# THERMAL CONTACT RESISTANCE

BORIVOJE B. MIKIC
WARREN M. ROHSENOW

September 1966

Report No. 4542-41
Contract No. NGR-22-009-065

Department of Mechanical Engineering
Massachusetts Institute of Technology



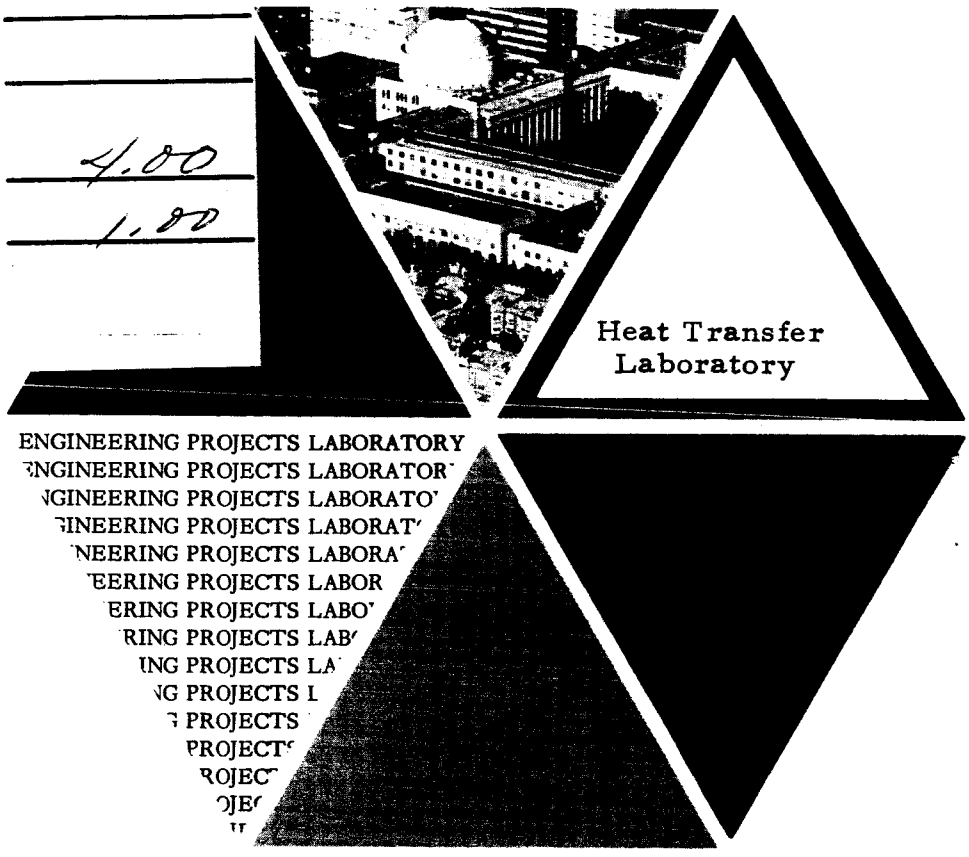

TECHNICAL REPORT NO. 4542-41

# THERMAL CONTACT RESISTANCE

by

Borivoje B. Mikic

Warren M. Rohsenow

Sponsored by the National Aeronautics
and Space Administration
Contract No. NGR 22-009-065

September 1966

Department of Mechanical Engineering
Massachusetts Institute of Technology
Cambridge 39, Massachusetts

# THERMAL CONTACT RESISTANCE

by

Borivoje Budimira Mikic
and
Warren Max Rohsenow

## ABSTRACT

This work deals with phenomena of thermal resistance for metallic surfaces in contact. The main concern of the work is to develop reliable and practical methods for prediction of the thermal contact resistance for various types of surface characteristics under different conditions. In particular, consideration is restricted to the following cases: (i) rough nominally flat surfaces in a vacuum environment; (ii) rough nominally flat surfaces in a fluid environment; (iii) smooth wavy surfaces in a vacuum environment (with either of the following three types of waviness involved; spherical waviness, cylindrical waviness in one direction and cylindrical waviness in two perpendicular directions) and (iv) rough wavy surfaces in a vacuum environment.

The problem is divided into three parts: thermal analysis, surface analysis and deformation analysis.

The thermal analysis, based upon the proposed models, investigates the analytical solutions for the thermal contact conductance under steady state conditions. It was found convenient, due to the extensive analytical work connected with various models and different methods used here, to present all details of the thermal analysis separately in the appendices.

The surface analysis, treating the surfaces as random processes with Gaussian distribution of height, relates the interface geometry to the actual contact area. The method suggested in this analysis has been checked against some autoradiographical experimental data.

The deformation analysis, in its two parts, gives dependence between the load supported by the interface and (i) the actual contact area and (ii) the contact spots distribution for rough spherically wavy surfaces, respectively. The result of the first part of

the analysis is based on the plastic deformation of the surface asperities. The second part considers, through the model of the equivalent contour area, the combined effect of spherical waviness and roughness on the problem of contact spots spreading at the interface.

Limitations and possible deviations of the proposed models are discussed.

Prediction of the thermal contact conductance is compared with experimental data obtained in this work (in a vacuum environment) together with some data obtained by other investigators (for which necessary surface parameters were available). Agreement between the measured and predicted values was good in the whole tested range of system variables.

## ACKNOWLEDGMENTS

This study was supported by the National Aeronautics and Space Administration.

Professors B. Rightmire and H. Fenech gave their time generously to discuss the program during the course of the investigation.

Mr. M. Yovanovich helped with very valuable discussions.

Mr. F. Johnson assisted in the experimental program.

Mrs. G. Benton typed the final manuscript.

We wish to express our thanks to all concerned.

# TABLE OF CONTENTS

# LIST OF FIGURES

## NOMENCLATURE

| | |
|---|---|
| a | radius of contact spot |
| a | half the width of contour strip |
| A | projected area |
| b | radius of heat channel |
| b | half the width of the heat channel |
| c | half the length of the heat channel |
| d | half the length of contour area |
| d | flatness deviation |
| D | diameter of contour area |
| E | modulus of elasticity |
| H | microhardness |
| h | contact conductance |
| $I_n, J_n, K_n$ | Bessel functions of order n |
| k | thermal conductivity |
| l | length of specimen |
| L | wave pitch |
| n | number of contacts per unit area |
| p | apparent pressure |
| Q | total heat flux rate per channel |
| r | radial coordinate |
| R | resistance |
| R | radius of curvature |
| T | temperature |
| $Y_o$ | yield stress |
| Y | distance between mean planes of contacting surfaces |

| | |
|---|---|
| x,y,z | Cartesian coordinates |
| $\alpha$ | eigenvalue |
| $\delta$ | mean height of interface gap |
| $\epsilon$ | a/b |
| $\Theta$ | mean of absolute value of slope |
| $\lambda$ | $^{D}/_{L}$ Eq. (4.3) |
| $\lambda$ | factor Eq. (2.17) |
| $\sigma$ | root mean square roughness |
| $\dot{\sigma}$ | root mean square slope |
| $\phi(\frac{a}{b})$ | resistance factor Eq. (2.14) |
| $\Psi(\frac{a}{b})$ | resistance factor Eq. (2.19) |

Subscripts

| | |
|---|---|
| 1,2 | metals 1 and 2 respectively, in contact |
| a | apparent |
| c | contact |
| conr | contour |
| f | void fluid |
| s | combination of 1 and 2 as in $k_s = \frac{2k_1k_2}{k_1+k_2}$ |
| t | total |

# I INTRODUCTION

## 1.1 Historical Background

For a long time it has been widely recognized that the calculation of heat flux through metallic joints formed by two bodies in contact, cannot be carried out in terms of the individual resistances of the bodies alone, by neglecting the temperature drop occuring in the region of the interface. Especially in the case of high heat flux, any prediction based on relations which do not include the interface effect would be unreliable. Consequently, when the problem of high heat flux arose in connection with the development of nuclear reactors, the necessity for better understanding of the phenomena of interface thermal resistance between two metals in contact - in this case between fuel elements and their metal cladding - resulted in a substantial number of works related to these problems. With the development of the spacecraft industry, where the knowledge of the interface resistance has been of even more importance for successful design of environmental control subsystems and energy conversion devices, the research in this area got further impulse, so that today we have a relatively extensive experimental, and in a somewhat lesser degree, theoretical work available. Although the noteworthy experimental work really started quite recently (about fifteen years ago) when the interest in this field became pronounced, it would be incorrect to conclude that the theoretical work was not much older; actually it started as early as 1873 by one of the best theoretical treatise on the subject [34].

The most significant publications related to this area are listed in the bibliography, and a very good review of those publications can be found in references [4], [5], [8] and [28]. Some investigators, [1], [3], [5], [6], [7] and [8] treated the problem analytically considering certain special cases.

This work, as a natural continuation of what has been done thus far, will represent an effort in the direction of obtaining more general knowledge relevant to the field of interface resistance. Our attention will be concentrated on the separate investigation of rough non-wavy surfaces, smooth wavy surfaces (with three different types of waviness), rough and wavy surfaces, all in a vacuum environment and rough non-wavy surfaces in a fluid environment.

## 1.2 Definition of Contact Conductance

In future we will use the term of thermal contact conductance which is defined by the following relation:

$$h = \frac{Q/A}{\Delta T} \tag{1.1}$$

where Q/A represents the heat flux per unit area and $\Delta T$ the temperature difference at the interface, interpreted, for steady state heat flow, as a difference between the respective interface temperatures which can be obtained by extrapolating the corresponding temperature profiles occurring far away from the contact surface (Fig: 1a).

The term thermal contact resistance, when used, will represent the reciprocal value of the contact conductance.

Turning now to the mechanism of contact resistance, we will consider two surfaces pressed together under condition of steady state heat flow. We may first conclude that the intimate contact

occurs only at a discrete number of locations; furthermore, those locations - which we will call contact spots - can be distributed uniformly or randomly or in some other particular manner over the contact surface, depending on the state of the surface and the nature of the load. We will investigate (Fig:1b) the case when the contact spots are confined inside contour areas which in turn could have their own distribution pattern. For a given load (normal to the surface of contact) and the given materials of the bodies in contact, the distribution of the contact spots, the shape of the contour areas and their distribution depend on the properties of the surfaces as roughness and waviness. The latter mainly, although not exclusively, determines the shape of the contour area and the former the contact spots distribution. In the case when the contour area is equal to the apparent area, i.e. when the contact spots are distributed over the whole area, we will say that we are dealing with nominally flat (or non-wavy)surfaces.

The heat across the interface generally can be transferred by conduction through a fluid, which might be present in gaps, by radiation and by conduction through the contact spots. When the interface is in a vacuum environment, only the last two modes will contribute in heat transmission.

We will restrict our interest primarily to the cases when the interface is in a vacuum under conditions of negligible radiation. Some theoretical work will be devoted also to the thermal contact conductance when a fluid is present in the gaps.

# II THERMAL ANALYSIS

## 2.1 Models

In order to solve analytically the problem of heat conduction through the interface of two metals in contact, the following models are adopted.

It is taken that all contacts are uniformly distributed inside the contour area and furthermore that all contact spots have the same area of contact, circular in shape whose radius is denoted by a. From the above it readily follows that inside the contour area there exist a number of identical heat channels in the form of hexagonal cylinders. In addition, for the contact in a vacuum, the contacting surface for each heat channel is considered to be flat; the last assumption can be justified by the fact that surface irregularities usually have a very small slope. One half of the elemental heat channel is given in Fig: 2a. By defining the elemental heat channel above, we do not want to imply that all the heat passing through contact spots under all circumstances flows in the pattern described by our model.

For contact in a fluid environment the model for a typical heat channel is given in Fig: 3a, where $\delta = \delta_1 + \delta_2$ is to be interpreted as the mean distance between surfaces in contact such that $\pi (b^2 - a^2) \delta$ represents the actual void volume for a heat channel; (b) stands for the radius of the typical heat channel).

The shape of the contour area, specified by the type of surface waviness, is assumed to be (i) circular for type of spherical waviness (Fig: 1b), (ii) in form of a strip for cylindrical waviness in

one direction only (Fig: 2b) and (iii) in form of a rectangle for cylindrical waviness in two principal directions (Fig: 2c).

Finally, it is assumed that the surfaces in contact are free from any kind of film and consequently, the whole problem of the thermal contact resistance is treated as the constriction phenomenon only, i.e. as the effect of constriction of heat flow in the region of contact.

## 2.2 Analytic Solution for an Elemental Heat Channel in a Vacuum Environment

For the model presented in Fig: 2a which will be considered like a semi-infinite cylinder, the temperature distribution and implicitly the thermal contact resistance is specified by the Laplace differential equation (for steady state conditions and thermal conductivity independent of temperature).

$$\nabla^2 T = 0 \tag{2.1}$$

and the following boundary conditions:

$$\left.\begin{aligned} T &= \text{const} \quad \text{at} \quad z = 0 \quad o<r<a \\ -k\frac{\partial T}{\partial z} &= 0 \quad \text{at} \quad z = 0 \quad a<r<b \end{aligned}\right\} \tag{2.2}$$

$$-k\frac{\partial T}{\partial z} = \frac{Q}{\pi b^2} \qquad z \to \infty \tag{2.3}$$

$$-k\frac{\partial T}{\partial r} = 0 \qquad \text{at} \quad r = b \tag{2.4}$$

$$k\frac{\partial T}{\partial r} = 0 \qquad \text{at} \quad r = 0 \tag{2.5}$$

where Q is the amount of heat passing through our model per unit of time and k stands for the conductivity of the material of the cylinder.

The solution of the above problem is obtained and discussed in detail in Appendix B. Summarizing here briefly the results of the Appendix, we want to emphasize several points. The mixed boundary

conditions at $z = 0$ (2.2) (where over a part of the area the temperature distribution is prescribed and over the rest of the area, the temperature gradient is given) did not allow for a direct analytical solution of our problem. Instead, two different indirect approaches are constructed, based on the known solution for the case when $b \to \infty$ (or rather $a/b \to 0$):

$$T = \frac{Q}{2\pi ka} \int_0^\infty e^{-\alpha z} \sin(\alpha a) J_o(\alpha r) \frac{d\alpha}{\alpha} \tag{2.6}$$

The derivation of (2.6) is presented in Appendix A.

2.2.1 Method of Superposition

In the first approach we considered the temperature field obtained by superposition of an infinite number of sources equally spaced on the surface at $z = 0$ (Fig: 4), where each source contribution on the resultant temperature field is of the form (2.6).

In this manner the expression for the thermal contact resistance for a half of an elemental heat channel was found to be:

$$R = \frac{1}{2\pi ka}\left\{\frac{\pi}{2} - \sin^{-1}\left(\frac{a}{b}\right) - \left(\frac{a}{b}\right)\left[1 - \left(\frac{a}{b}\right)^2\right]^{1/2} - \frac{3}{16}\left(\frac{a}{b}\right)\left[1 - \left(\frac{a}{b}\right)^2\right]\right\} \tag{2.7}$$

$$\equiv \frac{4}{\pi ka}\ \phi_2\left(\frac{a}{b}\right)$$

Where $\phi_2(\frac{a}{b})$ is presented in Fig: 5.

Expression (2.7) can be approximated by the linearized form as

$$R = \frac{1}{2\pi ka}\left[\frac{\pi}{2} - 2\left(\frac{a}{b}\right)\right] \tag{2.8}$$

which is a good approximation for $0 \leq \frac{a}{b} \leq 0.6$

$\phi_3(\frac{a}{b})$ related to (2.8) is also given for comparison in Fig: 5.

2.2.2 Alternative Approach

The other method presented in section one of Appendix B utilized

the fact that from (2.6) follows:

$$- k \frac{\partial T}{\partial z} = \frac{Q}{2\pi a\sqrt{a^2 - r^2}} \quad \text{at } z = 0 \quad o \leq r \leq a$$

and $$- k \frac{\partial T}{\partial z} = 0 \quad \text{at } z = 0 \quad a < r \qquad (2.9)$$

as well as $T = \text{const}$ at $z = 0$ $o \leq r < a$

(See Appendix A (A.6a), (A.7a) and(A.7b))

From the above it follows that one may use (2.9) to approximate ( 2.2) taking the temperature of the contact to be the mean temperature over the contacting area.

This procedure yields the expression for the thermal contact resistance in the form

$$R = \frac{2}{\pi ka} \left(\frac{a}{b}\right) \sum_{n=1}^{\infty} \frac{\sin (\alpha_n a) \, J_1 (\alpha_n a)}{(\alpha_n b)^3 \, J_o^2 (\alpha_n b)} \qquad (2.10)$$

$$\equiv \frac{4}{\pi ka} \phi_1 \left(\frac{a}{b}\right)$$

where eigenvalues $\alpha_n$ can be obtained from the relation:

$$J_1 (\alpha_n b) = 0 \qquad (2.11)$$

$\phi_1 (\frac{a}{b})$ is plotted in Fig: 5. The agreement between the two methods - as it is evident from Fig: 5 - is excellent.

2.2.3 Constant Heat Flux over the Contact Area

The case when the condition of constant heat flux prevails over the contact area, has been considered for two reasons: (i) since the constant heat flux over the contact area imposes a higher constriction of heat flow than the constant temperature condition over the same area, the former should always yield the higher thermal contact resistance and could serve as an upper bound check for

our previous solutions; and (ii) in certain cases, for example in the case of macroscopic constriction due to the waviness effect, the condition over the contour area depends on the contact spots distribution inside the area and hence, the actual situation over the contour area may approach that of the constant heat flux.

The exact solution for the thermal contact resistance (see section three of Appendix B) for this case, may be written as

$$R = \frac{4}{\pi k a} \left(\frac{b}{a}\right) \sum_{n=1}^{\infty} \frac{J_1^2 (\alpha_n a)}{(\alpha_n b)^3 \, J_o^2 (\alpha_n b)} \equiv \frac{4}{\pi k a} \phi_4 \left(\frac{a}{b}\right) \qquad (2.12)$$

$\alpha_n$ is determinable from (2.11). $\phi_4(\frac{a}{b})$ is given in Fig: 5.

2.2.4 Solution for a Finite Length of the Model

Since in practice the length of the elemental heat channel is always finite, we realize that it is of some interest to find: (i) the value of the minimum length for which the relations given in the previous sections are still applicable and further (ii) how the thermal contact resistance will behave when the length is less than that value. For this reason in Appendix C, section one, this problem specified by relation (2.1) with the boundary conditions (2.9), (2.4), (2.5) and

$$T = \text{const at } z = \ell$$

has been solved for the thermal contact resistance (C.13).

$$R = \frac{2}{\pi k a} \left(\frac{b}{a}\right) \sum_{n=1}^{\infty} \tanh (\alpha_n \ell) \frac{\sin(\alpha_n a) \, J_1 (\alpha_n a)}{(\alpha_n b)^3 \, J_o^2 (\alpha_n b)} \qquad (2.13)$$

where $\alpha_n$ is again the solution of (2.11). The alternative expression for the thermal contact resistance obtained by a method of superposition, which is of some theoretical importance, is presented in

section three of Appendix C. Also the case of constant heat flux over the contact area has been treated in section two of the same Appendix.

Comparison between (2.14) and (2.10) shows that the influence of the finite length of the elemental heat channel on the contact resistance is negligible for all values of $\ell \geq b$. This conclusion follows from the fact that the lowest $\alpha_n b$ is (from (2.11))

$$\alpha_1 b = 3.8317 \quad \text{and for } \ell \geq b$$

$$\tanh\left(\alpha_1 b \frac{\ell}{b}\right) \geq \tanh(\alpha_1 b) = \tanh 3.8317 = 0.999$$

and for all other values of $\alpha_n b$ in the subsequent terms of the series in (2.13), $\tanh(\alpha_n \ell)$ will be still closer to the value of one.

Another significant conclusion which follows from (2.14) is that the contact resistance will decrease with decreasing $\ell$ and will have the value zero for $\ell = 0$. Of course, this is a direct consequence of the imposed boundary condition: T = const at $z = \ell$ and formally it says that the mean temperature over the whole surface $z = 0$ approaches the contact temperature as $\ell$ approaches the value of zero, which is nothing but the statement of unique temperature; physically it says that as $\ell$ decreases for $\ell > b$, the deflection of flow lines will be less pronounced (i.e. heat flux contribution at $z = \ell$ will be highest directly opposite the contact area ($\pi a^2$) and will decrease rapidly with increasing r for r>a).

If we had imposed the constant heat flux at $z = \ell$ (rather than the constant temperature) the behavior of the contact resistance with decreasing $\ell$ would be quite the opposite of the one discussed above.

2.2.5 Application

The expressions found in this chapter of the form

$$R = \frac{4}{\pi k a} \phi \left(\frac{a}{b}\right)$$

do represent the contact resistance only for a half of the elemental heat channel. For the whole channel, it directly follows

$$R = R_1 + R_2 = \frac{8}{\pi k_s a} \phi\left(\frac{a}{b}\right) \qquad (2.14)$$

where

$$k_s \equiv \frac{2k_1 k_2}{k_1 + k_2}$$

$k_1$ and $k_2$ are the respective conductivities of two bodies in contact.

From the above one can obtain the thermal contact resistance per unit area as

$$R \equiv \frac{1}{h} = \frac{8}{\pi k_s a n} \phi(\varepsilon) = \frac{8\phi(\varepsilon)}{k_s \varepsilon \sqrt{\pi n}} \qquad (2.15)$$

where n represents the number of contacts per unit area and may be connected to the geometry of the elemental heat channel by the relation $n = \frac{1}{\pi b^2}$

Also

$$\varepsilon \equiv \frac{a}{b} = \left(\frac{Aconr}{Ac}\right)^{1/2}$$

is used as an abbreviation.

$\phi(\varepsilon)$ for a given $\varepsilon = \frac{a}{b}$ can be found in Fig: 5 or in the linearized form

$$\phi(\varepsilon) \simeq \frac{\pi}{16} - \frac{\varepsilon}{4}$$

## 2.3 Analytic Solution for an Elemental Heat Channel in a Fluid Environment

The problem of an elemental heat channel in a fluid environment, based upon the model given in Fig: 3a, has been considered in Appendix F. In the following we will briefly outline the procedure used in the Appendix and the result obtained by the same procedure.

The temperature distribution for this case is again determinable from relations (2.1),(2.3), (2.4), (2.5) and (instead (2.2)).

$$\left.\begin{aligned} T &= T_c = \text{const. at } z = 0 \quad o<r<a \\ -k_1 \frac{\partial T}{\partial z} &= \frac{k_f}{\delta_1} (T_c - T) \text{ at } z = 0 \quad a<r<b \end{aligned}\right\} \tag{2.16}$$

where $k_f$ is equivalent conductivity of the fluid present in the interface gaps. $\delta_1$ stands for the mean distance between the solid and the isothermal plane specified by temperature $T_c$.

In order to obtain a solution in closed form, the body of revolution which confines the amount of heat passing through the metallic contact, is approximated by the cylinder of radius $b_1$ (see Fig: 3b). With this approximation, together with the known solution for the cylinder in a vacuum environment, the expression for the contact conductance per unit area was obtained in the form:

$$h \equiv \frac{1}{R} = \frac{\varepsilon k_f \sqrt{\pi n}}{8\phi(\lambda\varepsilon)} + \frac{k_f}{\delta} \tag{2.17}$$

where

$$\lambda \equiv \sqrt{m^2 + \frac{\pi}{2}\frac{m}{\varepsilon} + 1} \quad - m$$

$$m \equiv \frac{bk_f}{\delta k_s} = \frac{k_f}{\delta k_s \sqrt{\pi n}}$$

and $\delta = \delta_1 + \delta_2$

## 2.4 Analytic Solution for the Contact Resistance due to the Various Types of Waviness

### 2.4.1 Spherical Waviness

The model for macroscopic heat channels in this case will be geometrically similar to the elemental heat channel given in Fig: 2a, and all expressions obtained for the latter are applicable here, provided that instead of $\varepsilon = \frac{a}{b}$, one uses $D/L$; D being the diameter of the contour area and L the wave length of the spherical waviness. So, from (2.15) it follows that the expression for the thermal contact resistance per unit of the apparent area due to the spherical waviness is:

$$R_w = \frac{4\,\phi(D/L)}{k_s(D/L)}\,L \qquad (2.18)$$

The values for $\phi\ (D/L)$ for different L/D can be found in Fig: 5 (formally taking $D/L = a/b$).

### 2.4.2 Cylindrical Waviness in One Direction

The analytical treatment of the heat flow through the macroscopic heat channel (Fig: 2b) where the contour area is of the form of a strip, is presented in Appendix D. The main results of the Appendix are as follows.

For the case when the contour area is kept at a constant temperature, the thermal contact resistance (for one half of the heat channel) was found to be:

$$R = \frac{1}{k\pi^2}\left(\frac{b}{a}\right)\sum_{n=1}^{\infty}\frac{1}{n^2}\,J_o\left(n\pi\,\frac{a}{b}\right)\sin\left(n\pi\,\frac{a}{b}\right) \qquad (2.19)$$

$$\equiv \frac{\psi_1\left(\frac{a}{b}\right)}{k}$$

where $\psi_1(\frac{a}{b})$ is given in Fig: 6.

The thermal contact resistance, when the heat flux over the contour area is taken to be a constant, can be expressed in the form

$$R = \frac{1}{k\pi^3}\left(\frac{b}{a}\right)^3 \sum_{n=1}^{\infty} \frac{1}{n^3} \sin^2\left(n\pi \frac{a}{b}\right) \equiv \frac{\psi_2(a/b)}{k} \tag{2.20}$$

$\psi_2\ (a/b)$ is presented in Fig: 6.

From the above one can derive the relation for the thermal contact resistance due to the cylindrical waviness per unit of the apparent area as

$$R_w = \frac{4\ \psi(a/b)}{k_s}\ b \tag{2.21}$$

2.4.3 Cylindrical Waviness in Two Perpendicular Directions

The contact resistance due to the cylindrical waviness in two principal directions (based on the model presented in Fig: 2c) has been considered in Appendix E only for the case of a constant heat flux over the contour area. The reason for this, together with the solution is given in the Appendix. The final result for the contact resistance per unit of the apparent area obtained there can be written as

$$R_w = \frac{4bc}{k_s\pi^3}\left[\frac{b^2}{ca^2}\sum_{n=1}^{\infty}\frac{\sin\left(\frac{n\pi a}{b}\right)}{n^3} + \frac{c^2}{bd^2}\sum_{m=1}^{\infty}\frac{\sin^2\left(\frac{m\pi d}{c}\right)}{m^3}\right] + \frac{8b^2c^2}{k_s\pi^2a^2d^2}\sum_{n=1}^{\infty}\sum_{m=1}^{\infty}\frac{\sin^2\left(\frac{n\pi a}{b}\right)\sin^2\left(\frac{m\pi d}{c}\right)}{n^2m^2\sqrt{\left(\frac{n\pi}{b}\right)^2+\left(\frac{m\pi}{c}\right)^2}} \tag{2.22}$$

where a, b, c and d are introduced in Fig: 2c.

# III SURFACE ANALYSIS

From the conductance equation involving roughness effect it is evident that the knowledge of the number of contacts per unit of the contour area as well as the ratio between the actual area and the contact area is required for prediction of the contact resistance. The ultimate goal of this whole work is to relate the thermal contact resistance to the apparent pressure through some surface characteristics and properties of materials which can be easily obtained.

The subject of this chapter is to find dependence between the number of contacts per unit area $\varepsilon$(square root of area ratio) as a function of geometrical parameters of surfaces, whereas the relation between $\varepsilon$ and the load will be discussed in the next chapter.

## 3.1 Description of the Surfaces

For each of the surfaces forming an interface contact, we assume the existence of an ensemble of the surface profiles, all taken from one surface, from which one can deduce statistical properties of the surface, i.e. we assume that there exists some probability measures related to the behavior of all the obtained profiles. As a consequence of the above, we can say that the surface profile y(x) (see Fig: 8a) is a random process which possesses a probability density function $\phi(y)$, where $\phi(Y)$, for example, is the probability that $y = Y$ and the quantity $p(Y)\,dy$ is the probability of the random variable y having the value between Y and Y + dy, i.e.

$$\lim_{\delta \to o} \frac{\phi(Y + \delta) - \phi(Y - \varepsilon)}{2\delta} = P(Y)$$

We will further assume that the random process y(x) is stationary, meaning that the statistical properties of the ensemble of surface profiles are invariant under arbitrary displacement in x direction.

In addition, it will be assumed that the probability density of height and slope are independent (i.e. the joint probability for height and slope may be written as $p(y,y') = p(y)\ p(y')$) and that the surface height is normally distributed, i.e. the probability density function for the surface height (measured from the mean plane) is given as

$$p(y) = \frac{e^{-y^2/2\sigma^2}}{\sigma\sqrt{2\pi}} \tag{3.1}$$

where $\sigma$ represents the standard deviation for height (or root mean square deviation) specified by the relation

$$\sigma \equiv \left[\frac{1}{L}\int_0^L y^2 dx\right]^{1/2} = \left[\int_{-\infty}^{\infty} y^2 p(y) dy\right]^{1/2} \tag{3.2}$$

Finally, we will state that for our purpose a surface under consideration is completely determined with the known probability density function for surface height p(y) together with the probability density function for profile slope p(y') (although, as it will be shown later, we will not need an explicit relation for p(y') but only the mean value at the slope).

## 3.2. Determination of Number of Contacts per Unit Area

Before starting to work direcdly on the problem of determination of the density of contact spots as a function of $\varepsilon$ and the geometry of the surfaces in contact, we recall the following known relation

from theory of probability [40]:

Let f(y) be a function of a random stationary variable y for which probability density distribution is known, then the mean value of f(y) over whole y distribution may be expressed as

$$\overline{f}\ (y(x)) = \frac{1}{L}\int_0^L f(y(x))\ dx = \int_{-\infty}^{\infty} f(y)\ p(y)\ dy \qquad (3.3)$$

or more generally

$$\overline{f}(y_1,y_2\ldots y_n) = \int_{-\infty}^{\infty}\ldots\ldots\int_{-\infty}^{\infty} f(y_1,y_2\ldots y_n)\ p(y_1,y_2\ldots y_n)\ dy_1,dy_2\ldots dy_n \qquad (3.3a)$$

We return now to random stationary distribution of the surface height, which can be formally presented as an all representative surface profile y(x) given in Fig:8a. Referring to the profile y(x) for a given surface, where y is measured from the mean line of the profile, we ask the question: what is the expected number of peaks per unit length above a certain level Y? Since we are dealing with all representative profiles, the actual interpretation of our question is: what is the expected value of $\sqrt{n}$, where n is the number of contacts per unit area, when a rough nominally flat surface is pressed to a smooth flat surface which is Y distance apart from the mean plane of the rough surface.

The above problem could be solved in more than one way. The method of counting functions suggested by Middleton [40] will be used here:

Let $u(\tau)$ be the step function with the following properties

$$u(\tau) = 1 \text{ for } \tau > 1 \text{ and } u(\tau) = 0 \text{ for } \tau < 1$$

Then $u(y(x) - Y)$ has the shape given in Fig: 8b.

Differentiating $u(y-Y)$ one can obtain the counting functional as

$$\frac{d}{dx}\,(u(y-Y)) = y'\delta(y-Y); \quad y' = \frac{dy}{dx} \tag{3.4}$$

where $\delta(y-Y)$ is known as unit impulse or Dirac delta, with property to vanish everywhere except at $y = Y$ and it satisfies the relation

$$\int_{-\infty}^{\infty} \delta\,(y-Y)\,dy = 1$$

from which follows

$$\int_{-\infty}^{\infty} f(y)\,\delta(y-Y)\,dy = f\,(Y) \tag{3.5}$$

and if for $a<x<b$ $y(x)$ assumes the value of Y once and only once, then

$$\int_{a}^{b} y'\,\delta(y - Y)\,dx = \pm\,1 \tag{3.6}$$

where the sign depends on the sign of $y'$.

From the above follows clearly that $\frac{du}{dx}$ consists of spikes with unit area directed upward or downward, depending on whether $y'$ is positive or negative (see Fig: 8c). Hence, the counting functional $|y'|\,\delta(y-Y)$ can be used for calculation (by virtue of (3.6)) of number of peaks crossed per unit lenghth of the profile (or square root of the number of contacts per unit area) as

$$\sqrt{n} = \frac{1}{2L} \int_{o}^{L} |y'|\,\delta(y-Y)\,dx \tag{3.7}$$

Since (3.7) is nothing but one half of the mean value of the counting functional, the use of (3.3a) will yield

$$\sqrt{n} = \frac{1}{2}\int_{-\infty}^{\infty}\int_{-\infty}^{\infty} |y'|\ \delta(y-Y)\ p(y)\ p(y')dy\ dy'$$

or with (3.5)

$$\sqrt{n} = \frac{P(Y)}{2}\int_{-\infty}^{\infty} |y'|\ p(y')\ dy' \qquad (3.8)$$

(The above expression could be derived also by a somewhat different approach developed by Rice, se [41], [43], [2]).

We can see that the integral of (3.8) represents the mean of the absolute value of the profile slope, and hence from (3.8) and (3.1) follows

$$\frac{2\sigma\sqrt{n}}{\tan\Theta} = \frac{e^{-Y^2/2\sigma^2}}{\sqrt{2\pi}} \qquad (3.9)$$

where

$$\tan\Theta \equiv \int_{-\infty}^{\infty} |y'|\ p(y')\ dy' = \frac{1}{L}\int_{o}^{L} |y'|\ dx \qquad (3.10)$$

Relation( 3.9) is presented in Fig: 9.

The value of $\varepsilon = (\frac{Ac}{Aa})^{1/2}$ may be similarly obtained. From Fig: 8a it is evident that $\varepsilon$ can be expressed as

$$\varepsilon = \frac{1}{L}\int_{o}^{L} u(y-Y)\ dx$$

and together with (3.3) and (3.1)

$$\varepsilon = \int_{-\infty}^{\infty} u(y-Y)\ p(y)\ dy = \int_{Y}^{\infty} p(y)\ dy$$

or finally

$$\varepsilon = \int_{Y}^{\infty} \frac{e^{-y^2/2\sigma^2}}{\sigma\sqrt{2\pi}}\ dy = \frac{1}{2}\left[1 - \operatorname{erf}\left(\frac{Y}{\sqrt{2}\sigma}\right)\right] \qquad (3.11)$$

The dependence $\varepsilon = f\ (^{Y}/\sigma)$ is given in Fig: 10.

Since both $\frac{2\sigma}{\tan\theta}\sqrt{n}$ and $\varepsilon$ are uniquely related to $^{Y}/\sigma$, there exists a unique relation

$$\frac{2\sigma}{\tan\theta}\sqrt{n} = \mu(\varepsilon) \tag{3.12}$$

Relation (3.12) is presented graphically in Fig: 11.

One can use the information given by Fig: 11 to relate the thermal contact conductance for nominally flat surfaces in contact to $\varepsilon$ in the form

$$\frac{h}{k_s \tan\theta} = \upsilon(\varepsilon) \tag{3.13}$$

Dependence (3.13) is given in Fig: 12.

All the relations derived so far in this chapter are based on the investigation of the contact between two nominally flat surfaces with the additional restriction that one of the surfaces must be smooth. In order to make the obtained results applicable for the case of two rough nominally flat surfaces in contact, we will modify the definitions of some parameters in the developed formulas.

Considering two rough surfaces in contact, with the mean planes at distance Y apart (again it was assumed that the distributions of height for both surfaces are random, stationary and Gaussian), we realize that at any point, whenever $y_1 + y_2 \geq Y$, the contact between the surfaces will occur ($y_1$ and $y_2$ are measured from the respective mean line). Consequently, one may apply all found relations by interpreting y(x) in Fig: 8a as

$$y(x) = y_1(x) + y_2(x)$$

and Y as the distance between the mean planes of the surfaces in contact. Standard deviation for distribution $y_1(x) + y_2(x)$, where both

$y_1(x)$ and $y_2(x)$ are normally distributed, is given as [44].

$$\sigma = \sqrt{\sigma_1^2 + \sigma_2^2} \tag{3.14}$$

The value for $\tan\theta$ in this case depends on the respective distributions of the slope for the two profiles.

If both slopes $|y'_1(x)|$ and $|y'_2(x)|$ are approximately constant, simple probability analysis shows that

$$\tan\theta \equiv \frac{1}{L}\int_0^L |y'_1 + y'_2|\, dx = \tan\theta_i \tag{3.15}$$

where $\tan\theta_i$ is the larger of the two slopes. In the case when each of the two $|y'(x)|$'s could have two different values (which can be the case for machined surfaces), the value of $\tan\theta$ will still approach the one given by (3.15).

If both slopes are normally distributed, i.e. if

$$p(y') = \frac{e^{-y'^2/2\dot{\sigma}^2}}{\dot{\sigma}\sqrt{2\pi}}$$

where $\dot{\sigma}$ is the standard deviation from the mean of the slope, then

$$\tan\theta = \frac{1}{L}\int_0^L |y'_1 + y'_2|\, dx = \int_{-\infty}^{\infty} |y'|p(y')dy = \sigma\sqrt{\frac{2}{\pi}}$$

$$= (\dot{\sigma}_1^2 + \dot{\sigma}_2^2)^{1/2}\sqrt{\frac{2}{\pi}} = \sqrt{(\tan\theta_1)^2 + (\tan\theta_2)^2} \tag{3.16}$$

The prediction of number of contacts per unit area based on the method developed above was compared with the predictions obtained from the other two existing methods, namely (i) from the graphical method (which can be executed on analog computers [45]) and (ii) from the method developed by Henry [2], which is based on the assumption of the random distribution of the height as well as the slope. For

five pairs of rough non-wavy surfaces, made of stainless steel 304, comparison between the three methods, and some experimental autoradiographical data is presented in Figs: 13 to 17. The predictions, except for the method suggested here, as well as the experimental data, were taken from [46]. The value for $\tan\theta$ in(3.12) was taken to be the larger of the two mean slopes of the contacting surfaces (which was justified by the behavior of the profiles slopes). In all the three methods $\varepsilon$ was related to the apparent pressure with the dependence: $\varepsilon^2 = \frac{P}{H}$, where H is microhardness (Vickers or Knoop). The conversion from $\varepsilon$ to pressure was done in order to enable the comparison with the experimental data. The relative agreement between the three methods, of course, does not depend on the validity of the assumed dependence between $\varepsilon$ and pressure (since in their original form the methods relate the number of contacts to $\varepsilon$).

# IV DEFORMATION ANALYSIS

The objective of this chapter is to give the final link between the thermal contact conductance and the apparent pressure. In the obtained relations in the previous chapters, the contact conductance has been expressed in terms of $\varepsilon = (\frac{Ac}{Aconr})^{1/2}$, the contour area and the wavelength, through some surface characteristics and properties of the materials in contact. In the following we will attempt, in the two separate sections, to relate $\varepsilon$ to the pressure over the contour area and to determine the contour area as a function of the apparent pressure for the case of rough spherically wavy surfaces.

## 4.1 Actual Contact Area

In Appendix H we have carried out an analysis with the purpose of estimating the real contact area when two rough non-wavy surfaces are brought into contact. The analysis is essentially constructed on a model which assumes that each contact point consists of two hemispherical asperities in symetric contact (Fig:19a)

The result of the analysis can be expressed by the following equation

$$\frac{Ac}{A_a} = \gamma \frac{p}{3Y_o} = \gamma \frac{p}{H}$$

where $\gamma$ is a function of the material properties of the contacting bodies, the pressure and the geometry of the surfaces in contact. For the geometry of the metallic surfaces we considered here ($\tan\theta \geq 0.1$) and the range of pressure we used ($p \geq 130$ psi), it is found that the value of $\gamma$ was very close to unity, and therefore it is permissible to use the relation

$$\frac{Ac}{A_a} = \frac{p}{H} \qquad (4.1)$$

The expression (4.1) agrees with the conclusions achieved by some other investigators ([47], [10])

From (4.1) it follows

$$\varepsilon^2 = \frac{Ac}{Aconr} = \frac{Aa}{Aconr} \frac{p}{H} = \frac{Pconr}{H} \tag{4.1a}$$

One may now use( 4.1a) and (3.13) to express the thermal contact conductance for the case of rough nominally flat surfaces in contact (Aa = Aconr) to the apparent pressure. The result is presented graphically in Fig: 18.

The same dependence can be expressed analytically as

$$\frac{\sigma h}{k_s \tan\theta} = 0.9 \left(\frac{p}{H}\right)^{16/17} \tag{4.2}$$

## 4.2 Contour Area for Spherically Wavy Surfaces in Contact

The model for spherical waviness, where only the mean line of the surface is presented, is given in Fig: 19b. We assume that the waviness is not too pronounced, i.e. (referring to Fig: 19b) $d/L \ll 1$. As a consequence of the above, the radius of curvature is expressed by

$$R = \frac{L^2}{8d}$$

We will call the distance d the flatness deviation and L the wavelength. For two such specimens in contact with the type of waviness described above, one can determine, by applying the Hertz theory [48], how the contour area (for smooth surfaces) varies with the load exerted between the contacting members. The final result may be written in the form

$$\lambda_H \equiv \frac{D}{L} = 1.285 \left| \left(\frac{p}{Em}\right) \left(\frac{L}{2d_t}\right) \right|^{1/3} \tag{4.3}$$

D being the radius of the contour area

$d_t = d_1 + d_2$

$E_s \equiv \frac{2E_1E_2}{E_1+E_2}$ ; $E_1$ and $E_2$ are respective moduli of elasticity for the materials in contact.

If the surfaces in contact are in addition rough, one can anticipate that the contour area will be larger than predicted by the Hertz theory. Also in this case, the effect of nonuniform distribution of the contacts will be present with the consequence that the density of the contact spots at the interface will decrease with increasing radius. In order to make the relations, based on the model which assumes uniform distribution of contacts inside the contour area, useful, we define here the effective contour area to be the area which would contain all the contact spots if they had been uniformly distributed inside this area. Using the definition given above, and the assumption that the mean surface would be deformed elastically according to the Hertz theory, the problem was investigated in Appendix H. The following result, which specifies the diameter of the effective contour area was obtained.

$$\lambda^2_{eff} = \lambda^2_H + 2\int_{\lambda_H}^{1} \exp\left\{-\frac{d_t}{\sigma}\lambda^2_H g(\frac{\lambda}{\lambda_H})\left[2\frac{Y}{\sigma} + \frac{d_t}{\sigma}\lambda^2_H\, g(\frac{\lambda}{\lambda_H})\right]\right\}\lambda d\lambda \quad (4.3)$$

where

$$\lambda_{eff} \equiv \frac{D_{eff}}{L} \text{ and } \lambda = \frac{2r}{L}$$

$$g(\lambda/\lambda_H) \equiv (\frac{\lambda}{\lambda_H})^2 - 2\left\{1 - \frac{1}{\pi}\left[(2 - \frac{\lambda^2}{\lambda^2_H})\sin^{-1}(\frac{\lambda_H}{\lambda}) + (\frac{\lambda^2}{\lambda^2_H} - 1)^{1/2}\right]\right\} \quad (4.4)$$

the waviness factor $g(\lambda/\lambda_H)$ is presented also graphically in Fig: 20. Since $(Y/\sigma)$ in (4.3) is the function of $\epsilon$ (see Fig: 10) where $\epsilon$ is

given by

$$\varepsilon = \frac{1}{\lambda_{eff}} \left(\frac{p}{H}\right)^{1/2} \tag{4.4a}$$

it is obvious that the process of calculating $\lambda_{eff}$ is an iterative process. However, from known $\lambda_H$ and some limited experience, one can make good estimation of $Y/\sigma$ in the first step so that only one evaluation of $\lambda_{eff}$ might be necessary.

4.3 Application

We will conclude this chapter by outlining the procedure for the prediction of the thermal contact resistance for two rough and spherically wavy surfaces in a vacuum environment.

From (2.15) and (2.18) follows

$$R = \frac{8\ \phi(\varepsilon)}{k_s \varepsilon \sqrt{\pi n}} + \frac{4\ \phi(\lambda_{eff})}{k_s \lambda_{eff}} L \tag{4.5}$$

where the first term in (4.5) is the resistance imposed by the roughness due to the amount of heat which might follow the pattern of the model for the elemental heat channel, and the second term represents the contribution due to the spherical waviness.

From the known parameters of the surfaces in contact ($\sigma_i$,$\tan\theta_i$, d,L) as well as the properties of the materials ($K_i$,$E_i$,$H_i$) one can use Eq. (4.5) to obtain $\lambda_{eff}$, Eq. (4.4) for $\varepsilon$, Fig:11 for determining $\sqrt{n}$ and Fig: 5 to evaluate $\phi(\varepsilon)$ and $\phi(\lambda_{eff})$. All this, together with (4.5) will enable the prediction for the thermal contact resistance.

In the case of nominally flat surfaces in contact, the prediction can be made directly from Eq. 4.2 (or Fig: 18)

# V EXPERIMENTAL DETERMINATION OF CONTACT RESISTANCE

## 5.1 Apparatus

The apparatus shown in Fig: 21 consists of a structure for support and loading, the test chamber, a vacuum system and an instrument console.

The lever system was designed to give mechanical advantage of 100. Dead weight loading is made to be independent of thermal strains. The load is measured by a strain gauge dynamometer, located in the test chamber and hence, the hysteresis effect due to bearing friction did not influence the accurate reading of the load.

The load in the test section may range from 0 - 20.000 pounds when the pressure in the test chamber is at one atmosphere. However, for a vacuum condition in the test chamber, the minimum load on the test section is 103 pounds (or 131 p.s.i. over the one-inch diameter specimens' interface). This is caused by the atmospheric pressure acting on the 3-inch diameter bellows, through which the load is transmitted to the test section. The cross-section of the test chamber is given in Fig: 22.

The chamber consists of a top plate, a base plate, an upper cylinder and a lower cylinder which can be lowered to expose the test section.

Referring to Fig: 22, the test section consists of the upper and lower main coolers (4,19), spacers (5,6,17) the upper and lower main heaters (7 and 8 respectively) the specimens (8,9), the dynamometer (18) and the guard ring with its upper and lower heaters (12,13), and upper and lower coolers (11,14).

The test section design allows for heat flow through the interface to be reversed. The heating elements are made from Kanthal

resistance wire. The heater cores are one-inch diameter stainless steel.

The temperature is measured by 28-guage chromel-alumel thermocouples cemented by means of Sauereisen. Four thermocouples are inserted into each specimen, spaced 3/8 of an inch apart along the centerline, beginning 2/8 of an inch from the tested interface. A Leeds and Northrup potentiometer, with the accuracy of 0.005 millivolts (corresponding to 0.25°F) was used for measuring e.m.t. produced by the thermocouples.

The load at the interface is measured by the dynamometer made of 1.5 inch diameter 2 inch long aluminum cylinder with semiconductor strain gauges attached near the base of the cylinder. The dynamometer was able to record the change of the load from one pound (at the basic sensitivity the load of one pound produced displacement on the Sanborn recorder of one millimeter).

The guard ring with its two coolers and two heaters is used to minimize the radiation effect on the specimens. It is done by adjusting the temperature gradient in the guard ring to be approximately the same as the temperature gradient in the two specimens. The temperature gradient in the guard ring is measured by the three thermocouples mounted along the guard ring.

The vacuum system consists of a mechanical pump, a diffusion pump and a three -way vacuum valve. The connection between the pumping system and the vacuum chamber is fitted with vacuum gauges. A thermocouple vacuum gauge is used for pressures between 5 and 1000 microus Hg, whereas the pressures from 5 microns to $10^{-7}$ mm are

covered by an ionization gauge. The pressure between the diffusion pump and the mechanical pump is measured by a thermocouple vacuum gauge.

The instrument console can be seen in Fig: 21. On the console are located: the thermocouple potentiometer, wattmeters for the heaters, the vacuum gauge control, the valves for controlling flows through the four coolers, four variacs for controlling the heaters and control switches for the pumps.

5.2 Specimen Preparation and Measurement of Surface Parameters

Specimens are made in the form of a one-inch diameter cylinders, 1.5 inch long. Both base surfaces of each specimen are lapped on a lapping machine. On one of the lapped bases, the spherical waviness is obtained by spinning the specimen on a lathe with the test surface pressed against a rubber base covered by polishing cloth with a thin layer of a diamond compound spread over it. The waviness produced in this manner is recorded on a surface analyzer with a basic vertical sensitivity of 0.94 μin per millimeter deflection of the Sanborn recorder. With the known waviness, smooth test surfaces were blasted by the Ballotini Division, Potters Bros.,Inc., Carlstadt, N.J., with glass spheres of various sizes under different pressures in order to achieve the desired roughness.

The surface profiles are recorded on the surface analyzer. From the recorded profiles, the mean of the absolute value of slope $\tan\theta = \frac{1}{L}\int_0^L |y'|dx$ is found graphically. The root mean square of roughness is calculated from the center line average value (C.L.A. $\equiv \frac{1}{L}\int_0^L |y|dx$), by assuming the normal distribution of the profile's height, i.e. $\sigma = \text{C.L.A.}\sqrt{\frac{\pi}{2}}$. The application of the Chi-square test

[2] showed that the assumption of the normal distribution of height was acceptable for this type of roughness. The value of the center line average is read directly from the "Talysurf" profilometer.

5.3 Experimental Procedure

The apparatus described in section 5.1, is used for the experimental determination of the contact resistance.

Two specimens, with fitted thermocouples, are aligned by a device in the form of a hollow cylinder (made of two removable halves). So aligned specimens are placed in the chamber and there aligned (as one unit) relatively to the chamber devices under a load of about 100 psi. Following the alignment of the whole chamber, the cylinder which is used for the specimens alignment is removed and the chamber closed. Simultaneously, the dead weight is gradually removed and the vacuum of about $5 \times 10^{-6}$ mm Hg is attained. At the minimum pressure (131 psi) and all heaters turned on, the system and the interface is allowed to outgas for about 36 hours.

After the outgassing is accomplished, the heaters and the coolers are adjusted to give the desired heat flow. The temperatures are measured every half-hour. After two identical successive readings, it was assumed that the steady state had been attained and the reading was followed by an increase of the load.

All data are taken for the ascending load.

The deformation and the surface analysis used in this work are valid only for the first application of the load, therefore the ascending load procedure had to be used in order to enable the comparison between the theory and the experiments.

# VI COMPARISON OF PREDICTED AND EXPERIMENTAL RESULTS

Discussion of the agreement between the prediction, based on the thermal, surface and deformation analyses presented in the first three chapters of this work, and the experimental results obtained here, together with some found by other investigators, will be the contents of this chapter.

## 6.1. Elemental Model in a Vacuum Environment

The artificial specimens (made of different materials and with various geometries), which resemble the model of the elemental heat channel related to a heat flow through a contact spot, are tested in a vacuum environment. The prediction of the contact conductance, specified by equation (2.14) is, as it can be seen from Fig: 23, in very good agreement with the experimental results.

In Figs: 24 and 25 we presented the result of the comparison between the prediction (from Eq. 2.21) and the experiments for the contact which comprises the conditions related to a cylindrical waviness. For both tested contacts, one of the specimens was a stainless steel with protruding stripes, whereas the other was made of a softer material with contacting surface smooth and nominally flat. The geometry of the contacts as well as the materials involved are indicated in Figs: 24 and 25. The agreement between prediction and the experiments can be described as satisfactory.

## 6.2 Rough Nominally Flat Surfaces in a Vacuum Environment

The prediction of the thermal contact conductance calculated from relation (4.2) was compared by the experimental data in Fig: 18.

The experimental results from this work are the readings obtained

from the rough spherically wavy surfaces for those values of pressure for which the contour area is identical with the apparent area, i.e. when the surfaces in contact behaved like nominally flat surfaces. Fig: 18 also contains the experiments from references [2] and [5]. All specimens have been made from stainless steel. The geometry for the surfaces tested are listed in Fig: 18. Except for data from reference [2], where $k = 14.6 \frac{Btu}{hr\ ft°F}$ and H = 375,000 psi (for stainless steel 416), the values for thermal conductivity are obtained from Fig: 33 (supplied from [62]) and hardness for the material considered was H = 370,000 psi.

It can be seen from Fig: 18 that fairly good agreement is obtained between the theory and the compared experimental data.

6.3 Rough and Wavy Surfaces in a Vacuum Environment

Three pairs of specimens made of stainless steel 305 with rough and wavy surfaces are used in the experiments. The geometry of the specimens' surfaces are listed below

| | | |
|---|---|---|
| Pair 1 | Specimen 1 | $\sigma_1$ = 190 μin, $d_1$ = 95 μin, $\tan\theta_1$ = 0.150 |
| | Specimen 2 | $\sigma_2$-negligible, $d_2$ = 55 μin, $\tan\theta_2 \simeq 0$ |
| Pair 2 | Specimen 1 | $\sigma_1$ = 132 μin, $d_1$ = 80 μin, $\tan\theta_1$ = 0.163 |
| | Specimen 2 | $\sigma_2$ = 76 μin, $d_2$ = 0 μin, $\tan\theta_2$ = 0.137 |
| Pair 3 | Specimen 1 | $\sigma_1$ = 292 μin, $d_1$ = 80 μin, $\tan\theta_1$ = 0.100 |
| | Specimen 2 | $\sigma_2$ = 174 μin, $d_2$ = 35 μin, $\tan\theta_2$ = 0.100 |

The resulting σ for each pair is given, together with the experimental results, in Figs: 26, 27 and 28. The theoretical prediction

is made from relation 4.5. $\tan\Theta$, for each pair is taken to be the larger of the two respective $\tan\Theta_i$ for the surfaces involved. $\upsilon \equiv \lambda_{eff}/\lambda_H$ varies with pressure, but the average one for range of pressures from 131 psi to the pressure which will eliminate the effect of deviation of flatness, is indicated in each figure. For comparison, the curve corresponding to $\upsilon = 1$ (i.e. when the contour area is assumed to be the same as one obtained by the Hertz theory for smooth surfaces) is presented for each pair of specimens. Hardness in all cases had the value of H = 370,000 psi, Young's modulus of elasticity $E = 26 \times 10^6$ psi and conductivity data are taken from Fig: 33.

For all the three pairs of specimens, the agreement between predicted and measured values was good.

6.4 Contacts in a Fluid Environment

The theory, which is developed in this work, for prediction of the contact conductance with the presence of an interstitial fluid, is compared to some experimental data obtained by Fenech [1] and Henry [2].

In Figs: 29 and 30 are given experimental results and prediction by the theories (one presented here and the other in reference [1]) for two different geometries of an artificial model with a fluid in the gap. Three types of fluids are used: air, water and mercury.

The agreement was satisfactory for all the three fluids. One may notice, that the fluids with relatively low conductivity (compared with the conductivity of the material of the model: stainless steel AMS 5613), the prediction for the thermal contact conductance was higher than the values obtained by experiments. This can be

explained by the influence of the finite height of the small cylinder which comprised the contact spot for the specimen experimentally tested. Since our theory is based on the model with zero height of the contact spot, it gave a somewhat smaller thermal resistance.

For the case of rough nominally flat surfaces with a fluid in the gaps, the validity of expression (2.17) was checked against the experimental (and theoretical) results obtained in reference [1] (Fig: 31) and reference [2] (Fig: 32).

For the prediction given in Fig: 31, dependence between $\delta$, $\sqrt{n}$ and $\varepsilon$ was taken from the graphically obtained data in reference [1], whereas $k_s$ for the particular combination of materials (Iron/Aluminum) had the value $k_s = 73.0 \frac{Btu}{hr\ ft^\circ F}$.

The interface parameters for the case considered, in Fig: 32 are listed in the figure.

The agreement between the predictions and the experiments was very good.

# VII CONCLUSIONS

## 7.1 Discussion of Results

The purpose of this, primarily theoretical work, was to provide certain relations which can be used to predict the thermal contact conductance for various conditions (rough non-wavy surfaces in a vacuum environment, rough non-wavy surfaces in a fluid environment, smooth wavy surfaces in a vacuum environment and rough and wavy surfaces in a vacuum environment). Furthermore, the effort was made to reduce the thermal contact conductance equation to the form which can be acceptable for practical application. It seems that the success in this respect was achieved in some cases, particularly for rough nominally flat surfaces in a vacuum environment (Eq.(4.2)) and, in a somewhat lesser degree for rough nominally flat surfaces in a fluid environment. We realize that the price paid for the attained simplicity is a degree of uncertainty in prediction imposed by the adaptation of various models and assumptions made in the process of deriving our relations. Although the experiments(Fig: 18), limited to the certain pressure range, gave quite a comfortable agreement, we do feel compelled to discuss limitations and possible deviations of the prediction.

Starting with the model for the elemental heat channel ( Fig:2a), we can say that the assumption of negligible height of contact button is a realistic one(justified by very small slope of surface asperities normally encountered in practice). The only different model, with contact button approximated by a small cylinder with a finite height, has been proposed in reference [1]. This less realistic model, leads to the more complicated conductance equation,

which in turn was obtained by satisfying the boundary conditions only in average, and assuming, that in the relations for the temperature distribution, it was sufficient to retain only the first term of an infinite series. As a consequence of these, when one lets the height of the contact button approach zero in the conductance equation developed in reference [1] (for the vacuum condition), the resulted prediction did not agree with the one obtained in this work.(Although in this way the two models have become identical.) The comparison between the two methods are given in Fig: 34. However, we should say that a prediction based on the original conductance equation from [1] would be better than was indicated by the situation observed from Fig: 34, since the resistance due to the fictitious finite height of the contact button, when taken into account, would tend to decrease the discrepancy between the two methods.

The assumption concerning the shape of the elemental heat channel with concentric circular contact spot, in spite of its artificialness, (the real contact, of course, has an irregular shape) cannot produce an essential error in the result for the thermal contact conductance prediction (this can be verified by comparing the conductance for two limiting cases: a cylinder with the concentric circular contact spot (Fig: 2a) and a rectangular heat channel with the contact area in the form of a strip (Fig: 2b) with the same contact area/apparent area ratio). The employed model further assumed that all the contact spots are of the same size and uniformly distributed over the apparent area. In our opinion, this simplification might have serious consequences on the accurate prediction of the contact conductance.

Especially at light pressures the actual situation could be quite different than our model assumes. The degree by which nonuniform distribution might effect the prediction could be deduced from the fact that such a distribution has the same effect on the contact conductance as some equivalent type of waviness. In Figs: 26, 27 and 28 we compared the predictions for rough spherically wavy surfaces and for the same surfaces if they were without waviness, i.e. if the contacts were uniformly distributed over the whole apparent area. The result of this comparison indicates the possible significance of nonuniform distribution of contacts.

The surface analysis, in which we related the number of contacts to $\varepsilon$, is based on probability analysis, starting with the assumption that the surface height is normally distributed. Even if our assumption were correct, and if we had sufficient information to determine the required statistical properties, the result of the probability analysis would represent, at best, only a good approximation. Nevertheless, we are confident that for surfaces large enough to qualify for statistical consideration, this analysis will yield the reliable results.

Finally, the deformation analysis provided an estimated dependence between area ratio and apparent pressure. The dependence is founded on the consideration of a symetric model (see Appendix H). It was concluded, as a result of such consideration, that the relation (4.1) could be used for the pressure range we had been interested in (130 psi to 15,000 rsi) with the known consequence, that at low pressures the actual area would be somewhat higher than predicted by (4.1) and at the high pressures, if we used the same hardness value in the entire pressure range, the actual area would be less than predicted,

due to the work-hardening of materials in contact.

In view of all the effects discussed above, together with the experimental findings (Fig: 18), we can conclude that the prediction of the contact conductance obtained from relation (4.2) might be somewhat low for low pressures( due to the combined effects of nonuniform distribution of contact spots and underestimation of real contact area) while at very high pressures the prediction could be too high due to the work-hardening effect of the materials engaged in the contact.

The waviness effect has been considered separately for smooth surfaces, for three different types of waviness as well as in combination with roughness. The latter case has significant practical interest, since all surfaces in practice will normally possess some type of waviness. On the other hand, this waviness could be irregular and very often indeterminable and therefore, any accurate prediction of the contact conductance, for these cases, would be impossible. However, the consideration of waviness was undertaken here in order to provide information concerning the relative importance of the waviness effect for surfaces in contact which were, in addition, rough. The waviness considered was of the spherical type specified by flatness deviation of the same order as roughness (this particular combination is likely to occur for real rough surfaces intended to be flat.)

The prediction, which agreed well with the experiments (Figs: 26, 27 and 28) indicated that the waviness effect is relatively significant and especially pronounced at low pressures with the tendency to

diminish with increasing pressure. The particular pressure for a given pair of surfaces, for which the waviness effect will disappear, depends on the elastic properties, flatness deviation and roughness of the specimens. The experiments done with wavy rough surfaces have been used also to confirm the theory for rough non-wavy surfaces, for those pressures for which the waviness will disappear (due to the elastic deformation of the specimens).

7.2 Recommendation for Further Research

The broad area of contact resistance is still largely unexplored Some topics have been examined mainly experimentally, for example, directional effect for dissimilar metals in contact (Rogers [24]), effect of cycling of the applied load on the thermal contact conductance (Cordier [19]), the thermal resistance with presence of interfacials foil (Fried [22]), plated surfaces in contact (Fried [9] and Weills and Ryder [11]). Since in those areas we are still without any correlation of available data, and still less without a theory which agrees with experiments, the problem of prediction of the contact resistance, for these cases, remains unsolved. We particularly wish to emphasize the significance of having contacting surfaces plated in connection, not only with an increase of actual contact area which can be achieved by plating contacting members with a soft metal, but also from the overlooked aspect of increasing conductivity of the layer through which constriction takes place. It is obvious from any conductance equation that the contact conductance is directly proportional to the value of $k_s \left( = \frac{2k_1 k_2}{k_1 + k_2} \right)$

where $k_1$ and $k_2$ are respective conductivities of the layers where

the heat flow is not parallel. From the conclusion of Appendix C, we saw that the thickness of this layer is approximately equal to the radius of one elemental heat channel ($=b=\sqrt{1/\pi n}$ (n being the number of contacts per unit area) and hence, for non-wavy surfaces, could be quite small. From the above it follows that considerable reduction in the contact resistance may be achieved by plating contacting surfaces with a material of high conductivity, even if in this way we do not increase the actual contact area. (Notice - from the expression for $k_s$ - that for good results both surfaces should be plated). The conclusion reached above may be generalized by realizing that any process or treatment which changes the conductivity of the materials in the immediate vicinity of contacting surfaces, will have significant influence on the contact conductance results. We think that the above phenomenon deserves closer investigation in future research.

Further work in the area of deformation analysis is needed in order to relate the actual contact area to the pressure in the region of very low pressures where elastic deformation of surface asperities might be a predominant factor.

Finally, we should mention investigation of the contact conductance under the condition of a vibrating load as well as the practically important case of transient conditions in their various forms (continuous heat flux variation and gradual evacuation of the interface fluid) as areas of future interest.

APPENDIX A

CONTACT RESISTANCE FOR A SEMI-INFINITE MEDIUM DUE TO HEAT SUPPLY OVER A FINITE CIRCULAR AREA

A.1 The circular area is kept under a constant temperature.

For a steady state condition, the temperature distribution in the semi-infinite medium should satisfy the Laplace differential equation

$$\nabla^2 T = 0 \qquad \begin{matrix} o \leq r < \infty \\ o \leq z < \infty \end{matrix} \tag{A.1}$$

The origin of the coordinate system is chosen so that it coincides with the center of the circular area through which heat is supplied, and the semi-infinite solid is extending in the positive z direction.

The boundary conditions of the problem are as follows

$$T = T_c = \text{constant} \quad \text{at } z = 0 \quad o \leq r < a \tag{A.2}$$

$$-k\frac{\partial T}{\partial z} = 0 \quad \text{at } z = 0 \quad r > a \tag{A.3}$$

$$\begin{matrix} T = 0 \text{ (arbitrary)} & \text{at } r = \infty \\ T = 0 & \text{at } z = \infty \end{matrix} \tag{A.4}$$

where a is the radius of the circular area, and k is thermal conductivity of the medium.

The differential equation (A.1) together with the boundary condition (A.4) has a solution in the form

$$e^{-\alpha z} f(\alpha) J_o(\alpha r)$$

for all values of $\alpha$ between zero and infinity. Hence

$$T = \int_o^\infty e^{-\alpha z} f(\alpha) J_o(\alpha r)\, d\alpha \tag{A.5}$$

The function $f(\alpha)$ will be determined in such a way as to fulfill the

the conditions (A.2) and (A.3), and this can be achieved by making use of the following known relations connected with Bessel functions (see for example [33] or [35]).

$$\int_0^\infty \frac{\sin(\alpha a)}{\alpha} J_o(\alpha r)\, d\alpha = \begin{cases} \pi/2 & o \leq r < a \quad (A.6a) \\ \sin^{-1}\left(\frac{a}{r}\right) & r > a \quad (A.6b) \end{cases}$$

and

$$\int_0^\infty \sin(\alpha a)\, J_o(\alpha r)\, d\alpha = \begin{cases} 0 & r > a \quad (A.7a) \\ \frac{1}{\sqrt{a^2 - r^2}} & o \leq r < a \quad (A.7b) \end{cases}$$

From the above it is evident that, by virtue of (A.6a) and (A.7a) the expression

$$T = \frac{2T_c}{\pi} \int_0^\infty e^{-\alpha z} \sin(\alpha a)\, J_o(\alpha r)\, \frac{d\alpha}{\alpha} \qquad (A.8)$$

satisfies (A.1) and all boundary conditions: (A.2), (A.3) and (A.4) (consequently $f(\alpha) = \frac{2T_c}{\pi} \frac{\mathrm{Sin}(\alpha a)}{\alpha}$ ).

Let Q be the total amount of heat transferred through the circular area per unit time, then from (A.7b) and (A.8) follows

$$Q = \int_b^a -k \left(\frac{\partial T}{\partial z}\right)_{z=0} 2\pi r dr = 4T_c k \int_0^a \frac{r dr}{\sqrt{a^2 - r^2}} = 4T_c k a \qquad (A.9)$$

The total thermal resistance between $z = 0$ and $z = \infty$ may now be written as

$$R = \frac{T_c - T_\infty}{Q} = \frac{T_c}{Q} = \frac{1}{4ka} \quad \left(= \frac{0.25}{ka}\right) \qquad (A.10)$$

Since the cross-sectional area of the conducting medium is infinite, all resistance is entirely due to the contact resistance.

## A.2 Heat is supplied at a constant rate over the contacting area

In some cases the condition over the contacting circular area

could be different from that of the constant temperature, and may in fact approach the constant heat flux condition (for example when a base of a cylinder or a wire is pressed or welded to the surface of a large body). For this reason the case of constant heat flux will be investigated in some detail below.

The temperature distribution should satisfy the differential equation (A.1) with boundary conditions given by (A.3),(A.4) and

$$-k\frac{\partial T}{\partial z} = \frac{Q}{\pi a^2} \quad \text{at } z = 0 \quad o \leq r < a \tag{A.11}$$

Q being the total amount of heat passing through the contacting area per unit time.

Relation (A.5) gives the form of the solution where $f(\alpha)$ may be obtained by applying boundary conditions (A.11) and (A.3) to the solution (A.5) and utilizing the following integral relation [33] and [35].)

$$\int_o^\infty J_o(\alpha r)\, J_1(\alpha a)\, d\alpha = \begin{cases} \frac{1}{a} & o \leq r < a \\ 0 & a < r \end{cases} \tag{A.12}$$

This procedure yields to

$$f(\alpha) = \frac{Q}{k\pi a}\,\frac{J_1(\alpha a)}{\alpha}$$

and further to

$$T = \frac{Q}{k\pi a}\int_o^\infty e^{-\alpha z}\,\frac{J_o(\alpha r)\, J\ (\alpha a)}{\alpha}\, d\alpha \tag{A.13}$$

Since the temperature over the contacting area for this case is not constant, the thermal contact resistance will be defined here with respect to the mean temperature over the area of contact ($o \leq r < a$, $z = 0$) i.e.

$$R = \frac{Tm - T\infty}{Q} = \frac{Tm}{Q}$$

where

$$T_m \equiv \frac{1}{\pi a^2}\int_0^a 2\pi\,[T(r)]_{z=0}\,rdr =$$

$$= \frac{2Q}{k\pi a^3} = \int_0^\infty [J_1(\alpha a)\int_0^a J_o\,(\alpha r)\,rdr]\,\frac{d\alpha}{\alpha} = \frac{2Q}{k\pi a^2}\int_0^\infty \frac{J_1^{\,2}(\alpha a)}{\alpha^2}\,d\alpha$$

The above integral can be evaluated in the form ( see [33],[35]).

$$T_m = \frac{2Q}{k\pi a^2}\left|\frac{\frac{a}{2}\;\Gamma(2)\;\Gamma(\frac{1}{2})}{2\;\;\Gamma(\frac{3}{2})\;\Gamma(\frac{5}{2})\;\Gamma(\frac{3}{2})}\right| = \frac{8}{3}\,\frac{Q}{k\pi^2 a}$$

Finally one may write

$$R = \frac{T_m}{Q} = \frac{8}{3}\;\frac{1}{k\pi^2 a}\;(=\frac{0.27}{ka}) \qquad (A.14)$$

Comparison between (A.10) and (A.14) reveals that there is no big difference (8%) in the values for the thermal resistances for the two cases considered. Also it is worthwhile to notice that the resistance for the case of the constant heat flux is higher than that of the constant temperature. This is quite in agreement with intuitive anticipation if one considers the disturbance of the flow lines (responsible for resistance) in the two cases.

APPENDIX B

CONTACT RESISTANCE FOR A SEMI-INFINITE CYLINDER IN A VACUUM

The temperature distribution in a semi-infinite cylinder (Fig:2a) for the case when heat is supplied over the circular area $\pi a^2$ at $z = 0$, will be considered below.

We seek the solution of

$$\nabla^2 T = 0 \tag{B.1}$$

with the following boundary conditions

$$\left.\begin{aligned} T &= \text{const} \quad \text{at } z = 0 \quad o \leq r < a \\ -k\frac{\partial T}{\partial z} &= 0 \qquad z = 0 \qquad r > a \end{aligned}\right\} \tag{B.2}$$

$$-k\left(\frac{\partial T}{\partial z}\right) = \frac{Q}{\pi b^2} \quad z \to \infty \tag{B.3}$$

$$-k\frac{\partial T}{\partial r} = 0 \qquad r = b \tag{B.4}$$

$$-k\frac{\partial T}{\partial r} = 0 \qquad r = o \tag{B.5}$$

The last condition, together with (B.3) restrict the temperature distribution to the form

$$T = -\frac{Q}{k\pi b^2} z + C e^{-\alpha z} J_o(\alpha r) + C_o \tag{B.6}$$

whereas (B.4) implies

$$\left.\begin{aligned} J_1(\alpha b) &= 0 \\ \text{i.e. } \alpha b &= 3.8317;\ 7.0156: \end{aligned}\right\} \tag{B.7}$$

Hence the problem stated by (B.1) through (B.5) has the solution expressible as

$$T = -\frac{Q}{\pi k b^2} z + \sum_{n=1}^{\infty} C_n e^{-\alpha_n z} J_o(\alpha_n r) \tag{B.8}$$

Where $\alpha, .. \alpha_n, ..$ can be obtained from (B.7). $C_n$ should be determined

by satisfying (B.2) while $C_o$ in (B.6), which by virtue of (B.7), represents the mean temperature over area $\pi b^2$, was taken to be zero (as the definition of zero temperature to be used in the first section of this Appendix.)

The mathematical difficulties imposed by the mixed boundary conditions (B.2) (where over a part of the area at z=0 the temperature is prescribed and over the rest of the area, the temperature gradient is specified) will force us to construct an approximate solution based on the exact temperature distribution for the case of semi-infinite medium (given in Appendix A).

Essentially there are three different methods by which one can obtain such approximate solution. Two methods will be demonstrated below, and the application of the third one will be postponed until the next Appendix.

B.1 Temperature gradient over the contact area is proportional to $(a^2-r^2)^{-1/2}$

It is evident that the solution obtained in Appendix A(A.8) represents the special case of the problem treated here, mainly the case when $b \to \infty$, or more precisely when $\frac{a}{b} \to 0$.

Furthermore, from (A.8), (A.9), (A.6a) and (A.7b) follows that for that case ($\frac{a}{b} \to 0$), boundary conditions

$$\left.\begin{aligned} -k\frac{\partial T}{\partial z} &= \frac{Q}{2\pi a\sqrt{a^2-r^2}} \quad \text{at} \quad z = 0 \quad o\leq r<a \\ -k\frac{\partial T}{\partial z} &= 0 \quad \text{at} \quad z = 0 \quad r>0 \end{aligned}\right\} \tag{B.9}$$

are equivalent to those given by (B.2). With an assumption that (B.9) can be used to approximate (B.2) even when $\frac{a}{b} \neq 0$ we may proceed by

determining $C_n$ in (B.8).

The above approach could be justified by the following arguments:

(i) The purpose of this analysis is primarily to obtain an estimation for the thermal resistance and not the exact temperature distribution in the cylinder. To achieve the former it is sufficient to know the temperature over the contacting area. Since here we will use the mean temperature obtained by integration over the mentioned area, an error introduced by the use of (B.9) will produce a second order effect in the expression for the mean temperature;

(ii) In an analogous situation for the two-dimensional case, it was found (see Appendix D) that the error in the expression for $\frac{\partial T}{\partial z} \sim (a^2 - r^2)^{-1/2}$ $o \leq r < a$ is only of the order of $(\frac{a}{b})^4$.

Before proceeding further with the solution, we will utilize the integral relation ([6])

$$\int_0^{\pi/2} J_o\ (w \cos\theta)\ \cos\theta d\theta = \frac{\sin w}{w} \qquad \text{(B.10)}$$

In order to evaluate the following, set $r = a\cos\theta$:

$$\int_0^a \frac{r\ J_o(\alpha r)\ dr}{\sqrt{a^2 - r^2}} = -\int_{-\pi/2}^{o} \frac{a\cos\theta\ a\sin\theta}{a\sin\theta}\ J_o(\alpha a\cos\theta)\ d\theta =$$

$$= a\int_0^{\pi/2} J_o(\alpha a\cos\theta)\ \cos\theta d\theta = \frac{\sin\alpha a}{\alpha} \qquad \text{(B.10a)}$$

Making use of the orthogonal properties of Bessel function and relations (B.8), (B.9), (B7) and (B.10a) one can write

$$\frac{Q}{\pi k_b^2}\int_o^b r\,J_o(\alpha_n r)\,dr + C_n\alpha_n\int_o^b r\,J_o^2(\alpha_n r)\,dr = \frac{Q}{2\pi ka}\int_o^a \frac{r\,J_o(\alpha_n r)\,dr}{\sqrt{a^2-r^2}}$$

$$C_n\alpha_n\ \frac{b^2}{2}J_o^2\ (\alpha_n b) = \frac{Q}{2\pi ka}\ \ \frac{\sin\alpha_n a}{\alpha_n}$$

or

$$C_n = \frac{Q}{\pi ka}\ \ \frac{\sin\ (\alpha_n a)}{(\alpha_n b)^2 J_o^2(\alpha_n b)} \tag{B.11}$$

The substitution of (B.11) into (B.8) yields

$$T = -\frac{Q}{\pi kb^2}z + \frac{Q}{\pi ka}\sum_{n=1}^{\infty} e^{-\alpha n z}\ \frac{\sin(\alpha_n a)J_o(\alpha_n r)}{(b\alpha_n)^2 J_o^2(\alpha_n b)} \tag{B.12}$$

The value for the mean temperature over the contact area follows from the above

$$T_m \equiv \frac{2\pi}{\pi a^2}\int_o^a (T)_{z=0}\,rdr = \frac{4Q}{\pi ka}\ \ (\frac{b}{a})\ \frac{1}{2}\ \sum_{n=1}^{\infty}\ \frac{\sin\ (\alpha_n a)\ J_1(\alpha_n a)}{(\alpha_n b)^3 J_o^2(\alpha_n b)} \tag{B.13}$$

The thermal resistance between z = o and z = ℓ (for large ℓ) is specified with

$$R_t = \frac{T_m - T_{z=\ell}}{Q} = \frac{Tm}{Q} + \frac{\ell}{k\pi b^2}$$

the contact resistance alone has the form

$$R = R_t - \frac{\ell}{k\pi b^2} = \frac{Tm}{Q} =$$

$$= \frac{4}{\pi ka}\ (\frac{b}{a})\ \frac{1}{2}\ \sum_{n=1}^{\infty}\ \frac{\sin(\alpha_n b\frac{a}{b})\ J_1(\alpha_n b\frac{a}{b})}{(\alpha_n b)^3\ J_o^2(\alpha_n b)} \tag{B.14}$$

We write (B.14) as

$$R = \frac{4}{\pi ka}\ \ \phi_1(\frac{a}{b}) \tag{B.15}$$

where

$$\phi_1\ (\frac{a}{b}) \equiv \frac{1}{2}\ (\frac{b}{a})\ \sum_{n=1}^{\infty}\ \frac{\sin(\alpha_n b\ \frac{a}{b})\ J_1\ (\alpha_n b\ \frac{a}{b})}{(\alpha_n b)^3\ J_o^2\ (\alpha_n b)}$$

with $J_1(\alpha_n b) = 0$

is represented in Fig: 5.

B.2 Solution obtained by the method of superposition

In order to obtain an approximate solution for the case of cylinder (Fig:2a) we will consider the field composed of an infinite number of heat sources equally spaced on the surface $z = 0$ which extends to infinity (Fig:4).

The temperature field is given by

$$T = \sum_{i=1}^{\infty} T_i(r,z) \qquad (B.16)$$

where $T_i$'s have the form of (A.8) and r in each $T_i$ represents the distance between the point considered and the particular source which contributes $T_i$.

By virtue of (A.6a), (A.6b) and (A.8) one may conclude that at $z = 0$ the contribution of each source is $T_c$ over its own source area and $\frac{2T_c}{\pi} \sin^{-1} \frac{a}{r_i}$ elsewhere (for $r_i > a$, where a and $r_i$ are measured from the center of the source).

From (A.7a), (A.7b) and (A.9) it is evident that heat has been transferred only through each source area and the amount for each contact spot is given by (A.9) i.e. $Q = 4T_c ka$.

In the further investigation the attention will be focussed on a cylinder with adiabate sides which separate heat flow coming from one contacting spot. The true shape of the cylinder is hexagonal, but here it will be approximated by a circular shape specified by its radius b. The radius itself depends on the density of sources and can be expressed by $b = (n\pi)^{-1/2}$ where n is the number of contact spots per unit area.

At this stage we want to introduce a small digression by

attempting to prove one significant point - namely that the contact resistance may be obtained from the expression

$$R = \frac{\frac{2}{a^2}\int_0^a [T]_{z=0}\, rdr - \frac{2}{b^2}\int_0^b [T]_{z=0}\, rdr}{Q} \qquad (B.17)$$

i.e. the knowledge of the temperature distribution at z = 0 contains all the information we need to solve the problem.

To reach the above conclusion we start from the exact form for the temperature distribution given with (B.8), noticing that it consists of the two parts: the linear part which dominates the solution for large values of z, and the disturbance part, which has its maximum effect at z = 0. The expression can also have a constant term which essentially defines the zero reference temperature. By virtue of (B.7) and (B.8) one may say that this constant would represent the mean temperature over $\pi b^2$ area or in other words - the temperature one would get at z = 0 by extrapolating the existing linear temperature profile occurring far away from the contact surface (or simply taking disturbance part equal zero).

Then from the definition of the contact resistance one may write (B.17)

Or proceeding in a more formal way

$$R = \frac{T_m - T_{z=\ell}}{Q} - \frac{\ell}{\pi k b^2} = \frac{\frac{2}{a^2}\int_0^a [T]_{z=0}\, rdr - \left(\frac{Q\ell}{k\pi b^2} + \frac{2}{b^2}\int_0^b [T]_{z=0}\, rdr\right)}{Q} - \frac{\ell}{\pi k b^2}$$

$$= \frac{\frac{2}{a^2}\int_0^a [T]_{z=0}\, rdr - \frac{2}{b^2}\int_0^b [T]_{z=0}\, rdr}{Q}$$

Returning now to the problem of determining the thermal resistance by the method of superposition, one can express the temperature distribution at z = 0 for one cylinder with adiabatic sides as

$$\left.\begin{aligned} T &= T_c + \frac{2T_c}{\pi} \sum_{i=1}^{\infty} \sin^{-1}\left(\frac{a}{r_i}\right) \qquad o \leq r < a \\ &= \frac{2T_c}{\pi} \sin^{-1}\left(\frac{a}{r}\right) + \frac{2T_c}{\pi} \sum_{i=1}^{\infty} \sin^{-1}\left(\frac{a}{r_i}\right) \quad a < r < b \end{aligned}\right\} \qquad (B.18)$$

where the terms summed from i = 1 to i = ∞ are contributions due to the sources outside of the area under consideration ($r_i$ being measured from the center of the source i).

Applying (B.17) to (B.18)

$$\frac{T_c - \left(\frac{T_c a^2}{b^2} + \frac{4T_c}{\pi b^2} \int_a^b \sin^{-1}\left(\frac{a}{r}\right) r\,dr\right)}{Q} +$$

$$+ \frac{2T_c}{\pi Q} \sum_{i=1}^{\infty} \left[\frac{1}{\pi a^2} \iint_{\pi a^2} \sin^{-1}\left(\frac{a}{r}\right) dA - \frac{1}{\pi b^2} \iint_{\pi b^2} \sin^{-1}\left(\frac{a}{r_i}\right) dA\right] \qquad (B.19)$$

To estimate the value of the last term in (B.19) we will use the fact that $\frac{a}{r_i} << 1$ and hence is permissible to write

$$\sin^{-1}\left(\frac{a}{r_i}\right) = \left(\frac{a}{r_i}\right) + \frac{1}{6}\left(\frac{a}{r_i}\right)^3 + \ldots \simeq \left(\frac{a}{r_i}\right)$$

With this and the relation $Q = 4kaT_c$ it was obtained

$$\frac{2T_c}{\pi Q} \sum_{i=1}^{\infty} \left[\frac{1}{\pi a^2} \iint_{\pi a^2} \sin^{-1}\left(\frac{a}{r_i}\right) dA - \frac{1}{\pi b^2} \iint_{\pi a^2} \sin^{-1}\left(\frac{a}{r_i}\right) dA\right] =$$

$$\simeq -\frac{1}{16\pi ka}\left(\frac{a}{b}\right)\left[1 - \left(\frac{a}{b}\right)^2\right] \sum_{i=1}^{\infty} \left(\frac{b}{R_i}\right)^3 \qquad (B.20)$$

where $R_i$ is distance between the center of the area considered (r=o) and the center of the particular source ($R_i = r_i$ for r = o).

After evaluation of the first part of (B.19) and making use of (B.20) follows the relation for the thermal contact resistance.

$$R = \frac{1}{2\pi ka}\left\{\frac{\pi}{2} - \sin^{-1}\left(\frac{a}{b}\right) - \left(\frac{a}{b}\right)\left[1 - \left(\frac{a}{b}\right)^2\right]^{1/2} - \frac{1}{8}\left(\frac{a}{b}\right)\left[1 - \left(\frac{a}{b}\right)^2\right]\sum_{i=1}^{\infty}\left(\frac{b}{R_i}\right)^3\right\} \quad (B.21)$$

The series $\sum_{i=1}^{\infty}\left(\frac{b}{R_i}\right)^3$ has been calculated for 300 nearest points with the result

$$\sum_{i=1}^{300}\left(\frac{b}{R_i}\right)^3 = 1.5 \quad \left(\left(\frac{b}{R_{300}}\right)^3 = \frac{1}{5000}\right)$$

So the finite form for the thermal resistance may be written as

$$R = \frac{1}{2\pi ka}\left\{\frac{\pi}{2} - \sin^{-1}\left(\frac{a}{b}\right) - \left(\frac{a}{b}\right)\left[1 - \left(\frac{a}{b}\right)^2\right]^{1/2} - \frac{3}{16}\left(\frac{a}{b}\right)\left[1 - \left(\frac{a}{b}\right)^2\right]\right\} \quad (B.22)$$

$$= \frac{4}{\pi ka}\phi_2\left(\frac{a}{b}\right)$$

Where $\phi_2\left(\frac{a}{b}\right)$ is given in Fig: 5.

The last term in (B.22) has a limited influence on the overall result e.g.

for $\frac{a}{b} = 0.1$ it contributes 1.5%

for $\frac{a}{b} = 0.2$ 3.5%

Furthermore, (B.22) could be simplified giving the good approximation of R for $0 \leq \left(\frac{a}{b}\right) \leq 0.6$ as

$$R = \frac{1}{4\pi ka}\left[\pi - 4\left(\frac{a}{b}\right)\right] \quad (B.22a)$$

B.3 Heat is supplied at a constant rate per unit of the contact area.

In order to obtain the upper limit for the thermal resistance, as well as for the reasons already stated in the previous Appendix, we will find the solution for the case of constant temperature gradient over the contact area.

The problem differs from that considered in the first section of this Appendix only in the boundary conditions at z = o, where now, instead of (B.9) we have

$$-k \frac{\partial T}{\partial z} = \frac{Q}{\pi a^2} \quad \text{at } z = 0 \quad o \leq r < a$$

$$-k \frac{\partial T}{\partial z} = 0 \quad \text{at } z = 0 \quad a < r < b \tag{B.23}$$

The routine procedure would lead to the following relation for the thermal resistance

$$R = \frac{4}{\pi k a} \phi_3 \left(\frac{a}{b}\right) = \frac{4}{\pi k a} \left(\frac{b}{a}\right) \sum_{n=1}^{\infty} \frac{J_1^2(\alpha_n b \frac{a}{b})}{(\alpha_n b)^3 J_o^2(\alpha_n b)} \tag{B.24}$$

## APPENDIX C

## CONTACT RESISTANCE FOR A FINITE CIRCULAR CYLINDER IN A VACUUM

In order to obtain the influence of the finite length of cylinders in contact on the expression for the thermal contact resistance, the solution obtained in Appendix B will be revised here by considering a cylinder limited with $o \leq r \leq b$ and $o \leq z \leq \ell$ when heat is supplied over a concentric circular area $\pi a^2$, $a \leq b$.

### C.1 Heat rate over the contact area is proportional to $(a^2-r^2)^{-1}/2$

The temperature distribution is determined by the following relations:

$$\nabla^2 T = 0 \tag{C.1}$$

$$-k \frac{\partial T}{\partial z} = \frac{Q}{2\pi a} \frac{1}{\sqrt{a^2-r^2}} \quad \text{at } z = 0 \quad o \leq r < a$$

$$-k \frac{\partial T}{\partial z} = 0 \quad \text{at } z = 0 \quad a < r < b \tag{C.2}$$

$$T = T_o = \text{const} \quad \text{at } z = \ell \tag{C.3}$$

$$-k \frac{\partial T}{\partial r} = 0 \quad r = b \tag{C,4}$$

$$-k \frac{\partial T}{\partial r} = 0 \quad \text{at } r = 0 \tag{C.5}$$

Imposing (C.3), (C.4) and (C.5) to (C.1) on arrives at the relation

$$T - T_o = \sum_{n=o}^{n=\infty} C_n e^{-\alpha_n \ell} \sinh[\alpha_n(\ell-z)] \, J_o(\alpha_n r) \tag{C.6}$$

where the solution of

$$J_1(\alpha b) = 0 \tag{C.7}$$

will give the values of $\alpha_n$ $(n = 0,1,2....)$

The boundary condition at $z = 0$ (C.2) can be expressed in the form of Faurier-Bessel series as

$$-\left(\frac{\partial T}{\partial z}\right)_{z=0} = \frac{Q}{\pi k b^2} + \frac{Q}{\pi k a} \sum_{n=1}^{\infty} \frac{\sin \alpha_n a \; J_o(\alpha_n r)}{b^2 \alpha_n \; J_o^2(\alpha_n b)} \qquad (C.8)$$

From (C.6) follows

$$\left(\frac{\partial T}{\partial z}\right)_{z=0} = -\sum_{n=o}^{\infty} C_n \alpha_n \; e^{-\alpha_n \ell} \cosh(\alpha_n \ell) \; J_o(\alpha_n t) \qquad (C.9)$$

Comparison of (C.8) and (C.9) will yield

$$C_o = \frac{Q}{\pi k b^2 \alpha_o \; e^{-\alpha_o \ell} \cosh \alpha_o \ell} \; ; \quad C_n = \frac{Q}{\pi k a} \frac{\sin(\alpha_n a)}{(\alpha_n b)^2 J_o^2(\alpha_n b) \; e^{-\alpha_n \ell} \cosh(\alpha_n \ell)} \qquad (C.10)$$

The first term for the temperature distribution may be obtained readily as

$$\lim_{\alpha_o \to o} \left[ \frac{Q}{\pi k b^2} \; \frac{\sinh[\alpha_o(\ell - z)]}{\alpha_o \cosh \alpha_o \ell} \right] = \frac{Q}{\pi k b^2} (\ell - z) \qquad (C.11)$$

The substitution of (C.10) and (C.11) into (C.6) will result in

$$T - T_o = \frac{Q}{\pi k b^2} (\ell - z) + \frac{Q}{\pi k a} \sum_{n=1}^{\infty} \frac{\sinh[\alpha_n(\ell - z)] \sin(\alpha_n a) \; J_o(\alpha_n r)}{\cosh(\alpha_n \ell) \; (\alpha_n b)^2 \; J_o^2(\alpha_n b)} \qquad (C.12)$$

From which the expression for the thermal contact resistance was found to be

$$R = \frac{4}{\pi k a} \left(\frac{b}{a}\right) \frac{1}{2} \sum_{n=1}^{\infty} \tanh\left(\alpha_n b \, \frac{\ell}{b}\right) \frac{\sin\left(\alpha_n b \, \frac{a}{b}\right) \; J_1\left(\alpha_n b \, \frac{a}{b}\right)}{(\alpha_n b)^3 \; J_o^2(\alpha_n b)} \qquad (C.13)$$

C.2 Heat is supplied over the contact area at constant rate

For the case when the constant heat flux is prescribed, the boundary condition (C.2) will change in

$$\left.\begin{aligned} -k \frac{\partial T}{\partial z} &= \frac{Q}{\pi a^2} \quad \text{at } z = 0 \quad o \le r < a \\ -k \frac{\partial T}{\partial z} &= 0 \quad \text{at } z = 0 \quad a < r < b \end{aligned}\right\} \qquad (C.14)$$

and the relation obtained for the thermal contact resistance (omitting the details of derivation) may be written as

$$R = \frac{4}{\pi k a}\left(\frac{b}{a}\right) \sum_{n=1}^{\infty} \tanh(\alpha_n b \frac{\ell}{b}) \quad \frac{J_1^2(\alpha_n b \frac{a}{b})}{(\alpha_n b)^3 J_o^2(\alpha_n b)} \tag{C.15}$$

C.3 Application of a method of superposition

In the following we will present the particular method of superposition which has some theoretical value. Although the result obtained here has less practical value than either (B.14), (B.19) or (C.13), the method deserves attention for the elegance of the idea of superposition as well as for the fact that the method itself is one of the first treatise on the mixed boundary conditions we had to deal with in our problem. The method is due to Weber (1873)([34],[35]).

As a first step, the infinite plate ($o \leq r \leq \infty$) with thickness $\ell$ ($o \leq z \leq \ell$) will be considered for the case when heat is supplied over the circular area $\pi a^2$ with center at $r = 0$, $z = \ell$.

The temperature distribution in the plate is defined by

$$\nabla^2 T_1 = 0 \tag{C.16}$$

and the following boundary conditions

$$\left.\begin{aligned} -k \frac{\partial T}{\partial z} &= \frac{Q}{2\pi k a} \frac{1}{\sqrt{a^2 - r^2}} \qquad z = \ell \quad o<r<a \\ -k \frac{\partial T}{\partial z} &= 0 \qquad\qquad\qquad z = \ell \quad a<r \end{aligned}\right\} \tag{C.17}$$

$$T_1 = 0 \text{ (arbitrary)} \quad \text{at } z = 0 \tag{C.18}$$

$$T_1 = 0 \qquad r \to \infty \tag{C.19}$$

$$k \frac{\partial T_1}{\partial r} = 0 \qquad \text{at } r = 0 \tag{C.20}$$

Utilizing (A.7a) and (A.7b) one can write the solution in the form of

$$T_1 = \frac{Q}{2\pi ka} \int_0^\infty \frac{\sinh(\alpha z)}{\cosh(\alpha \ell)} \sin(\alpha a)\, J_o(\alpha r)\, \frac{d\alpha}{\alpha} \qquad (C.21)$$

and at $z = \ell$

$$(T_1)_{z=\ell} = \frac{Q}{2\pi ka} \int_0^\infty \left(1 - \frac{2e^{-2\alpha\ell}}{1 + e^{-2\alpha\ell}}\right) \sin(\alpha a)\, J_o(\alpha r)\, \frac{d\alpha}{\alpha} \qquad (C.22)$$

From (C.22), (A.6a) and neglecting terms of order $(\frac{a}{e})^3$ and up, the following result has been found for the contact resistance ([33],[34])

$$R = \frac{1}{4ka} - \frac{\log 2}{2\pi k\ell} \qquad (C.23)$$

The solution for a finite circular cylinder may be obtained by superimposing the new temperature field $T_2$ to the one found above (C.21). The temperature distribution $T_2$ is specified by the following relations

$$\nabla^2 T_2 = 0 \qquad (C.24)$$

$$-k \frac{\partial T_2}{\partial z} = 0 \quad z=0 \qquad (C.25)$$

$$-k \frac{\partial T_2}{\partial z} = 0 \quad z=\ell \qquad (C.26)$$

$$k \frac{\partial T_2}{\partial r} = 0 \text{ at } r=0 \qquad (C.27)$$

$$-k\left(\frac{\partial T_1}{\partial r} + \frac{\partial T_2}{\partial r}\right) = 0 \quad r=b \qquad (C.28)$$

Where the above boundary conditions - especially (C.28) reveal the nature of superposition.

Satisfying (C.25), (C.26) and (C.27) one arrives at

$$T_2 = \sum_{n=1}^{\infty} C_n \sin\left(\frac{2n-1}{2\ell}\pi z\right) I_o\left(\frac{2n-1}{2\ell}\pi r\right) \qquad (C.29)$$

To implement (C.28) and thus to determine $C_n$ in (C.29) one has to express $T_1$(C.21) in the form of a series.

After the introduction of the approximation

$$\frac{\sin\alpha a}{\alpha} \simeq a \tag{C.30}$$

(C.21) may be written as

$$T_1 = \frac{Q}{2\pi k} \int_0^\infty \frac{\sinh(\alpha z)}{\cosh(\alpha \ell)} J_o(\alpha r)\, d\alpha =$$

$$= \frac{Q}{\pi k \ell} \sum_{n=1}^{\infty} \frac{\sin(\frac{2n-1}{2\ell}\pi z)}{\sin(\frac{2n-1}{2}\pi)} K_o(\frac{2n-1}{2\ell}\pi r) \tag{C.31}$$

for $r>o$

where the above transformation has been done by using Cauchy's residue theorem (for details see [33] or [35]).

Notice that (C.31) is not valid for r = o due to the behavior of $K_o(0)$, but since it will be employed only at r = b, the form is still useful.

From (C.29), (C.31) and (C.28) the expression for $C_n$ has been obtained and after substitution into (C.29) we may write

$$T_2 = \frac{Q}{k\pi\ell} \sum_{n=1}^{\infty} \frac{\sin(\frac{2n-1}{2\ell}\pi z)}{\sin(\frac{2n-1}{2}\pi)} \frac{K_1(\frac{2n-1}{2\ell}\pi b)}{I_1(\frac{2n-1}{2\ell}\pi b)} I_o(\frac{2n-1}{2\ell}\pi r) \tag{C.32}$$

Finally

$$T = T_1 + T_2 \qquad \text{and}$$

$$R = \frac{T_{z=\ell} - T_{z=o}}{Q} - \frac{\ell}{k\pi b^2}$$

or

$$R = \frac{1}{4ka} - \frac{\ell \log 2}{2\pi k \ell} + \frac{1}{k\pi\ell} \sum_{n=1}^{\infty} \frac{K_1(\frac{2n-1}{2\ell}\pi b)}{I_1(\frac{2n-1}{2\ell}\pi b)} - \frac{\ell}{k\pi b^2} \tag{C.33}$$

For $\frac{b}{\ell} >> 1$

$$\frac{1}{k\pi\ell}\sum_{n=1}^{\infty}\frac{K_1(\frac{2n-1}{2\ell}\pi b)}{I_1(\frac{2n-1}{2\ell}\pi b)} \to \frac{1}{k\pi\ell}\,\frac{8\ell^2}{\pi^2 b^2}\sum_{n=1}^{\infty}\frac{1}{(2n-1)^2} = \frac{8\ell}{k\pi^3 b^2}\,\frac{\pi^2}{8} =$$

$$= \frac{\ell}{k\pi b^2}$$

i.e. the solution (C.33) gets the form of (C.23) as one should expect.

The solution obtained in this section suffers from the lack of accuracy mainly due to the approximation (C.30). However, it is possible to improve the accuracy of the method by expressing integral (C.21) in the form of an infinite series without introducing (C.30). Because of the involvement of the procedure and the fact that we already have a good solution, it will not be done here.

## APPENDIX D

## CONTACT RESISTANCE FOR A SEMI-INFINITE RECTANGULAR SOLID DUE TO HEAT SUPPLY OVER A STRIP

### D.1 Heat is supplied over the contact area at a constant rate

With reference to Fig: 2b, the problem could be stated with the following relations

$$\nabla^2 T = 0 \tag{D.1}$$

$$-k \frac{\partial T}{\partial z} = \frac{Q}{2a} \quad \text{at } z = 0;\ -a<x<a$$

$$-k \frac{\partial T}{\partial z} = 0 \quad \text{at } z = 0;\ a<x<-a \tag{D.2}$$

$$-k \frac{\partial T}{\partial z} = \frac{Q}{2b} \qquad z \to \infty \tag{D.3}$$

$$k \left(\frac{\partial T}{\partial x}\right) = 0 \qquad x = \pm b \tag{D.4}$$

Where Q is heat flux per unit length of the strip.

The solution of (D.1) which satisfies (D.3) and (D.4) may be written as

$$T = -\frac{Q}{2kb} z + \sum_{n=1}^{\infty} C_n e^{\frac{-n\pi}{b} z} \cos\left(\frac{n\pi}{b} x\right) \tag{D.5}$$

From (D.2),(D.5) and the orthogonal property of trigonomerie function follows

$$\int_o^b \frac{Q}{2kb} \cos\left(\frac{n\pi}{b} x\right) dx + \int_o^b C_n \frac{n\pi}{b} \cos^2\left(\frac{n\pi}{b} x\right) dx = \frac{Q}{2ak} \int_o^a \cos\left(\frac{n\pi}{b} x\right) dx$$

from which

$$C_n = \frac{Qb \sin\left(\frac{n\pi}{b} a\right)}{kan^2\pi^2}$$

The temperature field is now defined by

$$T = \frac{Q}{2kb} z + \frac{Qb}{ka\pi^2} \sum_{n=1}^{\infty} \frac{1}{n^2} e^{-n\pi \frac{z}{b}} \sin\left(n\pi \frac{a}{b}\right) \cos\left(n\pi \frac{x}{b}\right) \tag{D.6}$$

The mean temperature over the contact area $-a<x<a$ at $z = 0$ can be found in the form

$$T_m = \frac{Qb^2}{ka^2\pi^3} \sum_{n=1}^{\infty} \frac{1}{n^2} \sin^2(n\pi\frac{a}{b})$$

The thermal contact resistance per unit length of the contact strip may be expressed from the above

$$R = \frac{1}{k\pi^3} (\frac{b}{a})^2 \sum_{n=1}^{\infty} \frac{1}{n^3} \sin^2(n\pi\frac{a}{b}) \qquad (D.7)$$

$R_k$ is presented in Fig:4.

D.2 Heat rate over the contact area is proportional to $(a^2-x^2)^{-1}/_2$

The problem is defined by the same relations considered in the previous section, except for the boundary condition at $z = 0$, where now, instead of (D.2) we have

$$-k \frac{\partial T}{\partial z} = \frac{Q}{\pi\sqrt{a^2-x^2}} \qquad \text{at } z = 0 \quad -a<x<a \qquad (D.8a)$$

$$-k \frac{\partial T}{\partial z} = 0 \qquad \text{at } z = 0 \quad a<x<-a \qquad (D.8b)$$

Relation (D.8a) approximates condition of constant temperature over the contact area. (More about this will be said later in this Appendix)

Expression (D.5) is still valid and $C_n$ will be determined by imposing boundary condition (D.8 ).

Since the following is true

$$\int_o^a \frac{\cos(\alpha x)}{\sqrt{a^2-x^2}} dx = \int_o^{\pi/2} \cos(\alpha a \sin \omega)\, d\omega = \frac{\pi}{2} J_o (\alpha a)$$

one may derive from (D.8 ) and (D.5) the following

$$C_n = \frac{Q}{nk\pi} J_o (n\pi\frac{a}{b})$$

or after substitution

$$T = -\frac{Q}{2kb}z + \frac{Q}{k\pi}\sum_{n=1}^{\infty} e^{-n\pi\frac{z}{b}} \frac{J_o(n\pi\frac{a}{b})\cos(n\pi\frac{x}{b})}{n} \qquad (D.9)$$

The thermal contact resistance per unit length of the strip has been found from (D.9) to be

$$R = \frac{1}{k\pi^2}\left(\frac{b}{a}\right)\sum_{n=1}^{\infty}\frac{1}{n^2} J_o(n\pi\frac{a}{b}) \sin\left(n\pi\frac{a}{b}\right) \qquad (D.10)$$

D.3 The use of the Schwarz-Christoffel transformation

From the fact that this Appendix deals with the two dimensional steady flow in the region bounded by a polygon, one may conclude that it is possible to use Schwarz=Christoffel transformation to obtain the solution. In the following we will use the mentioned transformation only to justify the statement that boundary condition (D.8a) represents very good approximation for the condition of constant temperature over the contact area.

In Fig: 7a, in the complex W=plane which comprises our problem (one can easily see the correspondence from Fig: 2b and Fig: 7a).

We consider heat flow restricted between two parallel planes, namely $v = 0$ and $v = b$, for the case of a heat source at $u = -\infty$ and a heat sink at $u = +\infty$. At $u = 0$ from $v = 0$ to $v = b-a$ there is a non-conducting partition.

The above flow may be transformed into the flow in the complex s-half plane (Fig;7b) by the use of the following transformation [10].

$$W = \frac{b}{\pi} \ln\left[\frac{f + (s^2 - d^2)^{1/2}}{f - (s^2 - d^2)^{1/2}}\right] \qquad (D.11)$$

where

$$f \equiv \cos\left(\frac{\pi}{2}\frac{b-a}{b}\right) = \sin\frac{\pi}{2}\frac{a}{b}$$

$$d \equiv \sin\left(\frac{\pi}{2}\frac{b-a}{b}\right) = \cos\frac{\pi}{2}\frac{a}{b}$$

The inverse of (D.11) being

$$S = [d^2 + f^2 \tanh^2 \frac{w\pi}{2b}]^{1/2} \qquad (D.12)$$

S-plane can be transformed into $\zeta$-plane

$$S = \frac{1 + \zeta}{1 - \zeta}, \quad \text{with its inverse}$$

$$\zeta = \frac{S - 1}{S + 1} \qquad (D.13)$$

The complex potential for the case of a sink in $\zeta$-half plane

$$\phi(\zeta) = \frac{Q}{2\pi k} \ell n \zeta \qquad (D.14)$$

where strength of the sink is $-Q/2$ and Q has the same meaning as in section 1 and 2.

By successive substitution of (D.13) and (D.12) into (D.14), the complex potential for the heat flow described in Fig:5a was determined to be

$$\phi(w) = \frac{Q}{2\pi k} \ell n \left\{ \frac{[d^2 + f^2 \tanh^2 \frac{w\pi}{2b}]^{1/2} + 1}{[d^2 + f^2 \tanh^2 \frac{w\pi}{2b}]^{1/2} - 1} \right\} \qquad (D.15)$$

From the above follows

$$T = \mathrm{Re}\,[\phi(w)] \qquad (D.15a)$$

Instead of using (D.15a) for obtaining the exact expression for the case considered in section 2, we will exploit (D.15) only for checking the reliability of the approximation made by (D.8a) i.e.

$$-\left(\frac{\partial T}{\partial z}\right)_{z=o} = \frac{Q}{\pi k b}\left[\left(\frac{a}{b}\right)^2 - \left(\frac{x}{b}\right)^2\right]^{-1/2}$$

After differentiation of (D.15) and certain rearrangement we can write

$$-\left(\frac{\partial T}{\partial z}\right)_{z=o} = \mathrm{Re}\left[\frac{d\phi(w)}{dw}\right]_{w=iv} =$$

$$= \frac{Q}{\pi k b} \frac{\pi}{2} \frac{\sin\left(\frac{v\pi}{2b}\right)}{\left[\sin^2\left(\frac{v\pi}{2b}\right) \sin^2\left(\frac{\pi a}{2b}\right) - \cos^2\left(\frac{v\pi}{2b}\right) \cos^2\left(\frac{\pi a}{2b}\right)\right]^{1/2}}$$

for b>v>b-a.

Introducing the relation v = b-x, simplifying and developing corresponding terms in series, one may proceed as shown below:

$$-\left(\frac{\partial T}{\partial z}\right)_{z=o} = \frac{Q}{\pi kb}\,\frac{\pi}{2}\left[\sin^2\frac{\pi a}{2b} - \cos^2\frac{\pi a}{2b}\,\tan^2\frac{\pi x}{2b}\right]^{-1}/2 =$$

$$= \frac{Q}{\pi kb}\left\{\left(\frac{a}{b}\right)^2 - \left(\frac{x}{b}\right)^2 - \left(\frac{\pi}{2}\right)^2\left[\frac{1}{3}\left(\frac{a}{b}\right)^4 + \frac{2}{3}\left(\frac{x}{b}\right)^4 - \left(\frac{a}{b}\right)^2\left(\frac{x}{b}\right)^2\right]+\ldots\right\}^{-1/2}$$

$$= \frac{Q}{\pi kb}\left[\left(\frac{a}{b}\right)^2 - \left(\frac{x}{b}\right)^2 + O\left(\frac{a^4}{b}\right)\right]^{-1/2} \text{ for } -a<x<a \qquad \text{(D.16)}$$

From expression (D.16) it follows that in order to approximate condition T = const. over the contact area, the use of (D.8a) is permissible.

APPENDIX E

CONTACT RESISTANCE FOR A SEMI-INFINITE RECTANGULAR PARALLELEPIPED

In this Appendix we will limit ourselves only to the consideration of the case when heat is supplied at constant rates over the contour area (Fig:3b).

The reasons for this are as follows

(i) The situation related to the geometry considered here primarily arises in connection with heat flow through a contour area. Since the contour area, by definition, is the area inside which all contact points are distributed, the condition over the area depends mainly on the character of this distribution. For the uniform distribution through each point passes the same amount of heat and consequently it might lead to (not completely justified) conclusion that the heat flux over the contour area is constant;

(ii) Even in the case when the actual situation over the contour area is different than that of constant heat flux, and approaches condition of constant temperature, the prediction for the thermal resistance obtained by either of the methods will be reliable due to the very small difference between the results of the two methods (as it was evident in the previous Appendix).

With reference to Fig: 3b, the problem is defined by the following relation:

$$\nabla^2 T = 0 \qquad \text{(E.1)}$$

$$\left.\begin{aligned} -k\left(\frac{\partial T}{\partial z}\right) &= \frac{Q}{4ad} \quad \text{at } z = 0 \quad -a<x<a,\ -d<y<d \\ -k\left(\frac{\partial T}{\partial z}\right) &= 0 \quad \text{at } z = 0 \quad a<x<-a,\ d<y<-d \end{aligned}\right\} \qquad \text{(E.2)}$$

$$-k\left(\frac{\partial T}{\partial x}\right) = 0 \quad \text{for } x = \pm b \tag{E.3}$$

$$-k\left(\frac{\partial T}{\partial z}\right) = 0 \quad \text{for } y = \pm c \tag{E.4}$$

$$-k\left(\frac{\partial T}{\partial z}\right) = \frac{Q}{4bc} \quad \text{as } z \to \infty \tag{E.5}$$

The solution of (E.1) which satisfies (E.3),(E.4) and (E.5) is expressible as

$$T = -\frac{Q}{4kbc} z + \sum_{n=1}^{\infty} C_{no} e^{-\frac{n\pi}{b} z} \cos\left(\frac{n\pi}{b} x\right) + \sum_{m=1}^{\infty} C_{om} e^{-\frac{m\pi}{c} z} \cos\left(\frac{m\pi}{c} y\right) + \sum_{n=1}^{\infty}\sum_{m=1}^{\infty} C_{nm} e^{-z\sqrt{\left(\frac{n\pi}{b}\right)^2 + \left(\frac{n\pi}{c}\right)^2}} \cos\left(\frac{n\pi}{b} x\right) \cos\left(\frac{m\pi}{c} y\right) \tag{E.6}$$

From (E.6) (after taking $\frac{\partial T}{\partial z}$ and evaluating at $z = 0$), (E.2) and the orthogonal properties of the trigonometric function, it follows

$$\frac{Q}{4ad} \frac{b}{n\pi} d \sin\left(\frac{n\pi a}{b}\right) = k C_{no} \frac{n\pi}{b} \frac{bc}{2}$$

$$\frac{Q}{4ad} \frac{c}{m\pi} a \sin\left(\frac{m\pi d}{c}\right) = k C_{om} \frac{m\pi}{c} \frac{bc}{2}$$

$$\frac{Q}{4ad} \frac{c}{m\pi} \frac{b}{n\pi} \sin\left(\frac{m\pi}{c} d\right) \sin\left(\frac{n\pi}{b} a\right) = k C_{nm} \sqrt{\left(\frac{n\pi}{b}\right)^2 + \left(\frac{m\pi}{c}\right)^2} \frac{cb}{y}$$

or

$$C_{no} = \frac{Qb}{2k\pi^2 ac} \frac{\sin\left(\frac{n\pi}{b} a\right)}{n^2}$$

$$C_{om} = \frac{Qc}{2k\pi^2 db} \frac{\sin\left(\frac{m\pi}{c} d\right)}{m^2} \tag{E.7}$$

$$C_{nm} = \frac{Q}{k\pi^2 ad} \frac{\sin\left(\frac{n\pi}{b} a\right) \sin\left(\frac{m\pi}{c} d\right)}{nm\sqrt{\left(\frac{n\pi}{b}\right)^2 + \left(\frac{m\pi}{c}\right)^2}}$$

Substitution of (E.7) into (E.6) determines the temperature distribution as

$$T = -\frac{Q}{4kbc} z + \frac{Q}{2k\pi^2}\left[\frac{b}{ac} \sum_{n=1}^{\infty} e^{-\frac{n\pi}{b} z} \frac{\sin\left(\frac{n\pi}{b} a\right) \cos\left(\frac{n\pi}{b} x\right)}{n^2} +\right.$$

$$+ \frac{c}{db} \sum_{m=1}^{\infty} e^{\frac{-m\pi}{c} z} \frac{\sin\left(\frac{m\pi}{b} d\right) \cos\left(\frac{m\pi}{c} y\right)}{m^2} \Bigg] +$$

$$+ \frac{Q}{k\pi^2 ad} \sum_{n=1}^{\infty} \sum_{m=1}^{\infty} e^{-z\sqrt{\left(\frac{n\pi}{b}\right)^2 - \left(\frac{m\pi}{c}\right)^2}} \frac{\sin\left(\frac{m\pi}{c} d\right) \sin\left(\frac{n\pi}{b} a\right) \cos\left(\frac{m\pi}{c} y\right) \cos\left(\frac{n\pi}{b} x\right)}{mn\sqrt{\left(\frac{n\pi}{b}\right)^2 + \left(\frac{m\pi}{c}\right)^2}}$$

the mean temperature over the contour area, and consequently the thermal contact resistance is immediately obtainable from the above expression

$$R = \frac{1}{2k\pi^3} \left[ \frac{b^2}{ca^2} \sum_{n=1}^{\infty} \frac{\sin\left(\frac{n\pi}{b} a\right)}{n^3} + \frac{c^2}{bd^2} \sum_{m=1}^{\infty} \frac{\sin^2\left(\frac{m\pi}{c} d\right)}{m^3} \right]$$

$$+ \frac{bc}{k\pi^4 a^2 d^2} \sum_{n=1}^{\infty} \sum_{m=1}^{\infty} \frac{\sin^2\left(\frac{n\pi}{b} a\right) \sin^2\left(\frac{m\pi}{c} d\right)}{n^2 m^2 \sqrt{\left(\frac{n\pi}{b}\right)^2 + \left(\frac{m\pi}{c}\right)^2}} \qquad \text{(E.8)}$$

It is easy to verify that relation (D.7) found in the previous Appendix is only special case of (E.8) namely for c = d.

Since in practice the shape of the contour area will be elliptic instead of rectangular one (as it was assumed here), we checked possible error due to such an assumption by comparing contact resistance for two cases: for a square bar with the concentric contour area and a circular cylinder with a concentric circular contour area. For both cases the cross-sectional area and the ratio between the contour area and the cross-sectional area were the same (for example considered square root of the ratio was equal 0.1); the agreement of comparison was satisfactory: 3.5% discrepancy.

Based on this, we might expect that the application of relation (E.8) to a case when the contour area has an elliptic shape, will not produce substantial error.

APPENDIX F

THERMAL RESISTANCE FOR A CONTACT IN A FLUID ENVIRONMENT

The model adopted for an elementary heat channel for the case treated here is given in Fig: 3a. Direct contact exists over the area $\pi a^2$ which is under a constant temperature $T_c$. For r>a a fluid is present in the gap. We denote with $\delta_1$ the mean distance (mean with respect to volume) between the solid and isothermal plane specified by the temperature $T_c$ ($T_c$ is not prescribed temperature, it stands only as an abreviation for a temperature at the contact area).

Considering only the solid (and assuming that it is permissible to treat the surface at z = 0 as a flat surface) one can seek the solution for the temperature distribution from the relations given in Appendix B, namely from (B.1), (B.3),(B.4) and (B.5), whereas, instead of (B.2) as the boundary condition at z = 0 we now have

$$T = \text{const} = T_c \quad \text{at } z = 0 \quad o \leq r < a \tag{F.1a}$$

$$-k\left(\frac{\partial T}{\partial z}\right) = \frac{k_f}{\delta}\,(T_c - T) \quad \text{at } z = 0 \quad a < r < b \tag{F.1b}$$

where $k_f$ is an equivalent conductivity of the fluid (taking into account all effects present in the gap).

The temperature distribution which is the solution of (B.1) and satisfies boundary conditions (B.3),(B.4) and (B.5) has the form of (B.8)

$$T = -\frac{Q}{\pi k b}\, z + \sum_{n=1}^{\infty} C_n e^{-\alpha_n z} J_o(\alpha_n r) \tag{F.2}$$

with

$$J_1(\alpha_n b) = 0 \tag{F.3}$$

where $C_n$ has to be determined from (F.1).

We will continue with our problem of estimating the thermal contact resistance for this case without obtaining the temperature distribution

by proceeding as follows.

First we will notice that expression (F.2) together with (F.3) defines the zero reference temperature as the mean temperature over area $\pi b^2$ at $z = 0$ (notice that the above conclusion holds regardless of what we would get for $C_n$). Consequently, by virtue of (B.17) follows the expression for the contact resistance:

$$R = \frac{T_c}{Q} \tag{F.4}$$

Furthermore, we may write

$$\int_0^a Trdr + \int_a^b Trdr = 0 \quad \text{at } z = 0 \tag{F.5}$$

or $$\int_a^b Trdr = -\frac{T_c a^2}{2}$$

Next we divide the total amount of heat passing through the surface $z = 0$ in the two parts:

$$Q = Q_1 + Q_2$$

where $Q_1$ stands for the amount passing through the solid contact area $\pi a^2$ and $Q_2$ represents the amount transferred through the fluid.

From (F.1b) and (F.5) one can express $Q_2$ as

$$Q_2 = 2\pi \int_a^b -k \left(\frac{\partial T}{\partial z}\right)_{z=0} rdr = 2\pi \frac{k_f}{\delta} \int_a^b (T_c - T)\, rdr =$$

$$= 2\pi \frac{k_f}{\delta_1} \left[ T_c \frac{b^2-a^2}{2} + T_c \frac{a^2}{2} \right] \quad \text{i.e.}$$

$$Q_2 = T_c \frac{k_f}{\delta_1} \pi b^2 \tag{F.6}$$

The expression for the thermal resistance (F.4) now acquires a new form

$$R = \frac{T_c}{Q_1 + Q_2} = \frac{1}{Q_1/T_c + \frac{k_f}{\delta_1} \pi b^2} \tag{F.7}$$

In order to estimate the value of $Q_1/T_c$ we will consider, see Fig;3b, the body of revolution specified by the streamline e-f which separates the part of the cylinder through which flows amount of heat $Q_1$. Far away from surface z = 0, where the streamlines are parallel, one can relate the distance of the streamline e-f from the axis of the cylinder, $b_1$ to the radius of the cylinder b, by using (F.6) as

$$\lambda^2 \equiv \frac{b^2}{b_1^2} = \frac{Q_1 + Q_2}{Q_1} = 1 + \frac{T_c}{Q_1} \frac{kf}{\delta_1} \pi b^2 \qquad (F.8)$$

Approximating the body of revolution, which confines the amount of heat $Q_1$, with the cylinder of radius $b_1$, treating the latter as in a vacuum (since the streamline e-f for the body of revolution represents the adiabatic wall), and using the results of Appendix B, one may write (from (B.14) and ( B.19))

$$\frac{T_c}{Q_1} = \frac{4}{\pi ka} \phi_1\left(\frac{a}{b_1}\right) = \frac{\phi}{\pi ka} \phi_1\left(\frac{a}{b}\lambda\right) \qquad (F.9)$$

From (F.8) and (F.9) it follows

$$\lambda^2 = 1 + \frac{4}{ka} \frac{k_t}{\delta_1} b^2 \phi_1\left(\frac{a}{b}\lambda\right) \qquad (F.10)$$

(F.10) implicitly determines $\lambda$. Due to the linear character of $\phi_1$ one can solve (in the range $0 \leq \frac{a}{b}\lambda \leq 0.6$) explicitly for $\lambda$. So linearizing $\phi$ by using (B.22a) (F.10) changes to

$$\lambda^2 + \left(\frac{kf}{\delta_1} \frac{b}{k}\right)\lambda - \left[1 + \frac{\pi}{4}\left(\frac{b}{a}\right)\left(\frac{kfb}{k_1\delta_1}\right) - 1\right] = 0$$

From which

$$\lambda = \sqrt{1 + \frac{1}{4} m_1^2 + \frac{\pi}{4}\left(\frac{b}{a}\right)m_1} - \frac{1}{2}m_1 \qquad (F.11)$$

where

$$m_1 \equiv \frac{bk_f}{\delta_1 k}$$

Knowing $\lambda$, the expression for thermal contact resistance follows from (F.7) and (F.9) as

$$R = \frac{1}{\frac{\pi k a}{4\phi_1(\frac{a}{b}\lambda)} + \frac{kf}{\delta_1}\pi b^2} \qquad (F.12)$$

To make (F.12) more useful for practical applications, we will consider two cylinders in contact with a fluid in the gap (Fig:3a).

Let the respective thermal conductivities of the two materials be denoted with $k_1$ and $k_2$. From (F.8) it is obvious that $\lambda_1 = \lambda_2 = \lambda(=\frac{b}{b_1})$. As a consequence of the above, from (F.11) follows $m_1 = m_2$, i.e.

$$\delta_1 k_1 = \delta_2 k_2 \qquad (F.13)$$

Relation (F.13) specifies the position of the isothermal plane $T_c$ in the gap.

Let $$k_s \equiv \frac{2k_1k_2}{k_1+k_2} \quad \text{and} \quad \delta \equiv \delta_1 + \delta_2$$

then from (F.13)

$$\delta_1 k_1 = \delta_2 k_2 = \frac{\delta k_s}{2} \qquad (F.13a)$$

Hence one can obtain from (F.11) $\lambda$ without knowing separately $\delta_1$ or $\delta_2$ as

$$\lambda = \sqrt{1 + m^2 + \frac{\pi}{2}(\frac{b}{a})\, m} \quad - m \qquad (F.14)$$

with $$m \equiv \frac{bk_f}{\delta k_s}$$

The total contact resistance, for the two cylinders together, may be written now as

$$R = R_1 + R_2 = \frac{1}{\frac{\pi k_1 a}{4\phi_1(\frac{a}{b}\lambda)} + \frac{k_f}{\delta_1}\pi b^2} + \frac{1}{\frac{\pi k_2 a}{4\phi_1(\frac{a}{b}\lambda)} + \frac{k_f}{\delta_2}\pi b^2}$$

with

$\delta_1 = \frac{\delta k_s}{2k_1}$ and $\delta_2 = \frac{\delta k_s}{2k_2}$, the relation for $R_c$ simplifies into

$$R = \frac{k_1 + k_2}{k_1 k_2 \left(\frac{\pi a}{4\phi_1(\frac{a}{b}\lambda)} + 2\frac{k_f}{\delta k_s}\pi b^2\right)} = \frac{1}{\frac{k_s a}{8\phi_1(\frac{a}{b}\lambda)} + \frac{k_f}{\delta}\pi b^2} \qquad \text{(F.15)}$$

The thermal contact conductance per unit area can be found from (F.15) as

$$h_c = \frac{(a/b)k_s}{8b\phi(\frac{a}{b}\lambda)} + \frac{k_f}{\delta} \qquad \text{(F.16)}$$

(F.16) now is in the form suitable for direct application since one determined $\lambda$ from (F.14), $\phi$ from Fig: 3(or from the linearized form: $\phi(\frac{a}{b}\lambda) = \frac{\pi}{16} - \frac{\lambda}{4}(\frac{a}{b})$) and b from the relation $\pi b^2 = \frac{1}{n}$, where n is the number of contact points per unit of the contour area. Of course, $h_c$ for vacuum conditions is only the special case of (F.16) when $k_f = 0$ and $\lambda = 1$.

APPENDIX G

ESTIMATION OF MEAN PRESSURE OVER CONTACT AREA

In order to estimate the mean pressure over the contact area we will consider a model which consists of two rough, nominally flat surfaces made of the same material with Poison's ratio $\upsilon = 0.3$. The irregularities on the surfaces are approximated by spherical caps. Furthermore, it will be assumed that for each point of contact we have two spherically shaped asperities with the same radius of curvature R in symetric contact (Fig: 19a).

After the moment when two asperities just touch each other, any relative approach between the two asperities of $\Delta C$ will produce, by the Hertz theory [48], the normal force

$$F = \frac{E}{1.934} (\Delta C)^{3/2} R^{1/2} \qquad (G.1)$$

and the area of contact

$$\pi a^2 = \pi \frac{\Delta C \, R}{2} \qquad (G.2)$$

where E represents Young's modulus of elasticity, and R the radius of curvature. Relations (G.1) and (G.2) are applicable provided that plastic flow did not occur. If $\Delta C$ is large enough so that the mean pressure over the contact area reaches the value of 1.1Yo, i.e.

$$P_m = 1.1Yo$$

the elastic limit will be just exceeded at the point $z \simeq 0.5a$ due to the shear stress at that point ([47]). (z is measured from the center of the contact in the normal direction). Yo is the initial elastic limit of the material found in pure tension.

When the mean pressure reaches the value of approximately 3Yo, the whole region of contact is flowing plastically. Theoretically

([51],[52]) it was shown that further increase in $\Delta C$ will not change the mean pressure over the contact area. The above conclusion is subject to limitation ([47]) if the deformed area is comparable with the size of the specimens and if there is work-hardening of the material during the contact.

Based on the above known relation, namely: (G.1) and (G.2) for elastic deformation, the mean pressure for which onset of plasticity will occur, the behavior of the material when the full plastic flow is reached, together with some relations from the surface analysis, one may estimate the mean pressure over the contact area.

From (G.1) and (G.2) it follows

$$P_m = \frac{F}{\pi a^2} = \frac{2}{1.934} \frac{E}{\pi} \left(\frac{\Delta C}{R}\right)^{1/2} \qquad (G.3)$$

The radius of curvature R can be approximated with

$$R = \frac{h}{2 \tan^2\theta}$$

where h being the height of the asperity and $\tan\theta$ the mean absolute slope of the surface profile (defined in Ch.III). Substitution of R in (G.3) and rearrangement will yield

$$\frac{\Delta C}{h} = 0.467 \left(\frac{\pi P_m}{\tan\theta E}\right)^2 \qquad (G.4)$$

the value of $\left(\frac{\Delta C}{h}\right)_Y$ - for which the material will just start to flow plastically, could be found from (G.4) by setting $P_m = 1.1Yo$. Using the data for stainless steel (303) for $\frac{Yo}{E}$ ($= 4.4 \times 10^{-3}$) and taking $\tan\theta = 0.1$ (that has been the minimum value we dealt with) it was obtained

$$\left(\frac{\Delta C}{h}\right)_Y = 1.1 \times 10^{-2} \qquad (G.5)$$

Considering now our model, we can conclude that if at a certain stage we had n - number of contacts per unit area, then after approaching the two surfaces closer by $(\Delta C)_Y$ all n contacts would experience plastic flow and only new contact points obtained in the process of approaching would be in elastic state.

From Ch.III (Eq. 3.9 ) the following relation holds

$$n = Ce^{-(y/\sigma)^2}$$

where C is a constant, y, the distance between the mean planes of the two surfaces in contact, and $\sigma$ is the standard deviation for the joined distribution ($\sigma = \sqrt{\sigma_1^2 + \sigma_2^2}$).

If one goes from $y_1$ to $y_2$ then as a consequence of the above, the percentage of the new contacts can be determined form the expression,

$$\frac{n_2 - n_1}{n_2} = 1 - e^{-[(\frac{y_1}{\sigma})^2 - (\frac{y_2}{\sigma})^2]} \qquad (G.6)$$

If we choose for our initial position the one for which $\varepsilon = (\frac{Ac}{A_a})^{1/2} = 0.02$ (i.e. $\frac{Ac}{A_a} = 0.0004$), and further estimate h by asserting

$$h(y) = \frac{y}{2}$$

(i.e. assuming that the sum of the heights of the two asperities just touching each other is equal, in average, to the distance between the mean planes), then after using Fig:10 to obtain $y_1/\sigma$, (G.6) will reveal that at the end of the approach $(\Delta C)_Y$ only 5% of all contacts will be in elastic state. Furthermore, the approach of $(\Delta C)_Y$ will produce the total increase of the contact area of 17% (from Fig:10), which together with the percentage of the new contacts allows us to conclude that not more than 0.85% of the total area in contact belongs to the new contacts.

For initial $\varepsilon$ is greater than that used here, the percentage of

the area for which the mean pressure is less than 1.1Yo will be still less due to the smaller $(y/\sigma)$ and the slower increase of the contact area for the same increment of $(\frac{\Delta C}{h})_Y$.

The immediate conclusion from the above analysis would be, that for the cases we are interested in, the amount of the contact area with the mean pressure less than 1.1Yo - the value which will produce onset of plasticity - is negligibly small. Although this information is significant it still does not tell us more about the value of the mean pressure than that it lies somewhere between 1.1Yo and 3Yo.

To achieve somewhat closer estimation than the previous one, we will proceed by making an assumption that the validity of relations (G.1) and (G.2) may be extended until the whole region of contact starts to flow plastically, i.e. until $P_m = 3Yo$. (Notice that although the assumption can be considered quite crude, since when the onset of plasticity occurs, both force F and the contact area will increase faster with an increase in $\Delta C$ than (G.1) and (G.2) predict, we use the above relations only in the form of the ratio (G.3) and hence, the overall effect of the inaccuracy will be smaller).

Setting $P_m = 3Y_o$ in (G.4) we obtain

$$(\frac{\Delta C}{h})_p = 8.2 \times 10^{-2}$$

Similarly as before, if we move the two surfaces closer for $(\Delta C)_p$ only the new contacts will have the mean pressure less than $3\ Y_o$.

Proceeding exactly as in the previous case, starting with $\varepsilon = 0.02$ it was obtained that at the end of the approach of $(\Delta C)_p$, less than 9% of the total contact area had the mean pressure less than $3Y_o$. Since, as it was found earlier, the amount of the contact area with the pressure less than $1.1Y_o$ is negligible, we may assume that the whole

9% of the contact area is at the pressure between $1.1Y_o$ and $3Y_o$. For the purpose of calculation we will take the mean pressure for this portion of the contact area to be $2Y_o$.

Let Ap stand for the part of the contact area for which the mean pressure is equal $3Y_o$; $A_c$ - the whole contact area, then we may write

$$P_m A_c = Ap\ 3Y_o + (A_c - Ap)\ 2Y_o \quad \text{or}$$

$$P_m = Y_o\ (2 + \frac{Ap}{A_c})$$

For the example we considered

$$P_m = 2.915\ Y_o \quad \text{or}$$

$$\epsilon^2 = (\frac{A_c}{Ap}) = \frac{p}{P_m} = 1.03\ \frac{p}{3Y_o}$$

where p is apparent pressure and $A_{ap}$ - the apparent area.

In the case when $\epsilon > 0.02$ the mean pressure calculated in the above manner would be closer to the value of $3Y_o$.

It is not difficult to change our rather artificial model (of two identical surfaces in contact) to more of a realistic one, consisting of the two surfaces with different characteristics and made of different materials.

For the latter case, the only modification in expressions (G.1) (G.2) and (G.3) would be

$$E = E_s = \frac{2E_1E_2}{E_1+E_2} \quad \text{and}$$

$$R = R_s = \frac{2R_1R_2}{R_1+R_2} = \frac{h_1}{\frac{h_1}{h_2}(\tan\Theta_2)^2 + (\tan\Theta_2)^2}$$

or taking, in average

$$\frac{h_1}{h_2} = \frac{\sigma_1}{\sigma_2} \quad \text{and} \quad h_1 + h_2 = y$$

$$R_s = \frac{y/(1+\sigma_2/\sigma_1)}{\frac{\sigma_1}{\sigma_2}(\tan\theta_1)^2 + (\tan\theta_2)^2}$$

where $y_1$, $\sigma_1$, $\sigma_2$ and $\tan\theta$ are already introduced in this Appendix.

One can proceed further similarly as in the former case, using the value for $Y_o$ of the softer material. The numerical result so obtained would depend on the particular combination of the surfaces, but essentially it should not differ considerably from the one already calculated.

APPENDIX H

EFFECTIVE CONTOUR AREA FOR SPHERICALLY WAVY ROUGH SURFACES IN CONTACT

Considering a spherically shaped body with an ideally smooth surface pressed on a rigid smooth plane (Fig:19c) one can obtain from the Hertz theory [37] the following relations from the displacement of the surface in the z direction due to the local deformation

$$w(r) = \frac{1}{2R}\left(\frac{D^2}{2} - r^2\right) \qquad r < D/2 \tag{H.1a}$$

and

$$w(r) = \frac{2}{\pi R}\int_0^{\sin^{-1}\left(\frac{D}{2r}\right)}\left(\frac{D^2}{4} - r^2\sin^2\Psi\right)\,d\Psi =$$

$$= \frac{D^2}{4\pi R}\left[\left(2 - \frac{4r^2}{D^2}\right)\sin^{-1}\left(\frac{D}{2r}\right) + \sqrt{\frac{4r^2}{D^2} - 1}\right]; r > D/2 \tag{H.1b}$$

where R is the radius of curvature and $D/2$ is the radius of contact.

The vertical distance between the surface of the body and the rigid plane for $r > \frac{D}{2}$ and $\frac{r}{R} << 1$ may be found from (H.1b) as

$$\delta(r) = \frac{1}{2R}\left\{r^2 - \frac{D^2}{2}\left[1 - \frac{1}{\pi}\left[\left(2 - \frac{4r^2}{D^2}\right)\sin^{-1}\left(\frac{D}{2r}\right) + \sqrt{\frac{4r^2}{D^2} - 1}\right]\right]\right\} \tag{H.2}$$

In the case of when two bodies with spherical waviness of the type shown in Fig: 19C are pressed together, the vertical distance between smooth surfaces beyond the contact area ($\frac{L}{2} > r > \frac{D}{2}$) can be expressed, by using (H.2) in the form

$$\delta(r) = \delta_1 + \delta_2 = \lambda^2_H d_t\left\{\left(\frac{\lambda}{\lambda_H}\right)^2 - 2\left\{1 - \frac{1}{\pi}\left[\left(2 - \frac{\lambda^2}{\lambda_H^2}\right)\sin^{-1}\left(\frac{\lambda_H}{\lambda}\right) + \sqrt{\frac{\lambda^2}{\lambda_H^2} - 1}\right]\right\}\right\} =$$

$$\equiv \lambda_H^2\, d_t\, g\left(\frac{\lambda}{\lambda_H}\right) \tag{H.3}$$

where g ($\lambda/\lambda_H$) is given graphically in Fig: 20,

$$\lambda \equiv \frac{2r}{L} \; ; \quad d_t \equiv d_1 + d_2 \qquad \text{and}$$

$$\lambda_H \equiv \frac{D}{L} = 1.285 \left[\left(\frac{p}{E_s}\right)\left(\frac{L}{2d_t}\right)\right]^{1/3} \tag{H.4}$$

where p is an apparent pressure given as

$$p = {}^{4F}/_{\pi L^2} \quad \text{and} \quad E_s = \frac{2E_1E_2}{E_1+E_2}$$

Extending now our attention to the case of wavy rough surfaces in contact, we will consider a model which can be obtained from the previous one by superimposing roughness on the smooth wavy surface (which we will call the mean surface). It will be further assumed that under the contact pressure, the mean surface will be deformed in the same manner as the smooth surface considered at the beginning of the section, i.e. it will be assumed that the relations (H.1a) and (H.1b) are specifying the deformation of the mean surface. Consequently, the mean surfaces of two rough surfaces in contact for $o \leq r \leq {}^{D}/L$ will be parallel and at a relative distance Y, where Y is a function of characteristics of the surfaces and the applied load. The vertical distance between the mean surfaces for $\frac{D}{2} \leq r \leq \frac{L}{2}$ is being now $[\delta(r) + Y]$.

The contact points will be spread not only over the area $\pi D^2/4$ (specified by (H4)) but also beyond that area. Since the distance between the mean surfaces will increase with an increase of r for $r > {}^{D}/2$, the density of contact points will decrease with an increase of r.

The number of contact points per unit area for $o \leq r \leq {}^{D}/2$ is given (from Eq. 3.9) with

$$n = C e^{-Y^2/\sigma^2} \tag{H.5a}$$

and for $\frac{D}{2} \leq r \leq \frac{L}{2}$

$$n(r) = C e^{-\left\{\frac{[Y+\delta(r)]^2}{\sigma^2}\right\}} \qquad \text{(H.5b)}$$

The effective radius of the contour area has been defined here by the relation:

$$n(D/2)\ (r_{eff}^2 - \frac{D^4}{4}) = 2 \int_{D/2}^{L/2} n(r) r dr \qquad \text{(H.6)}$$

Which states that if the effective area had the uniform density $n(D/2)$ it would contain all the contact points.

From (H.6), (H.5a) and (H.5b) one can obtain

$$\lambda_{eff}^2 = \lambda^2_H + 2 \int_{\lambda_H}^{1} e^{-\frac{\delta}{\sigma}(2\frac{Y}{\sigma} + \frac{\delta}{\sigma})} \lambda d\lambda \qquad \text{(H.7)}$$

with $\lambda_{eff} \equiv \frac{2r_{eff}}{L}$

Together with (H.3), (H.7) can be written as

$$\lambda^2_{eff} = \lambda^2_H + 2 \int_{\lambda_H}^{1} e^{-\frac{dt}{\sigma}\lambda^2_H\, g(\frac{\lambda}{\lambda_H})[2\,Y/\sigma + \frac{dt}{\sigma}\lambda^2_H\, g(\frac{\lambda}{\lambda_H})]} \lambda d\lambda \qquad \text{(H.8)}$$

## BIBLIOGRAPHY

1. Fenech, H. & Rohsenow, W.M., "Prediction of Thermal Conductance of Metallic Surfaces in Contact", ASME Transactions Paper No. 62-HT-32, Journal of Heat Transfer, September 1962.

2. Henry, J.J., "Thermal Contact Resistance", A.E.C. Report MIT-2079-2 June 1964.

3. Clausing, A.M. & Chao, B.T., "Thermal Contact Resistance in a Vacuum Environment". National Aeronautics and Space Administration, University of Illinois, ME-TN-242-1, August 1965.

4. Clausing, A.M., "Some Influences of Macroscopic Constrictions on the Thermal Contact Resistance", National Aeronautics and Space Administration, University of Illinois, ME-TN-242-2, April 1965.

5. Yovanovich, M.M., "Thermal Contact Conductance in a Vacuum", National Aeronautics and Space Administration, MIT, November 1965.

6. Centinkale, T.N. & Fishenden, Dr. Margaret, "Thermal Conductance of Metal Surfaces in Contact", International Conference on Heat Transfer, Institution of Mechanical Engineers, London, 1951.

7. Laming,L.C. "Thermal Conductance of Machined Metal Contacts," International Developments in Heat Transfer, ASME 1961.

8. Fried, E.,"Study of Interface Thermal Contact Conductance", NASA Document No. 645D652, May 1964.

9. Fried, E. "Study of Interface Thermal Contact Conductance", NASA Document No. 655D4395, March 1965.

10. Holm,R. "Electrical Contacts Handbook" Springer Verlag, Berlin 1958.

11. Weills, N.D. & Ryder, E.A., "Thermal Resistance Measurements of Joints Formed between Stationary Metal Surfaces".

12. Bloom, M.F. "Thermal Contact Conductance in a Vacuum Environment". Missile and Space Systems Division, Douglas Aircraft Company Report SM-47700, December 1964.

13. Held, W. "Heat Transfer between Worked Surfaces," Redstone Scientific Information Center - Transaction No. 76, October 1963.

14. Kouwenhoven, W.B. & Potter J.H. "Thermal Resistance of Metal Contacts" Journal of American Welding Society, Vol. 27, Part 2, 1949,

15. Barzelay, M.E., Tong, K.N. & Holloway, G.F., "Thermal Conductance of Contacts in Aircraft Joints", National Advisory Committee for Aeronautics, Technical Note 3167, March 1954.

16. Barzelay, M.E., Tong, K.N. & Holloway, G.F. "Effect of Pressure on Thermal Conductance of Contact Joints", National Advisory Committee for Aeronautics, Technical Note 3295, May 1955.

17. Boeschoten, F. & Van der Held, E.F.M., "Thermal Conductance of Contact between Aluminum and other Metals", Physica, Vol XXIII, 1957.

18. Barkan, P. & Tuohy, E.J., "A Contact Resistance Theory for Rough Hemispherical Silver Contacts in Air and in Vacuum", IEEE Transaction on Power Apparatus and Systems Vol. PAS-84, No. 12, December 1965.

19. Cordier, H., "Experimental Study of the Influence of Pressure on Contact Thermal Resistance", Redstone Scientific Information Center (RSIC-116) 1961.

20. Bory, C. & Cordier, H., "Resistances Thermiques de Contact", Journal de la Transmission de la Chaleur, Institut

21. Wheeler, R.G., "Thermal Conductance of Fuel Element Materials" AEC Report HW 60343, 1959 and HW 53598, 1957.

22. Fried, E. & Costello, F.A.,"Interface Thermal Contact Resistance Problem in Space Vehicles", ARS Journal, Vol. 32, No.2, 1963.

23. Aron, W. and Colombo, G.,"Controlling Factors of Thermal Conductance Across Bolted Joints in a Vacuum Environment", ASME paper No. 63-WA-196, August 26, 1963.

24. Rogers, G.F.C., "Heat Transfer at the Interface of Dissimilar Metals" International Journal of Heat and Mass Transfer, Vol. 2, 1961.

25. Stubstad, W.R., "Measurements of Thermal Contact Conductance in Vacuum", ASME Paper No. 63-WA-150, August 1, 1963.

26. Jacobs, R.B. & Starr, C., "Thermal Conductance of Metallic Contacts", Review of Scientific Instruments, Vol. 10, 1939.

27. Graff, W.J., "Thermal Conductance Across Metal Joints", Machine Design, Vol. 32, September 1960.

28. Minges, L.M. "Thermal Contact Resistance", Vol. I - A review of the literature:" Technical Report AFML-TR-65-375, Vol. I April 1966.

29. Berman, R. "Some Experiments on Thermal Contact at Low Temperatures", Journal of Applied Physics, Vol. 27, No. 4 April 1956.

30. Schmidt, E.H.W., & Jung, E. "Measurement of the Thermal Contact Resistance from Stainless Steel to Liquid Sodium", Modern Developments in Heat Transfer, Academic Press, New York, 1963.

31. Shlykov, Yu. P. & Ganin, E.A. "Thermal Contact Resistance", Atomnaya Energiya, Vol. 9, No. 6 December 1960.

32. Shylkov, Yu.P. & Ganin, E.A. "Experimental Study of Contact Heat Exchange", Redstone Scientific Informa;tion Center (RSIC-128) 1961.

33. Watson, G.N., "Theory of Bessel Function:" Cambridge, University Press 1922.

34. Gray, A. & Mathews, A.B., "Bessel Functions", London, Macmillan 1895.

35. Weber, "Ueber Besselsche Functionen", Crelle Bd. 75,74, 1873.

36. McLachlan, "Bessel Function", Oxford, Clarendon Press, 1955.

37. Sonin, N.I. "Issledovania o Tsilindricheskih Funktsiah", Gos. Izd-vo Tekh-teoret lit-ry Moskva, 1954.

38. Titchmarsh, E.C. "Fourier Integrals", Oxford, Clarendon Press 1948.

39. Carslaw, H.S., Jaeger, J.C. "Conduction of Heat in Solids", Oxford Clarendon Press, 1959

40. Middleton, D. "An Introduction to Statistical Communication Theory" New York, McGraw-Hill, 1960.

41. Crandall, S.H. "Zero-Crossings, Peaks and Other Statistical Measures of Random Responses", Journal of Acoustical Society of America, November 1962.

42. Crandall, S.H. "Random Vibration", John Wiley & Sons Inc. New York 1958.

43. Crandall, S.H. "Random Vibration" Volume 2, The MIT Press, Cambridge Mass., 1963.

44. Wadsworth, G.P. & Bryan, J.G., "Introduction to Probability and Random Variables", McGraw-Hill Book Co. Inc. New York, 1960.

45. Henry, J.J. & Fenech,H. "The Use of Analog Computer for Determining Surfaces Parameters Required for Prediction of Thermal Contact Conductance", ASME Paper No. 63-WA-104, Journal of Heat Transfer, September 1964.

46. Foster, E.T. "Prediction of Contact Population in Bimetallic Surface Junctions," MIT, M.S. Thesis, August 1964.

47.
Bowden, F.P. & Tabor, D. "Friction and Lubrication" New York, John Wiley & Sons Inc. 1956

48. Timoshenko, S. & Goodier, J.N., "Theory of Elasticity", McGraw-Hill 1951.

49. Kragelskii, I.V., "Friction and Wear", Butter worths, Washington 1965.

50. D'yachenco, P.E. et al., "The actual Contact Area between Touching Surfaces", Consultants Bureau, New York, 1964.

51. Hencky, H., Z.angew Math. Mech. 3,241, 1923.

52. Ishlinsky, A.J., J. Appl/Math.Mech (USSR) 8,233, 1944.

53. Archard, J.F. "Contact and Rubbing of Flat Surfaces" Journal of Applied Physics, Vol. 24 No. 8, Aug. 1953.

54. Archard J.F. "Elastic Deformation and the Laws of Friction", Research Correspondence, Vol. 9, 1956.

55. Archard, J.F. "Single Contacts and Multiple Encounters" Journal of Applied Physics, Vol. 32, No.8, Aug. 1961.

56. Greenwood, J.A. & Williamson, J.B.P., "The Contact of Nominally Flat Surfaces", Burndy Research Division, Research Report No. 15 July 1964.

57. Greenwood, J.A. & Tripp, J.H., "Elastic Contact of Rough Spheres".

58. Ling, F.F., "Some Factors Influencing the Area-Load Characteristics for Semi-smooth Contiguous Surfaces under Static Loading", ASME Paper No, 57-A-246, September 1957.

59. Ling, F.F., "On Asperity Distributions of Metallic Surfaces", Journal of Applied Physics, Vol. 29, No.8 August 1958.

60. Tsukizoe, T. Hisakado, T., "On Mechanism of Contact between Metal Surfaces - The Penetrating Depth and the Average Clearance", ASME Journal of Basic Engineering. September 1965.

61. Velissaropoulos, P.D., "Apparatus for Measurement of Contact Resistance", MIT, M.S. Thesis, Aug. 1965.

62. Ryerson Data Book, Joseph T. Ryerson and Sons Inc. 1960.

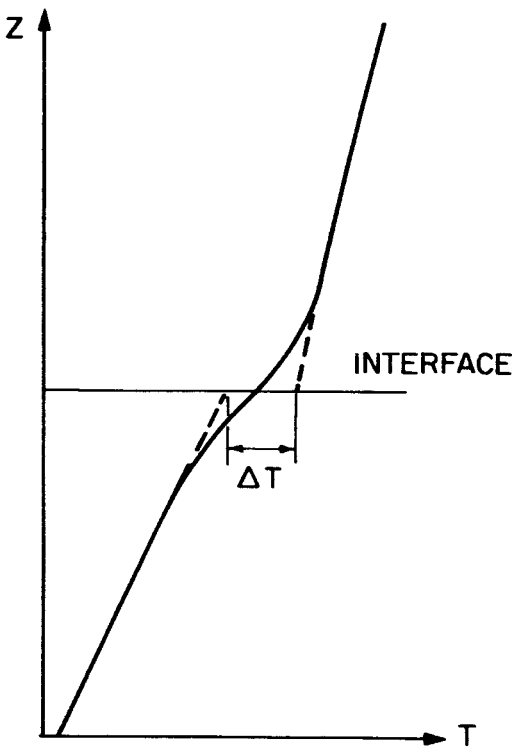


a) TEMPERATURE DISTRIBUTION

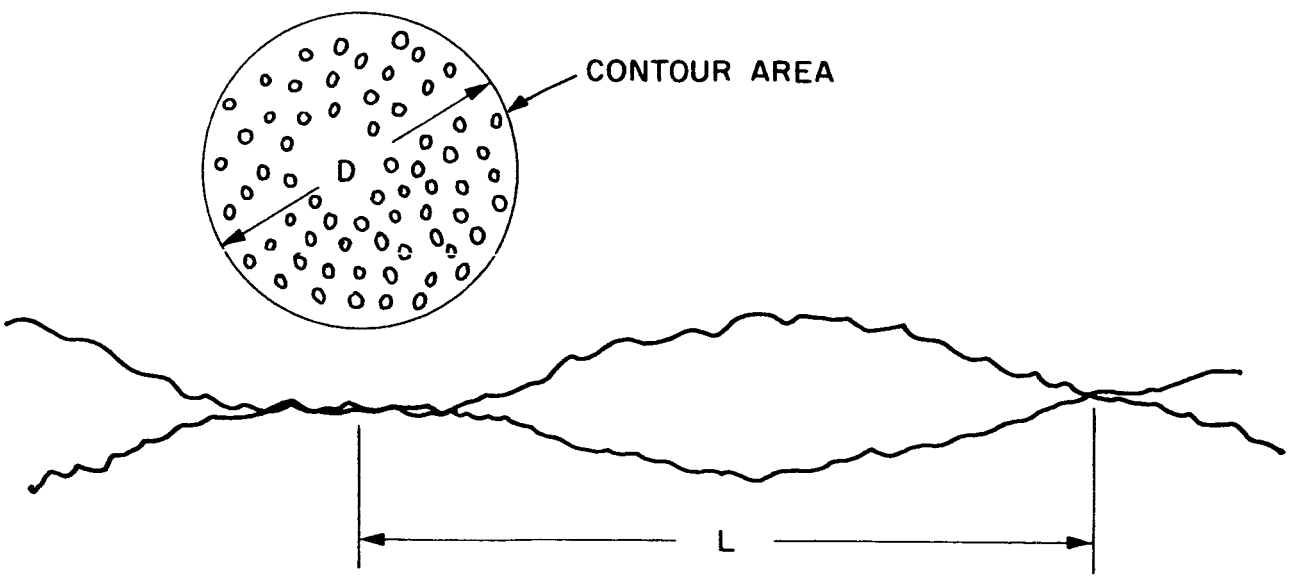


b) CONTOUR AREA (FOR CASE OF SPHERICAL WAVINESS)

FIG. 1 DEFINITIONS

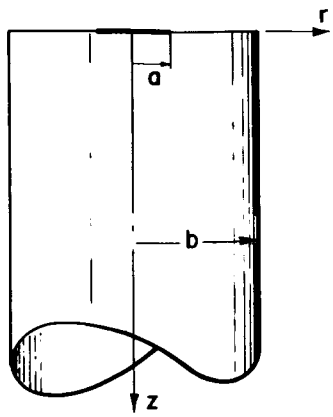


a) MODEL OF A CONTACT

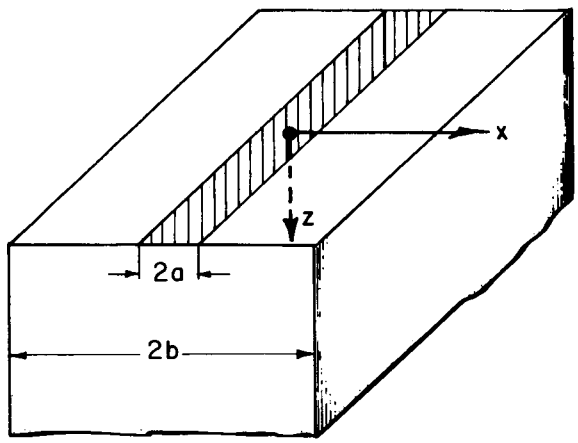


b) MACROSCOPIC HEAT CHANNEL FOR CYLINDRICAL WAVINESS IN ONE DIRECTIONS

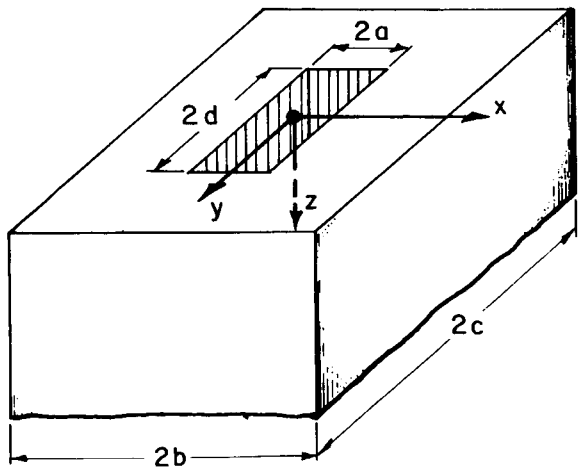


c) MACROSCOPIC HEAT CHANNEL FOR CYLINDRICAL WAVINESS IN TWO DIRECTIONS

FIG. 2 MODELS FOR HEAT CHANNELS

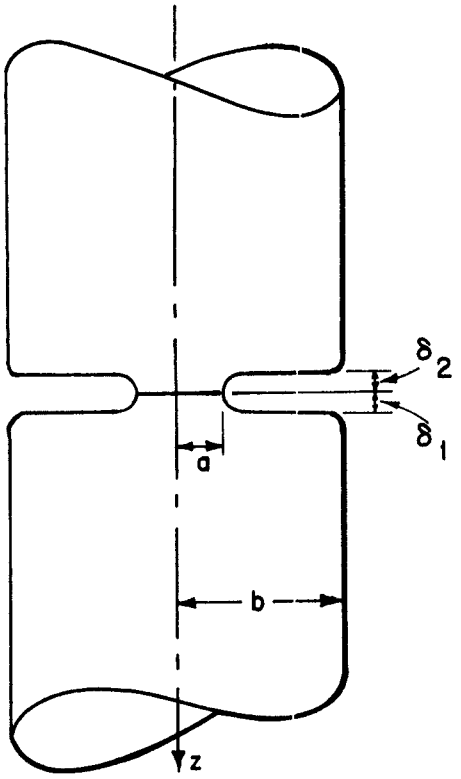


a) TYPICAL HEAT CHANNEL

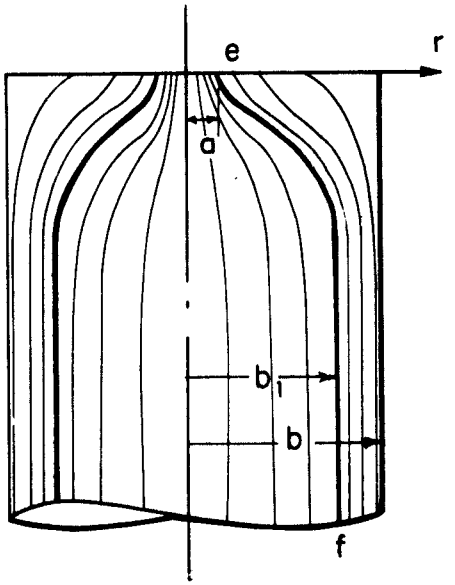


a) HEAT FLOW REPRESENTATION

FIG. 3 MODEL FOR A CONTACT IN A FLUID ENVIRONMENT

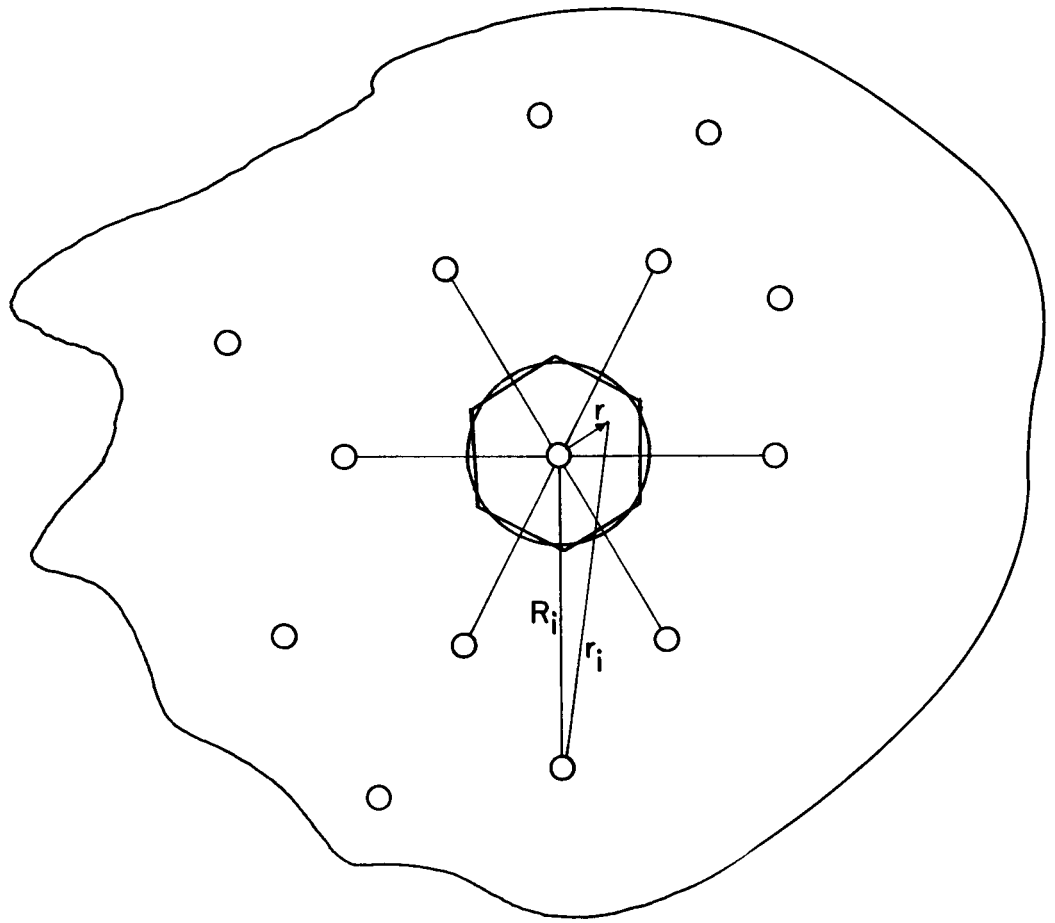


FIG. 4 CONTACT SPOTS DISTRIBUTION

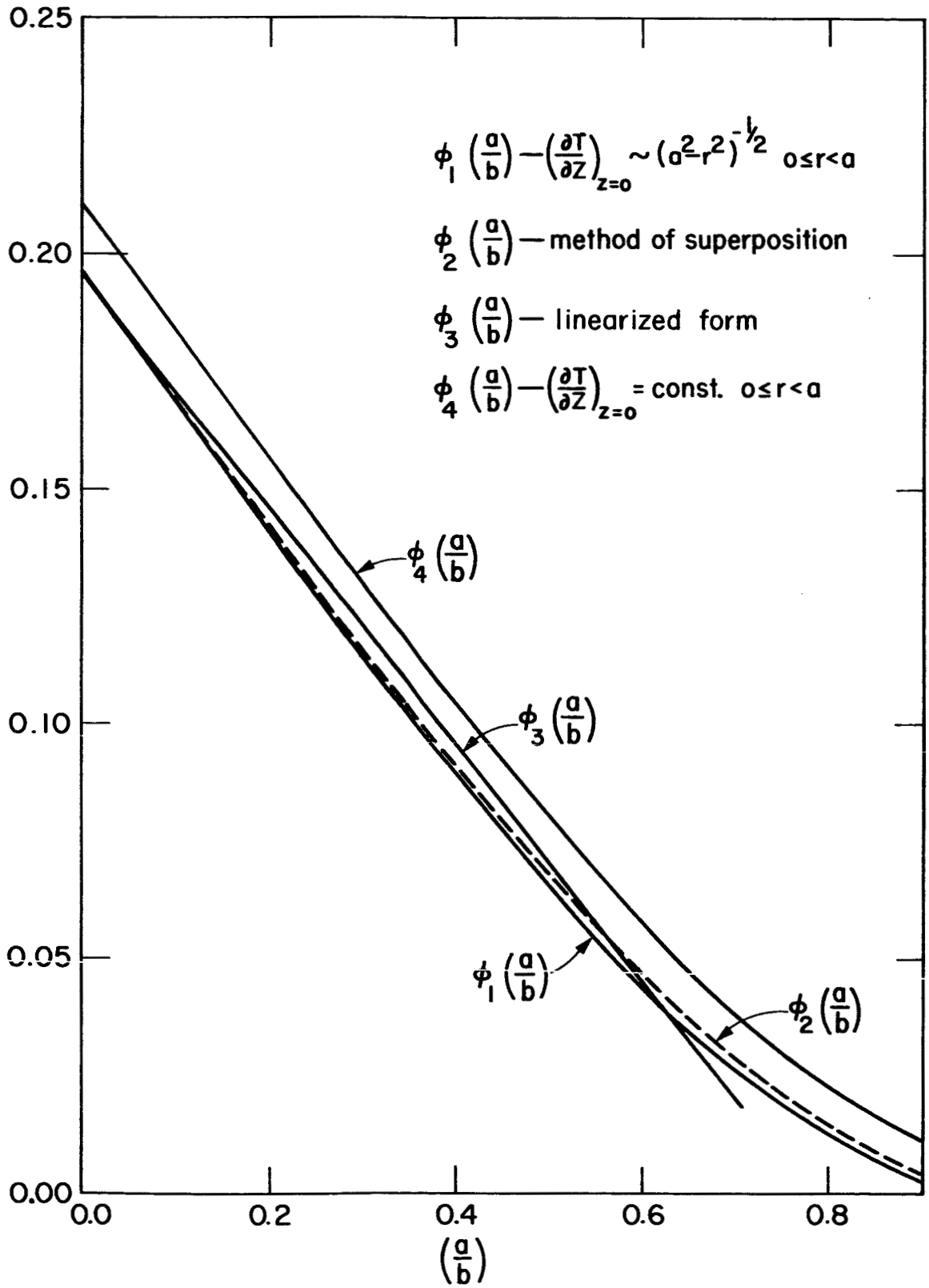


FIG. 5 CONTACT RESISTANCE FACTOR

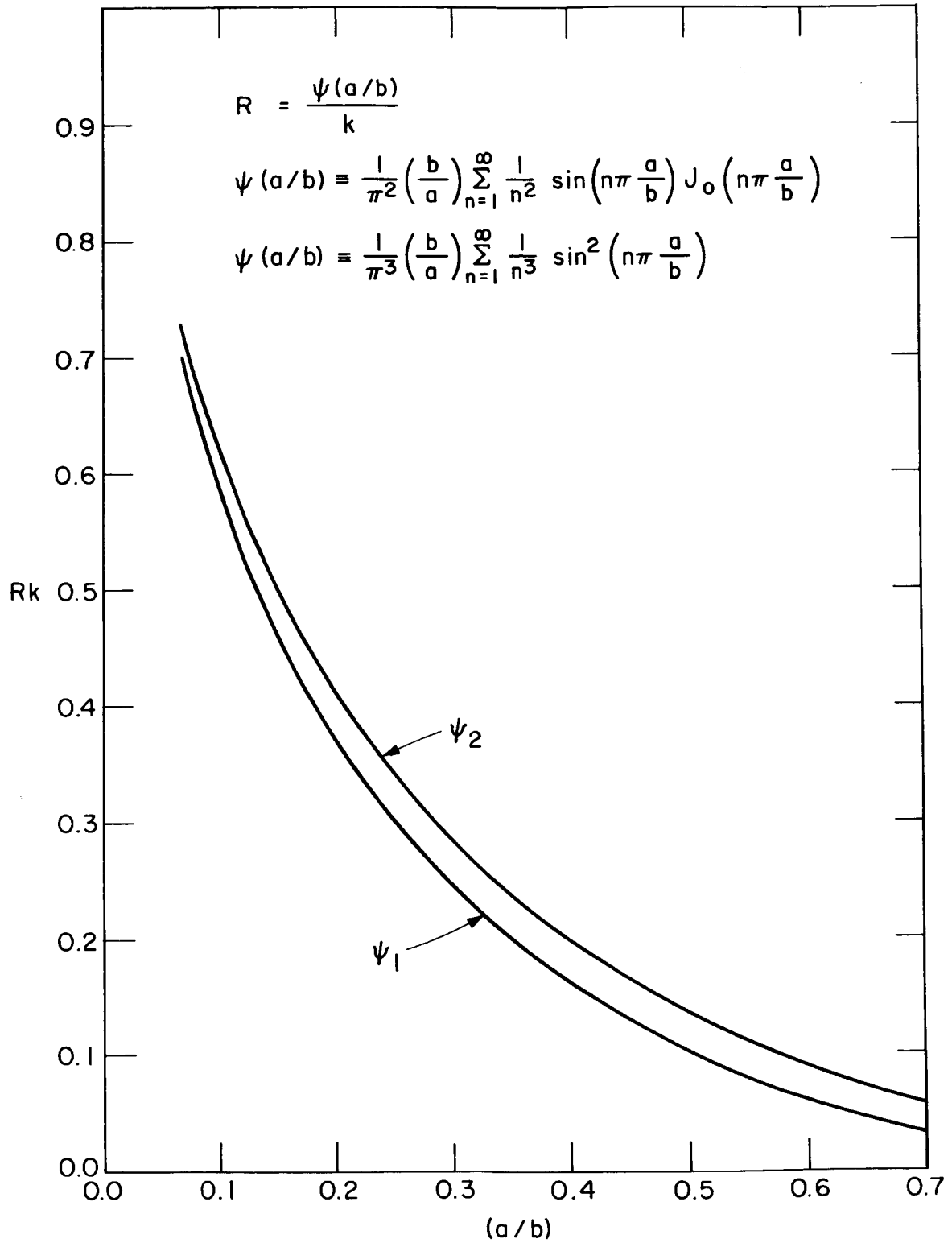


FIG. 6 CONTACT RESISTANCE FACTOR FOR CYLINDRICAL WAVINESS

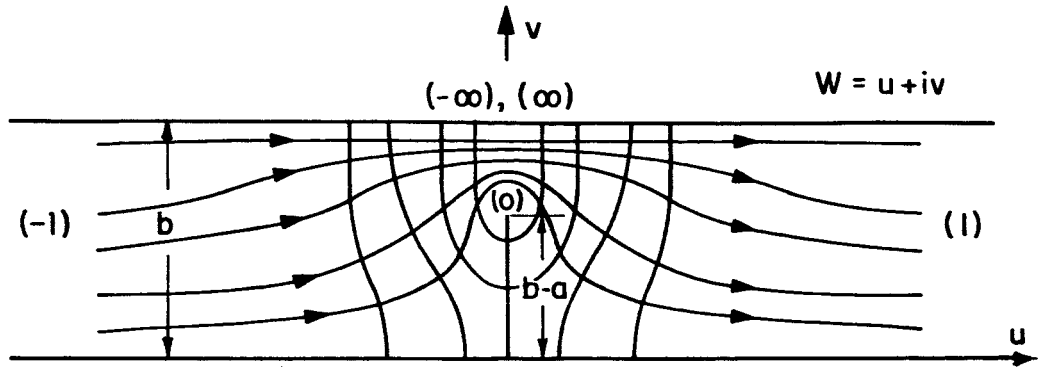


a) HEAT FLOW BETWEEN TWO PARALLEL PLANES WITH CONSTRUCTION OF FLOW AT U=0

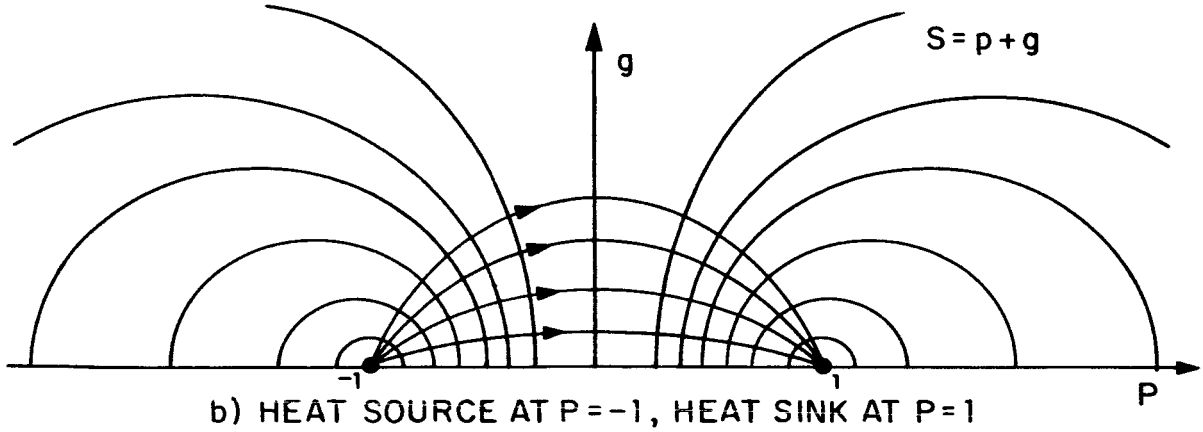


b) HEAT SOURCE AT P=-1, HEAT SINK AT P=1

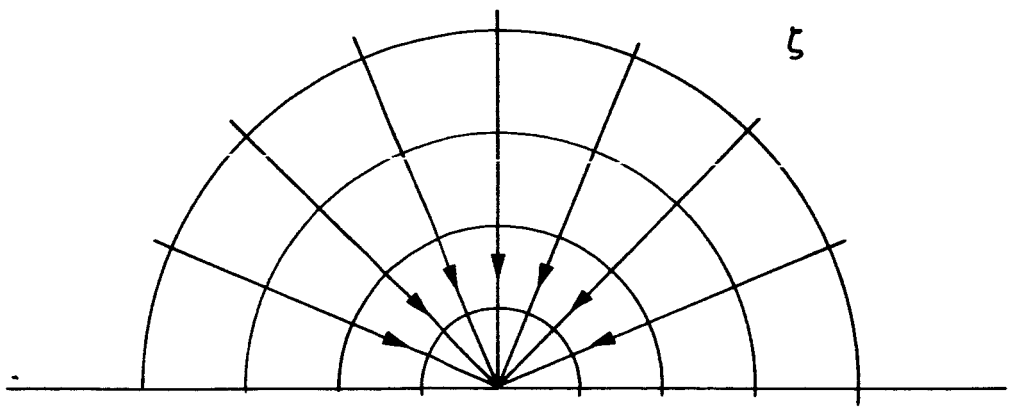


c) HEAT SOURCE AT $\zeta = \infty$ ; HEAT SINK AT $\zeta = 0$

FIG.7 TRANSFORMATIONS IN COMPLEX PLANE

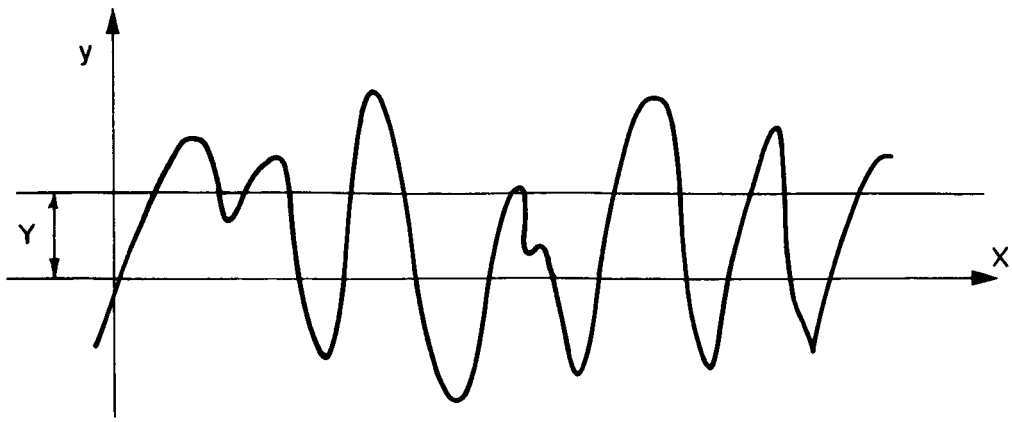


a) SURFACE PROFILE

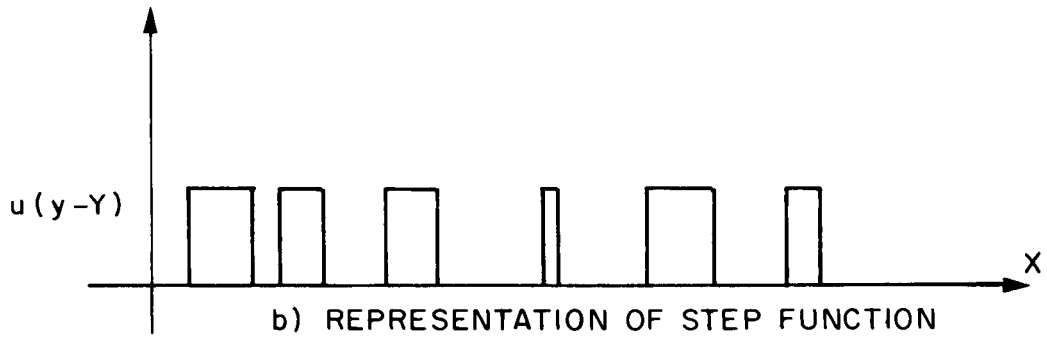


b) REPRESENTATION OF STEP FUNCTION

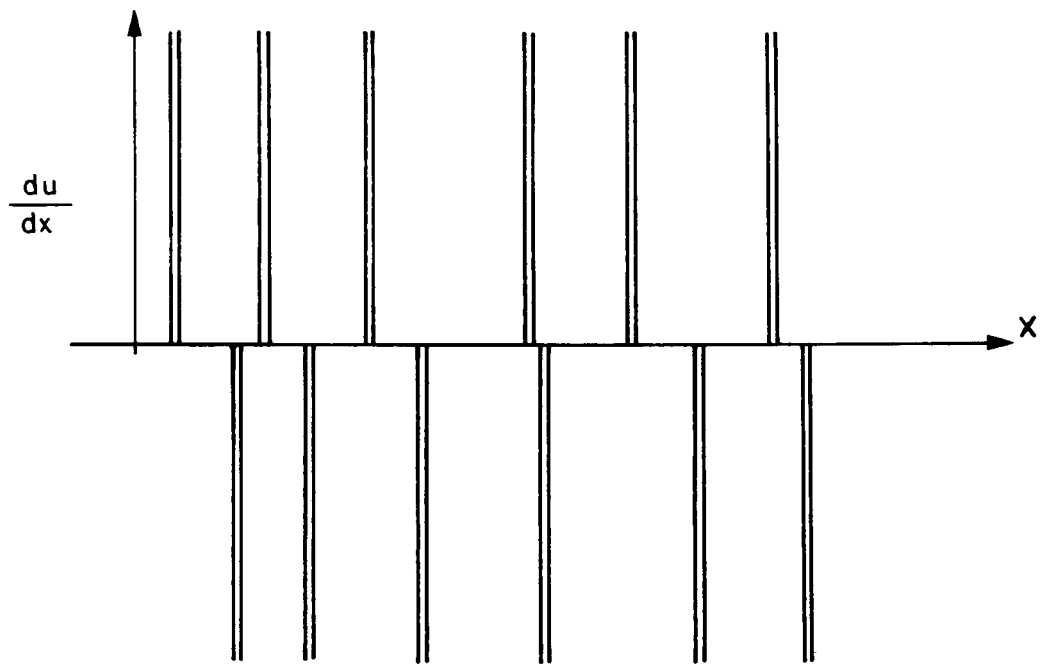


c) COUNTING FUNCTIONAL

FIG. 8 NUMBER OF CROSSING AT y=Y FOR TYPICAL SURFACE PROFILE

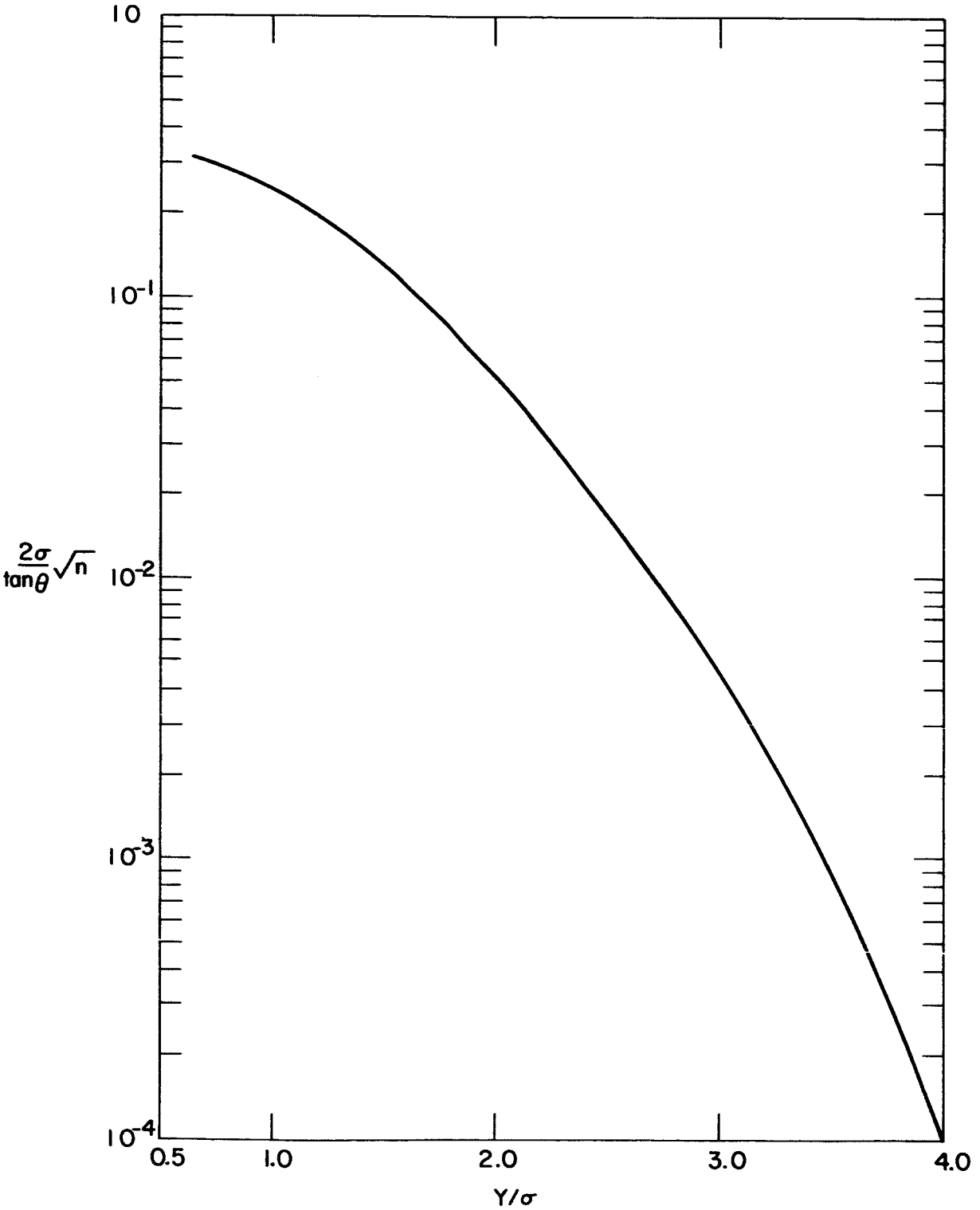


FIG. 9 NUMBER OF CONTACT POINTS VS. DISTANCE BETWEEN MEAN PLANES

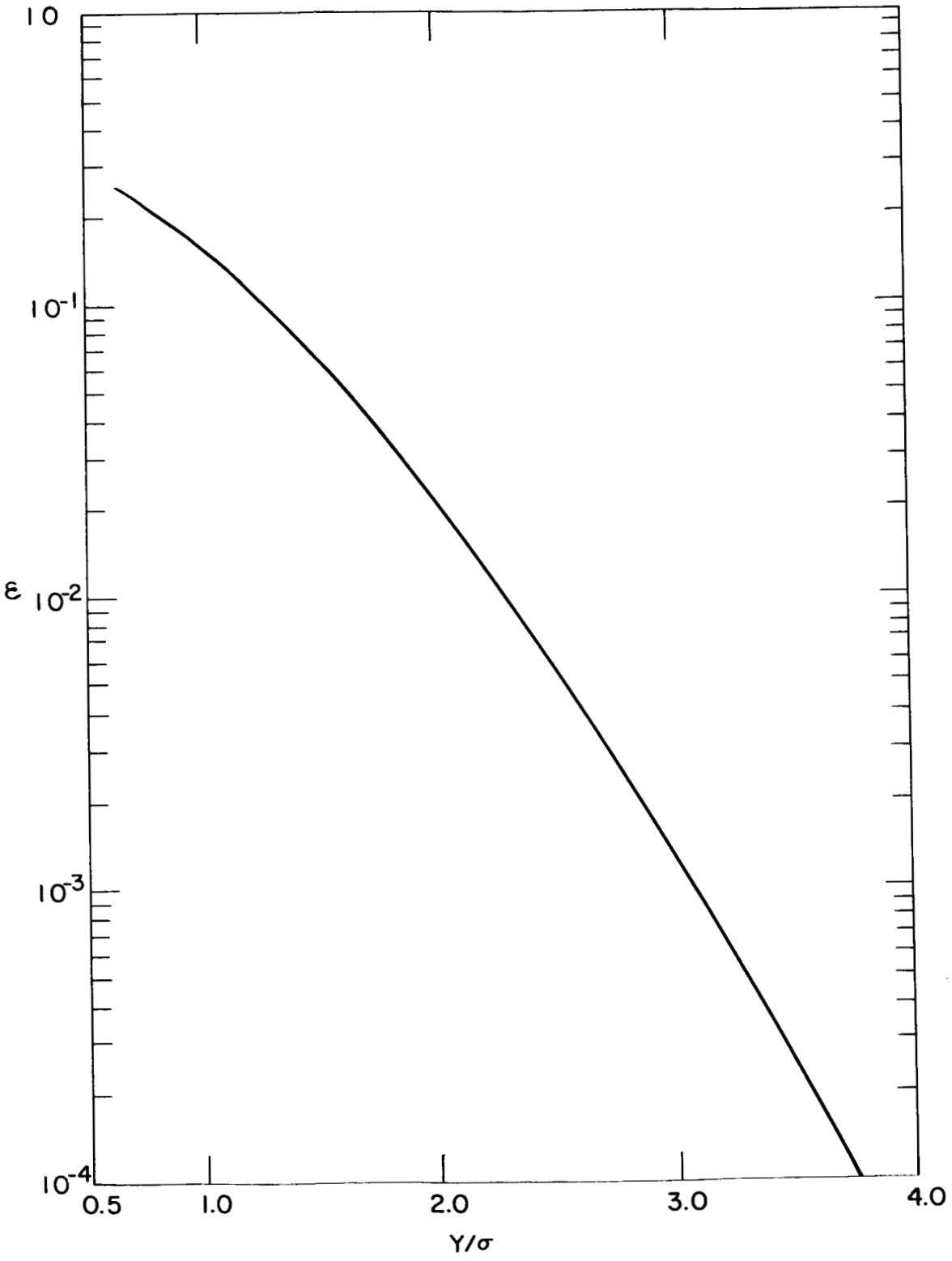


FIG. 10 CONTACT AREA RATIO VS. DISTANCE BETWEEN MEAN PLANES

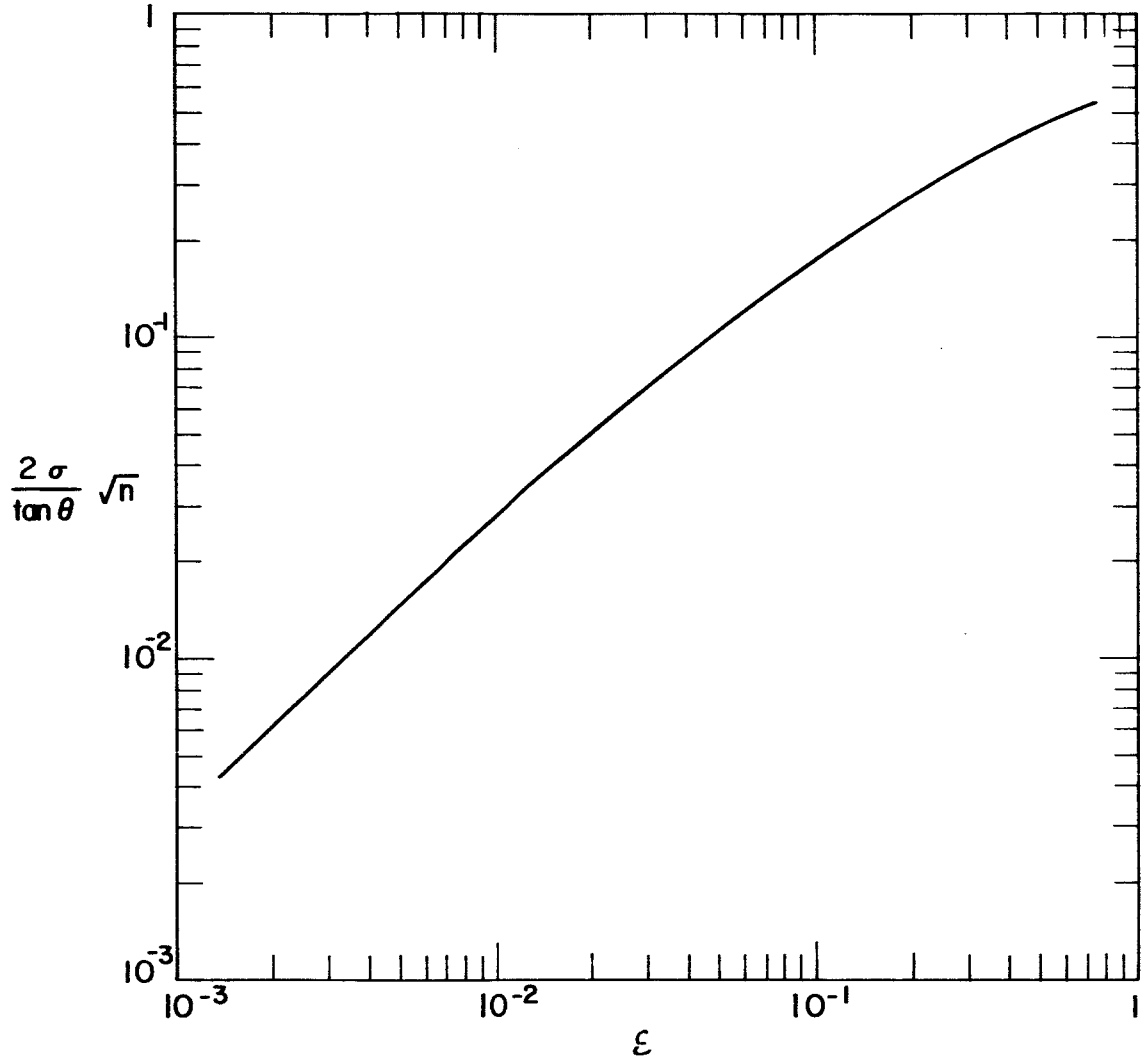


FIG. 11 NUMBER OF CONTACTS VS. CONTACT AREA RATIO

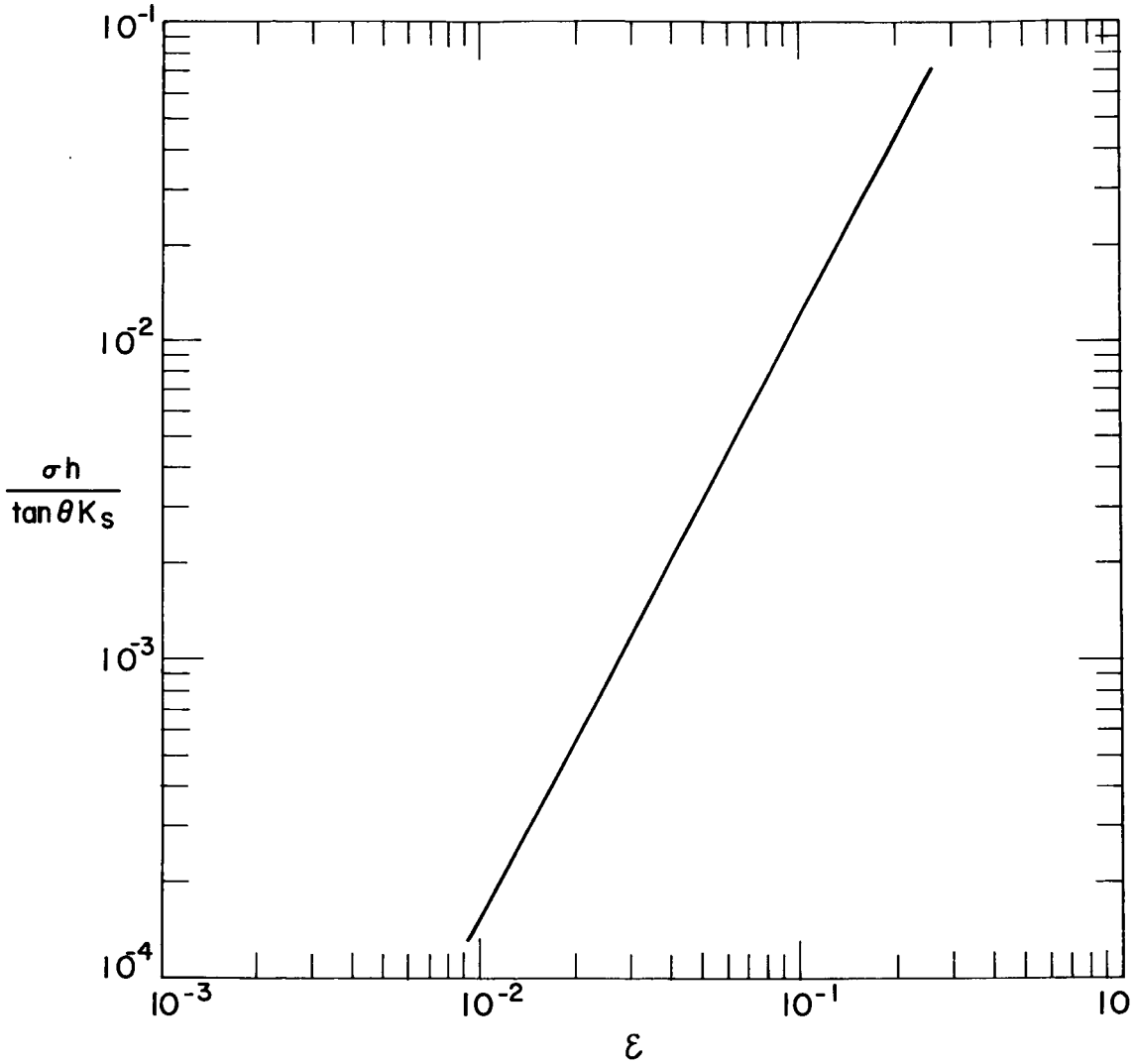


FIG. 12 THERMAL CONTACT CONDUCTANCE VS. CONTACT AREA RATIO

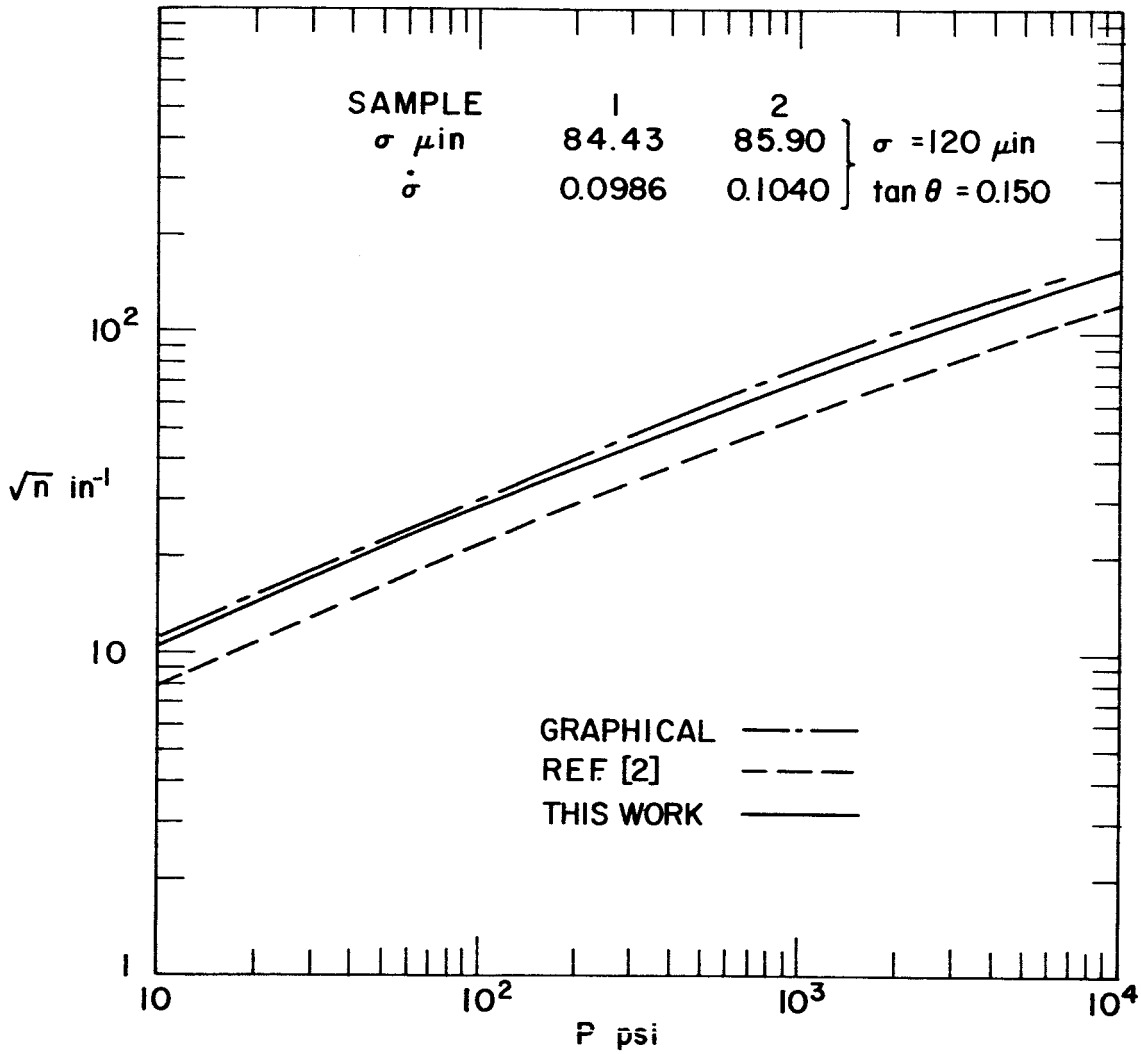


FIG. 13 NUMBER OF CONTACTS VS. PRESSURE : PAIR I

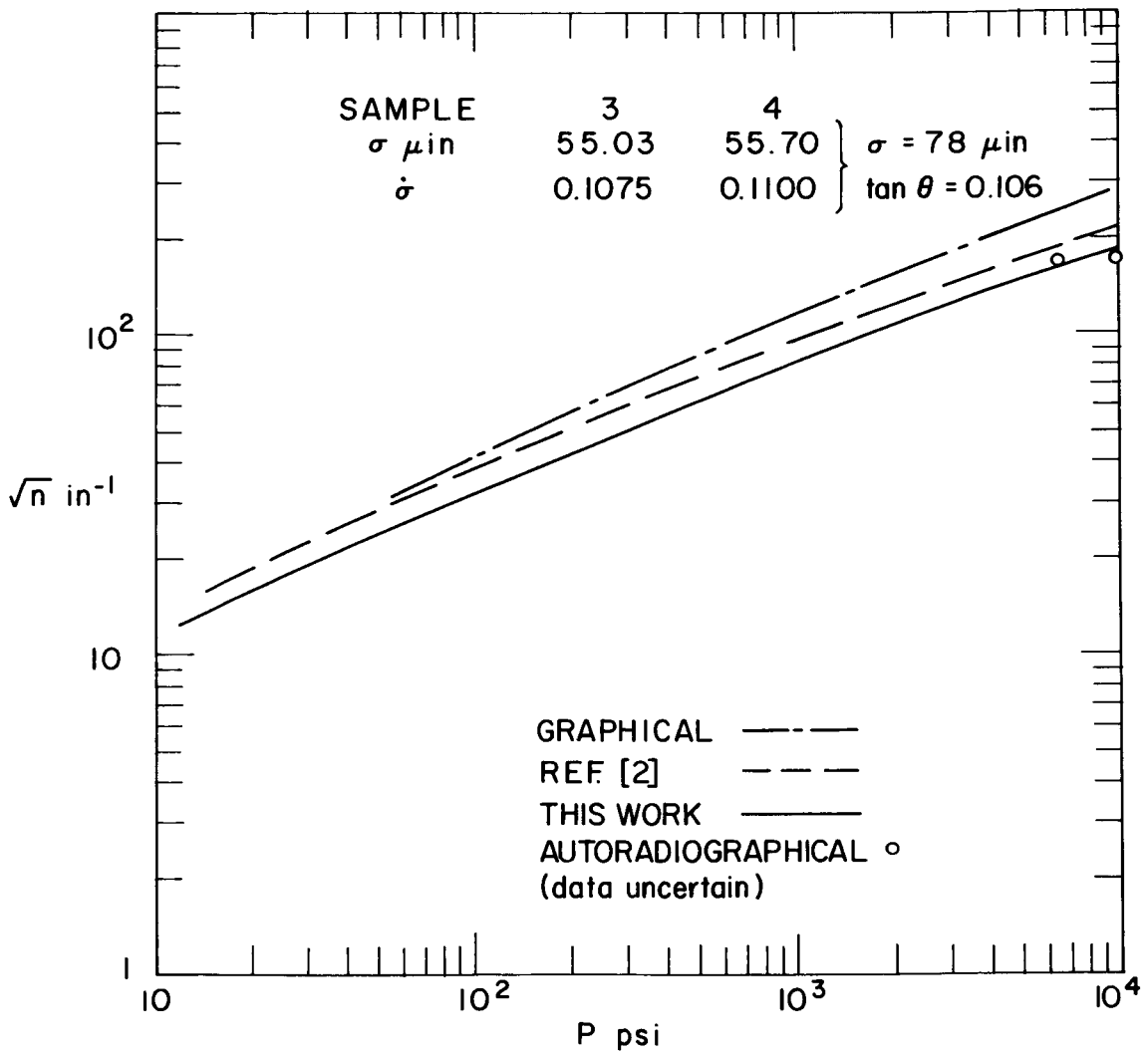


FIG. 14 NUMBER OF CONTACTS VS. PRESSURE: PAIR II

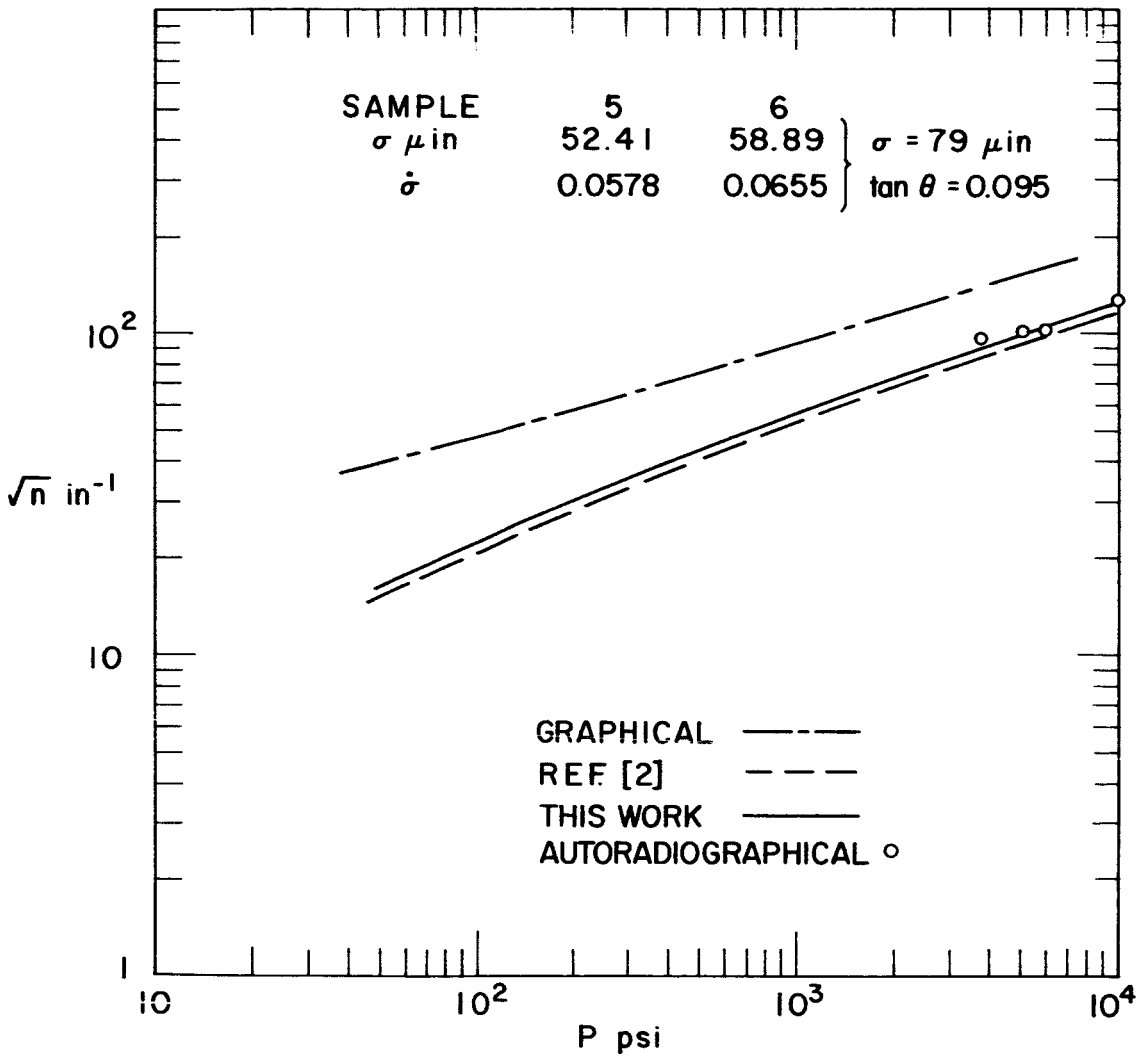


FIG. 15 NUMBER OF CONTACTS VS. PRESSURE: PAIR III

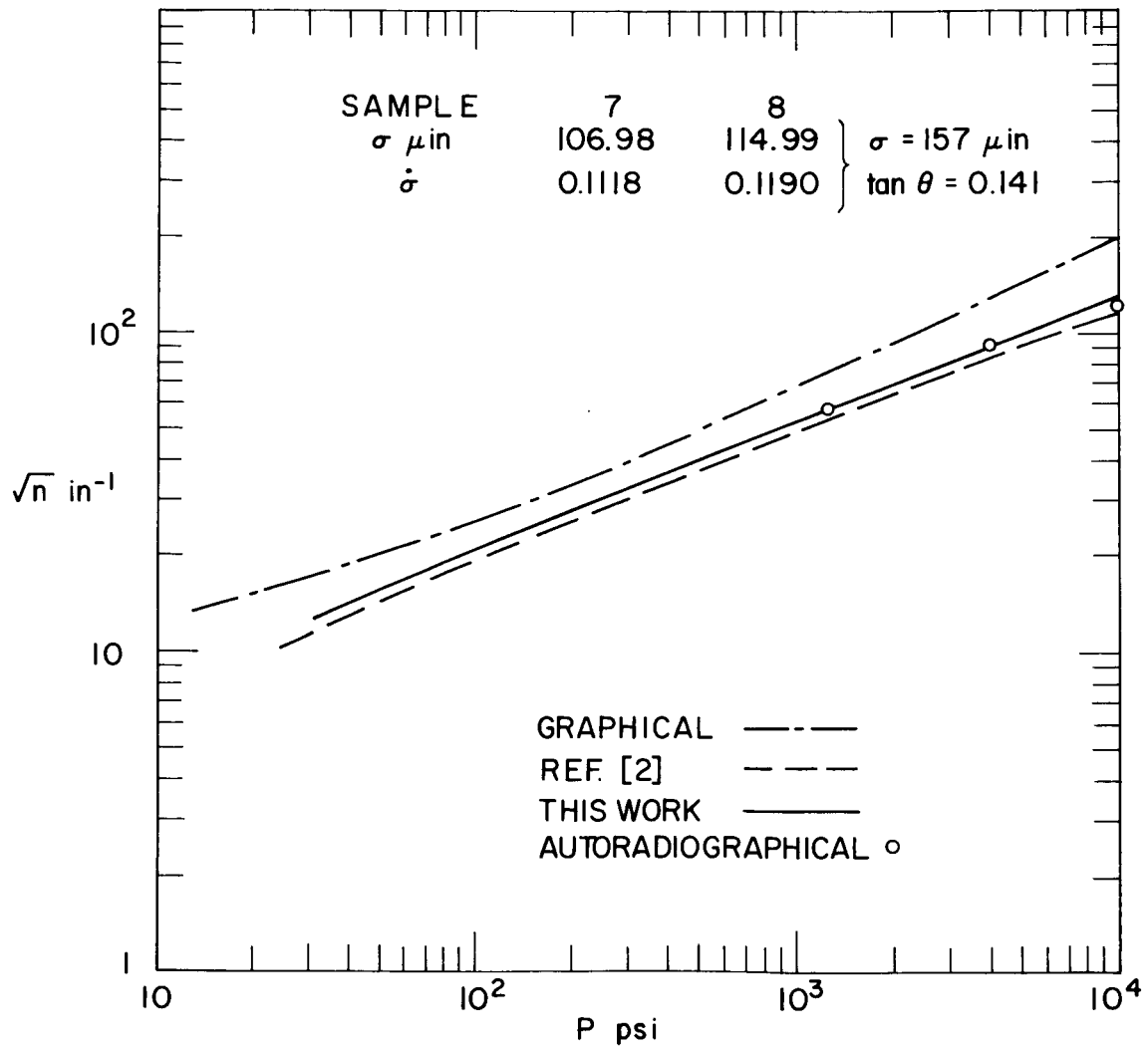


FIG. 16 NUMBER OF CONTACTS VS. PRESSURE : PAIR IV

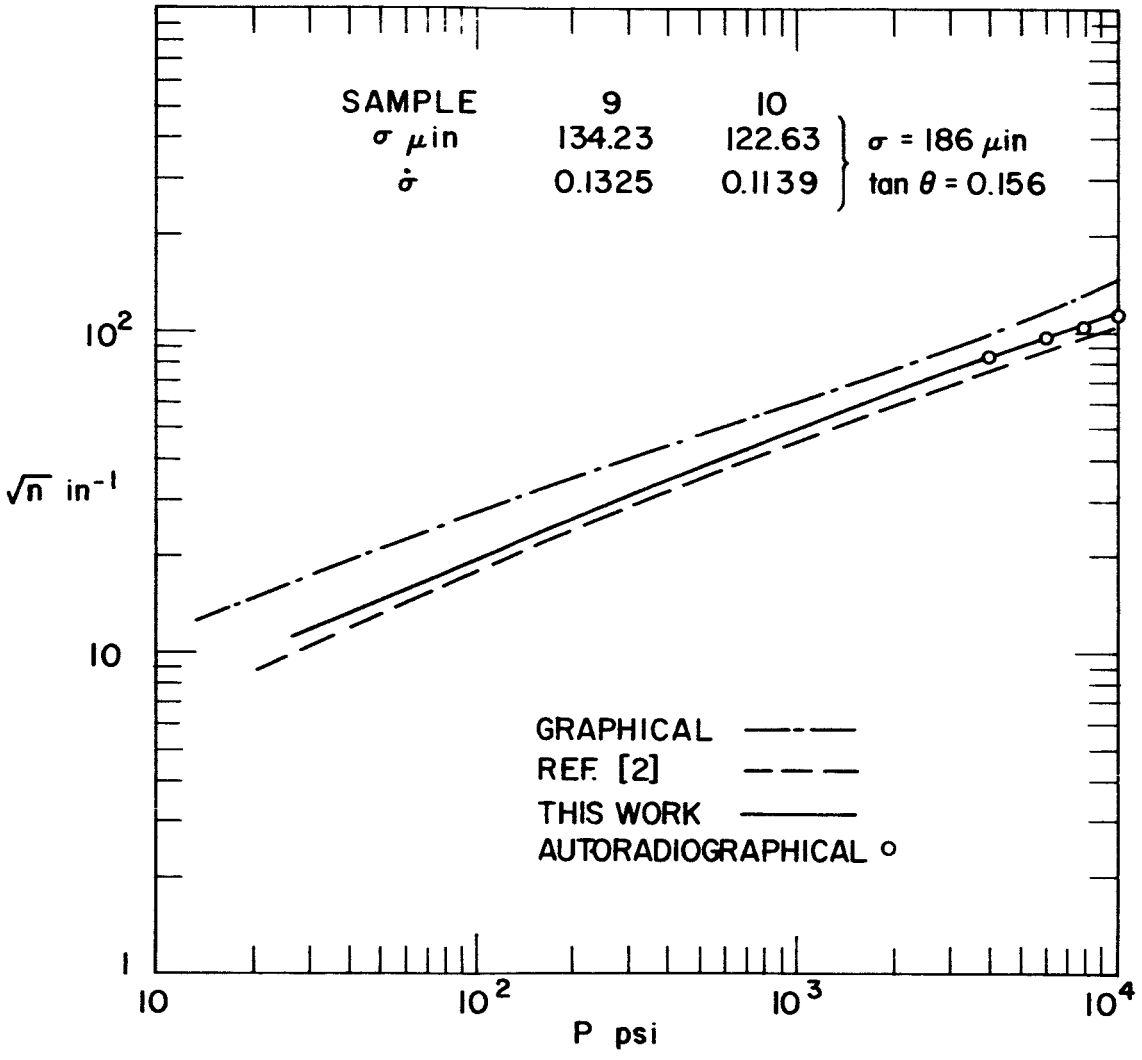


FIG. 17 NUMBER OF CONTACTS VS. PRESSURE : PAIR V

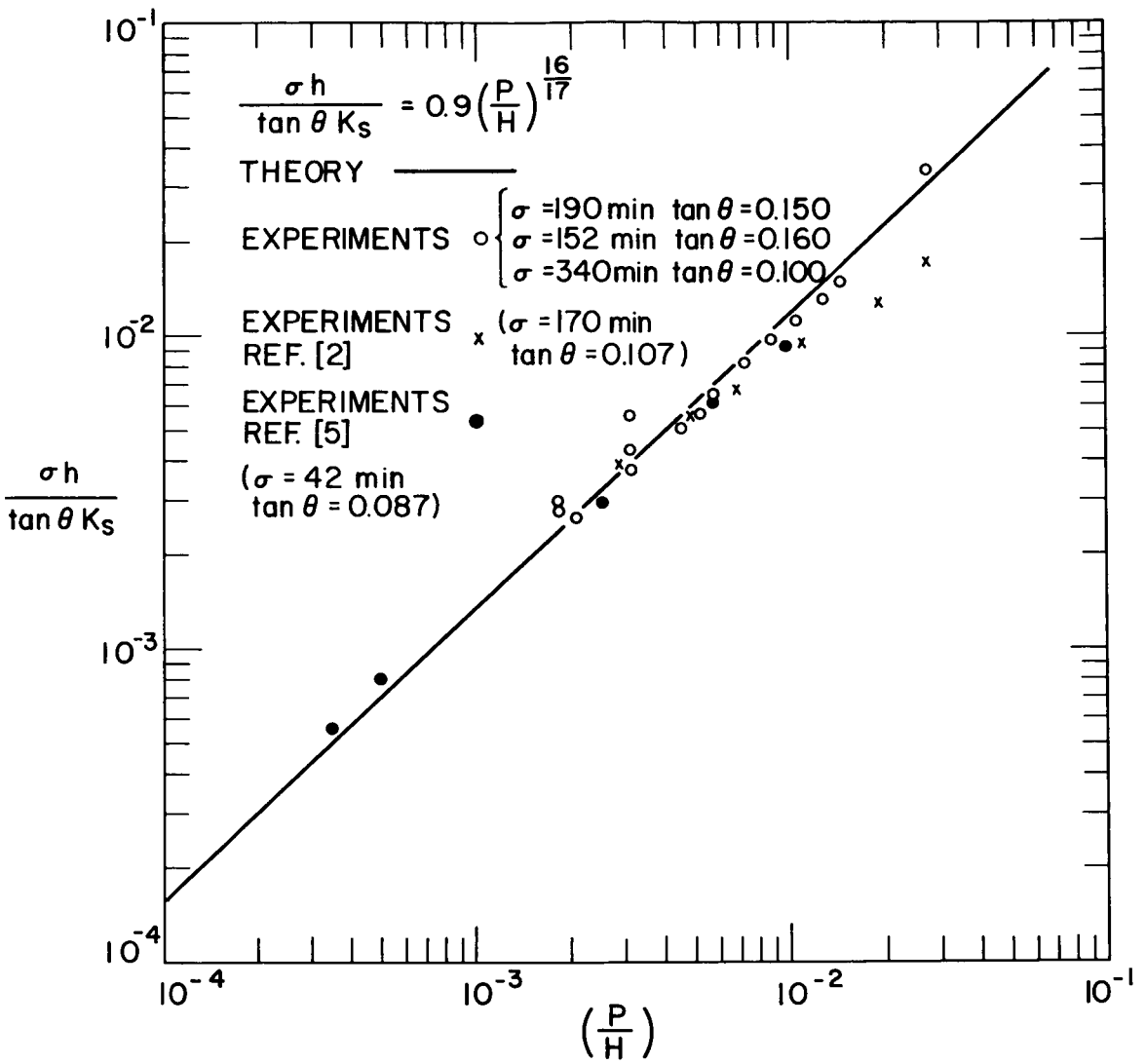


FIG. 18 CONTACT CONDUCTANCE VS. PRESSURE FOR NOMINALLY FLAT SURFACES IN A VACUUM

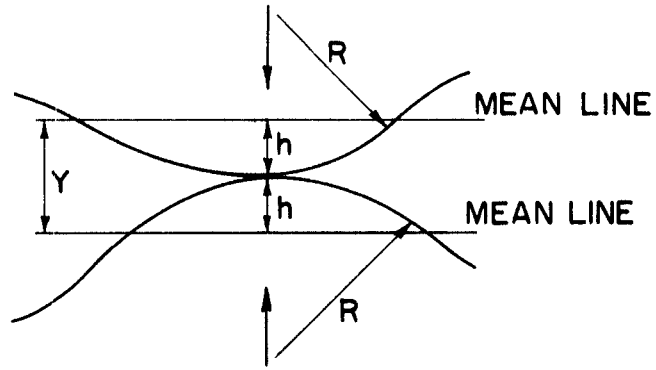


a) MODEL FOR TWO ASPERITIES IN CONTACT

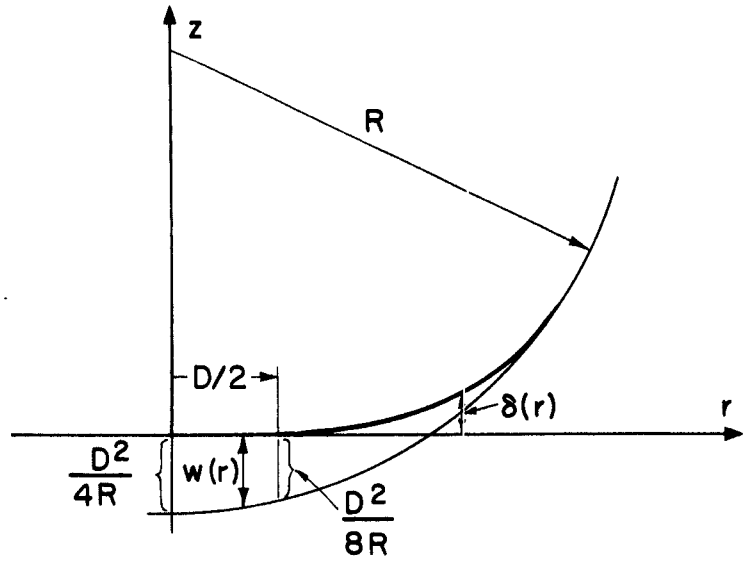


b) LOCAL DEFORMATION OF A SPHERE PRESSED AGAINST A RIGID PLANE

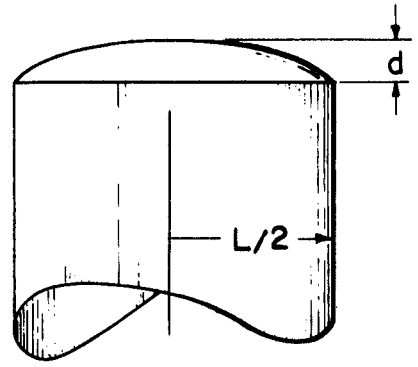


c) SPECIMEN FLATNESS DEVIATION

FIG. 19 MODELS USED IN DEFORMATION ANALYSIS

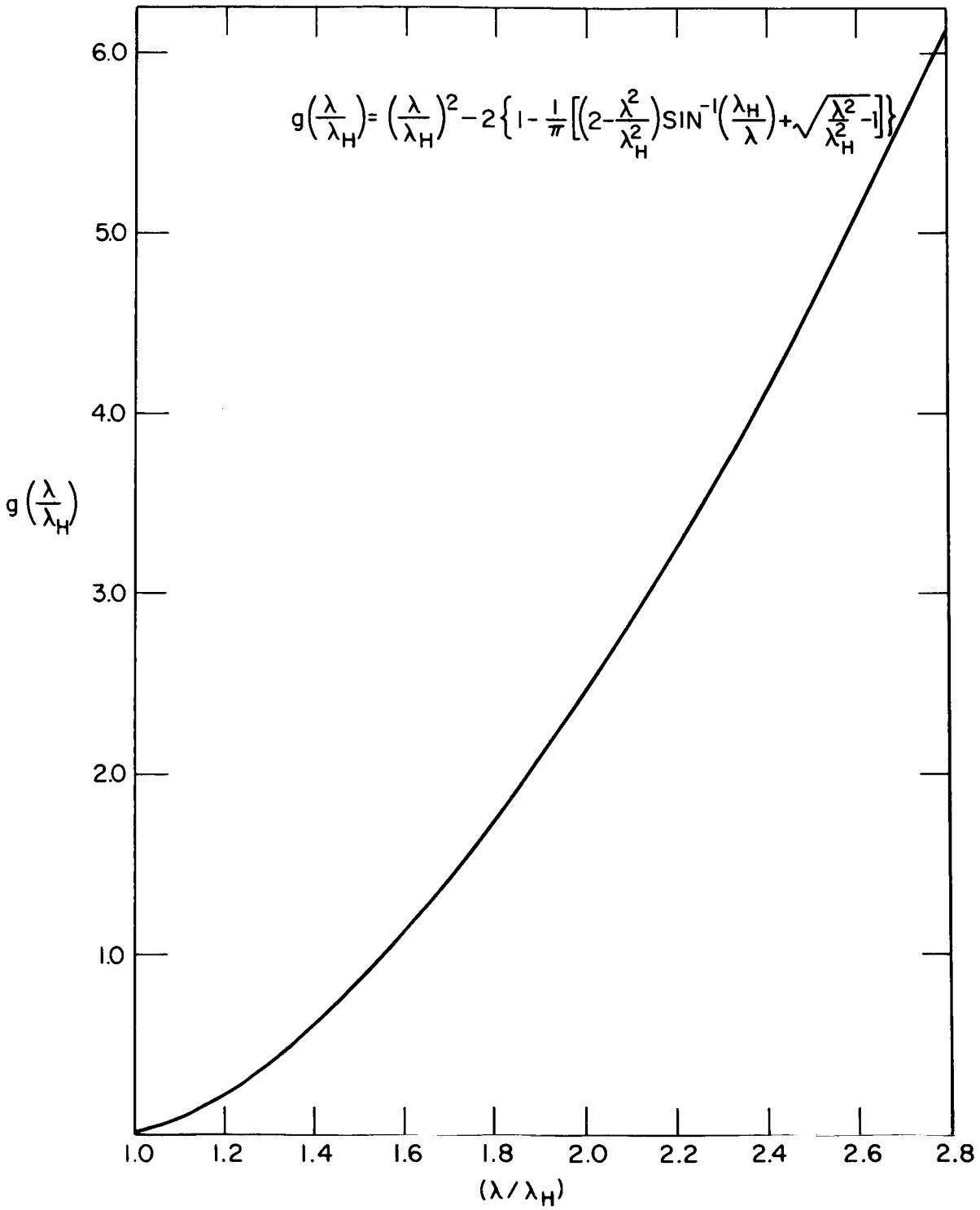


FIG. 20 WAVINESS FACTOR

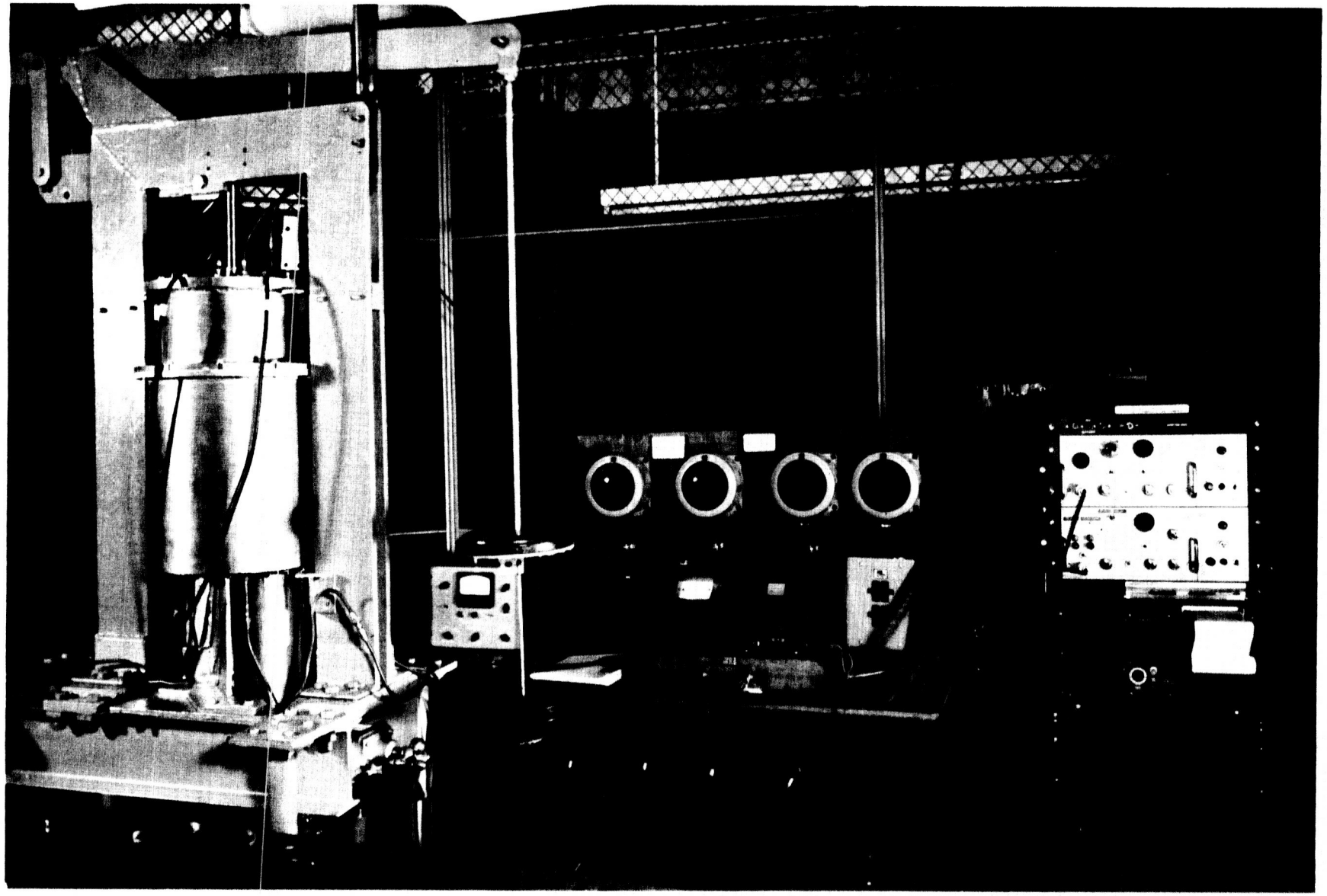

FIG. 21 CONTACT RESISTANCE APPARATUS

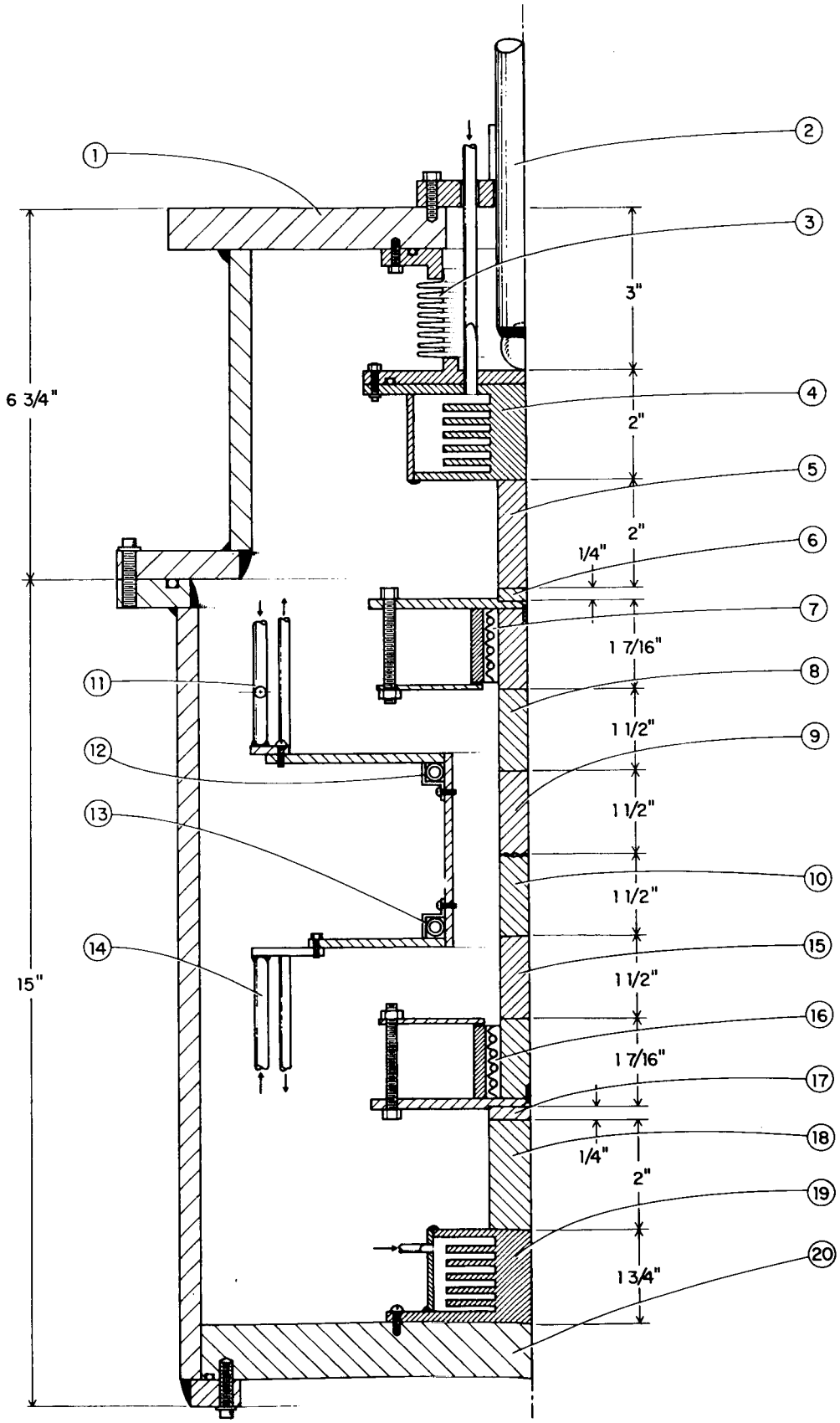


FIG. 22 TEST SECTION AND CHAMBER

PARTS LIST FOR FIGURE 22

Part No:

| | |
|---|---|
| 1 | Top Plate |
| 2 | Loading Mechanism |
| 3 | Bellows |
| 4 | Upper Main Cooler |
| 5 & 6 | Spacers |
| 7 | Upper Main Heater |
| 8 | Upper Heat Meter |
| 9 & 10 | Specimens |
| 11 | Upper Guard Ring Cooler |
| 12 | Upper Guard Ring Heater |
| 13 | Lower Guard Ring Heater |
| 14 | Lower Guard Ring Cooler |
| 15 | Lower Heat Meter |
| 16 | Lower Main Heater |
| 17 | Spacer |
| 18 | Dynamometer |
| 19 | Lower Main Cooler |
| 20 | Base Plate |

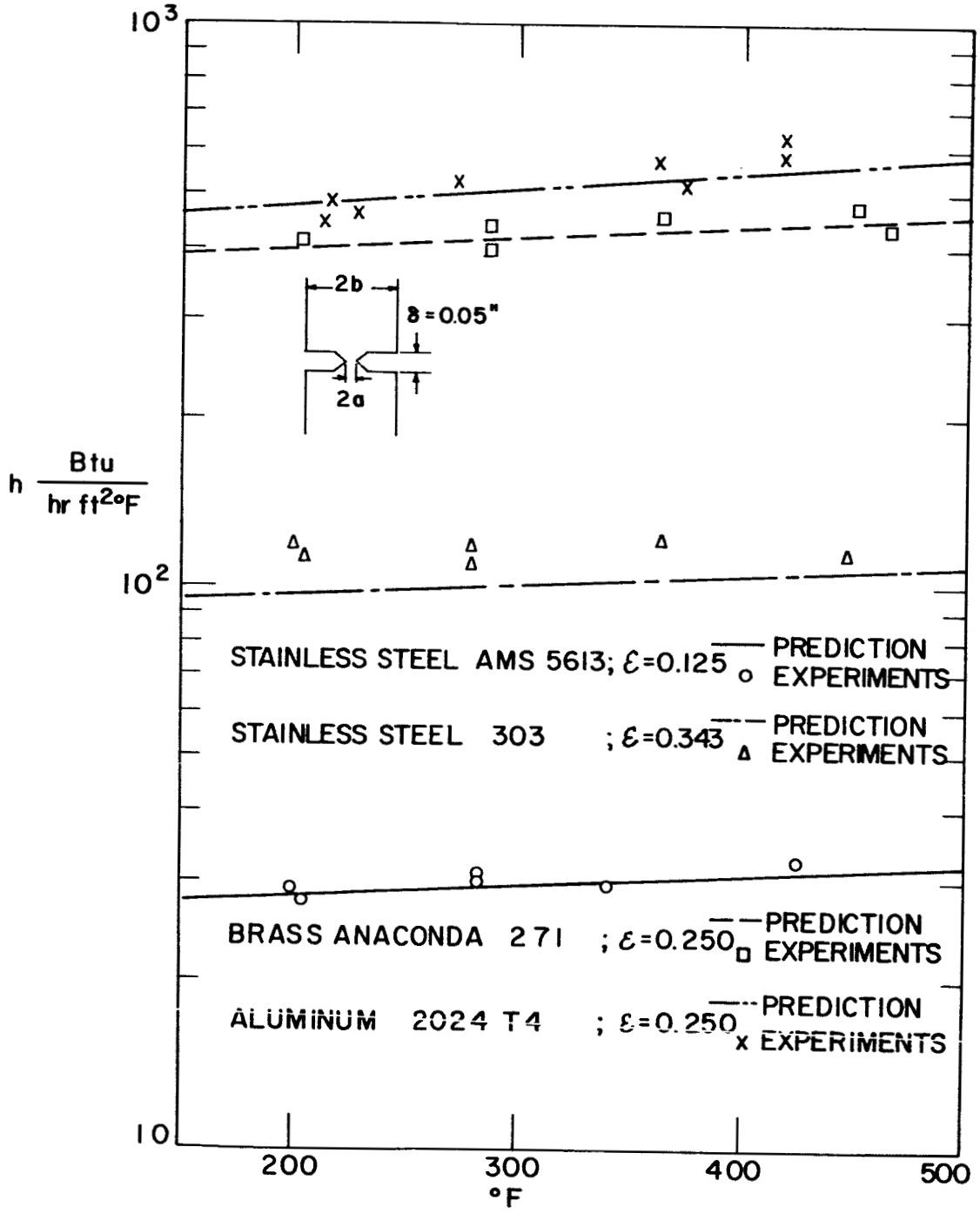


FIG. 23 IDEALIZED MODEL IN A VACUUM ENVIRONMENT

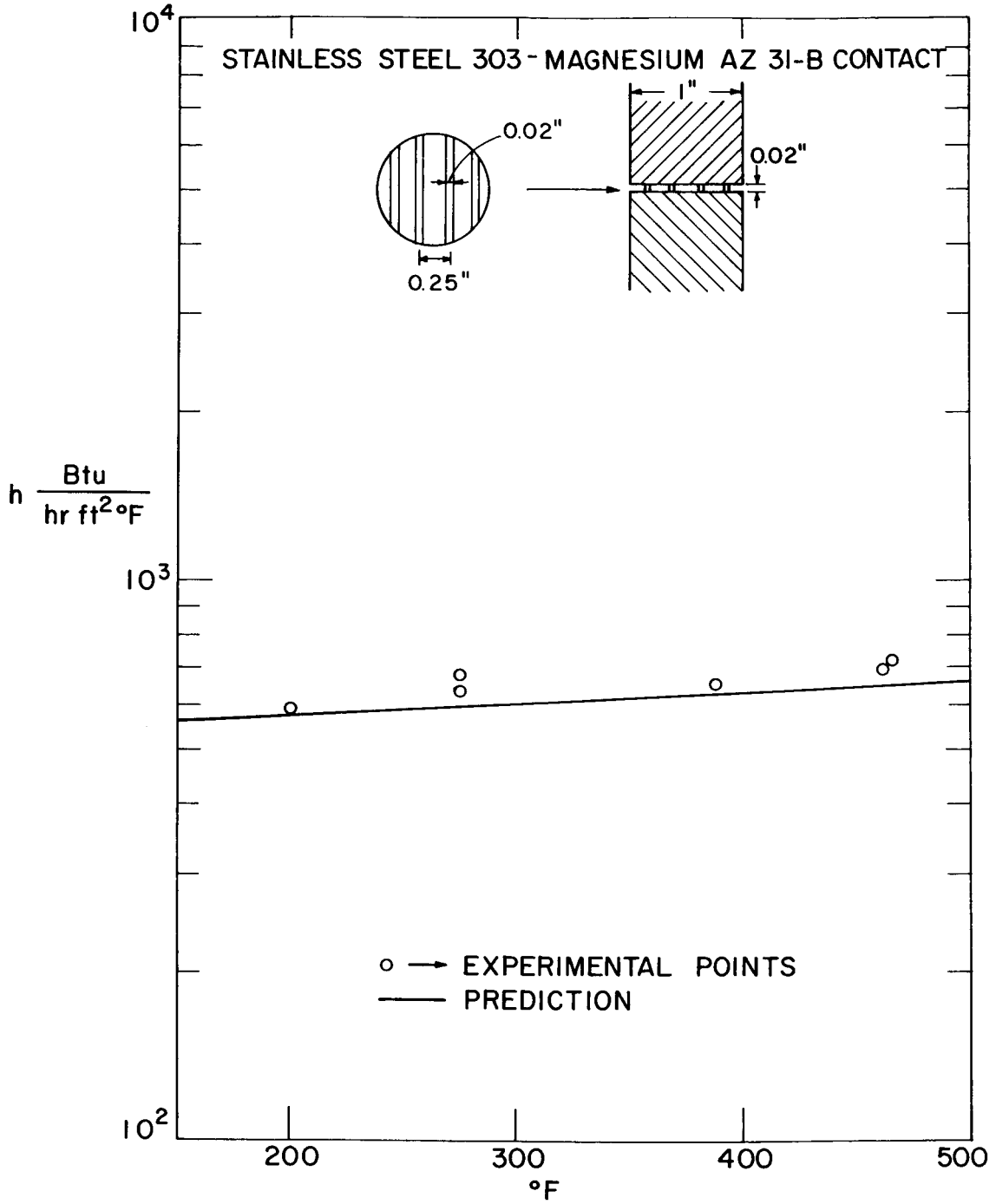


FIG. 24 IDEALIZED CYLINDRICAL WAVINESS MODEL: STAINLESS STEEL / MAGNESIUM CONTACT IN A VACUUM ENVIRONMENT

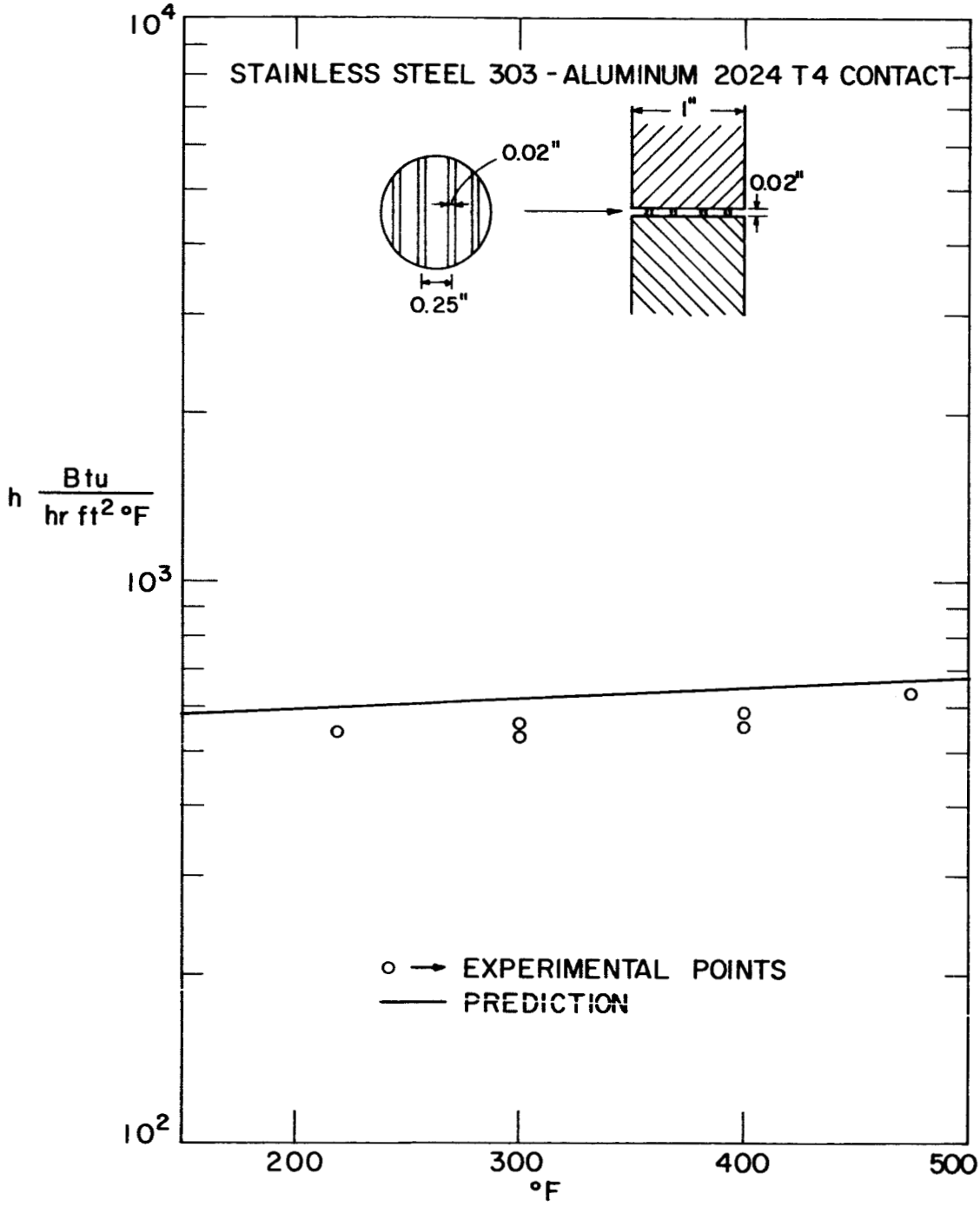


FIG. 25 IDEALIZED CYLINDRICAL WAVINESS MODEL: STAINLESS STEEL / ALUMINUM CONTACT IN A VACUUM ENVIRONMENT

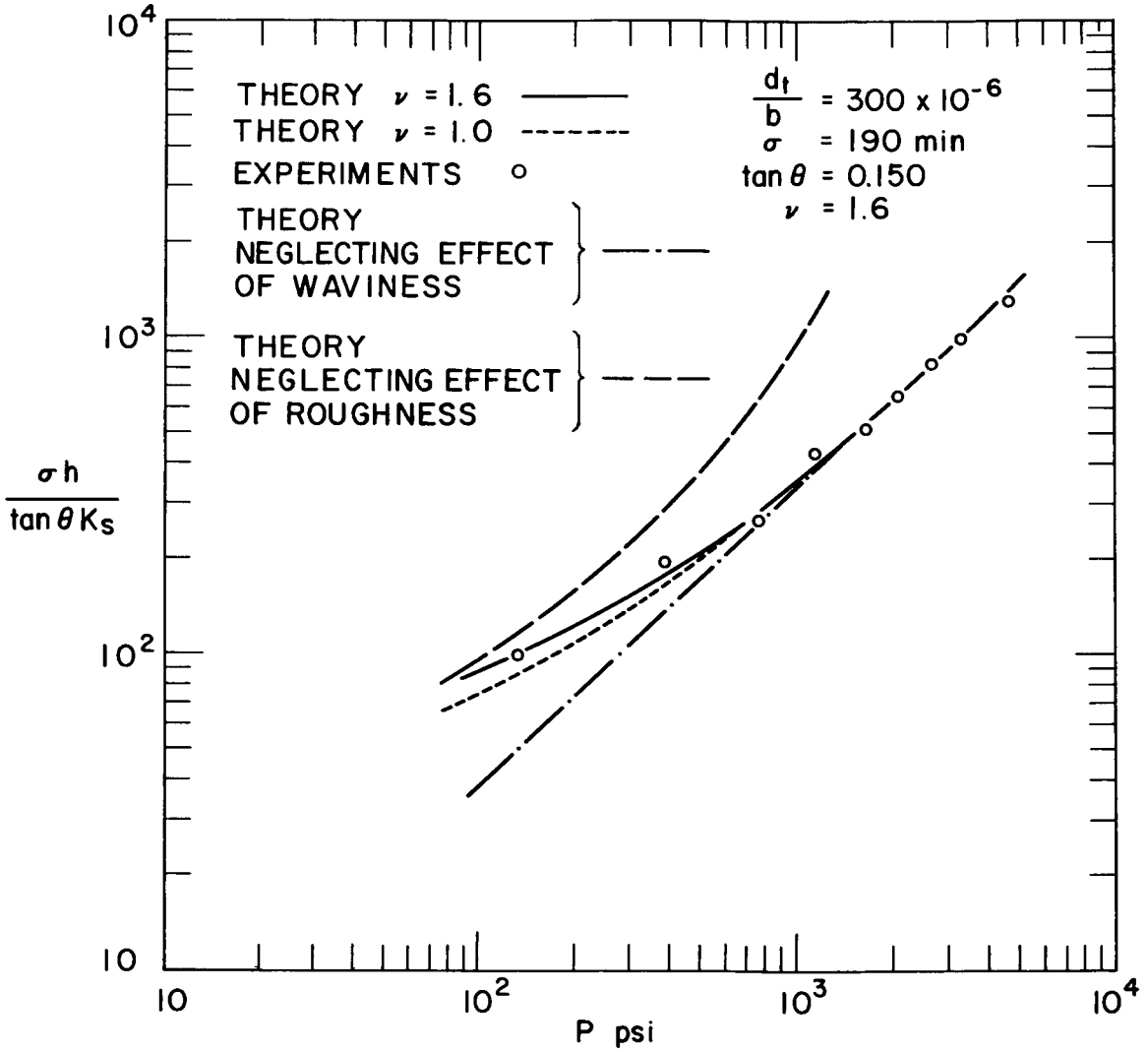


FIG. 26 CONTACT CONDUCTANCE VS. PRESSURE: STAINLESS STEEL PAIR NO. 1

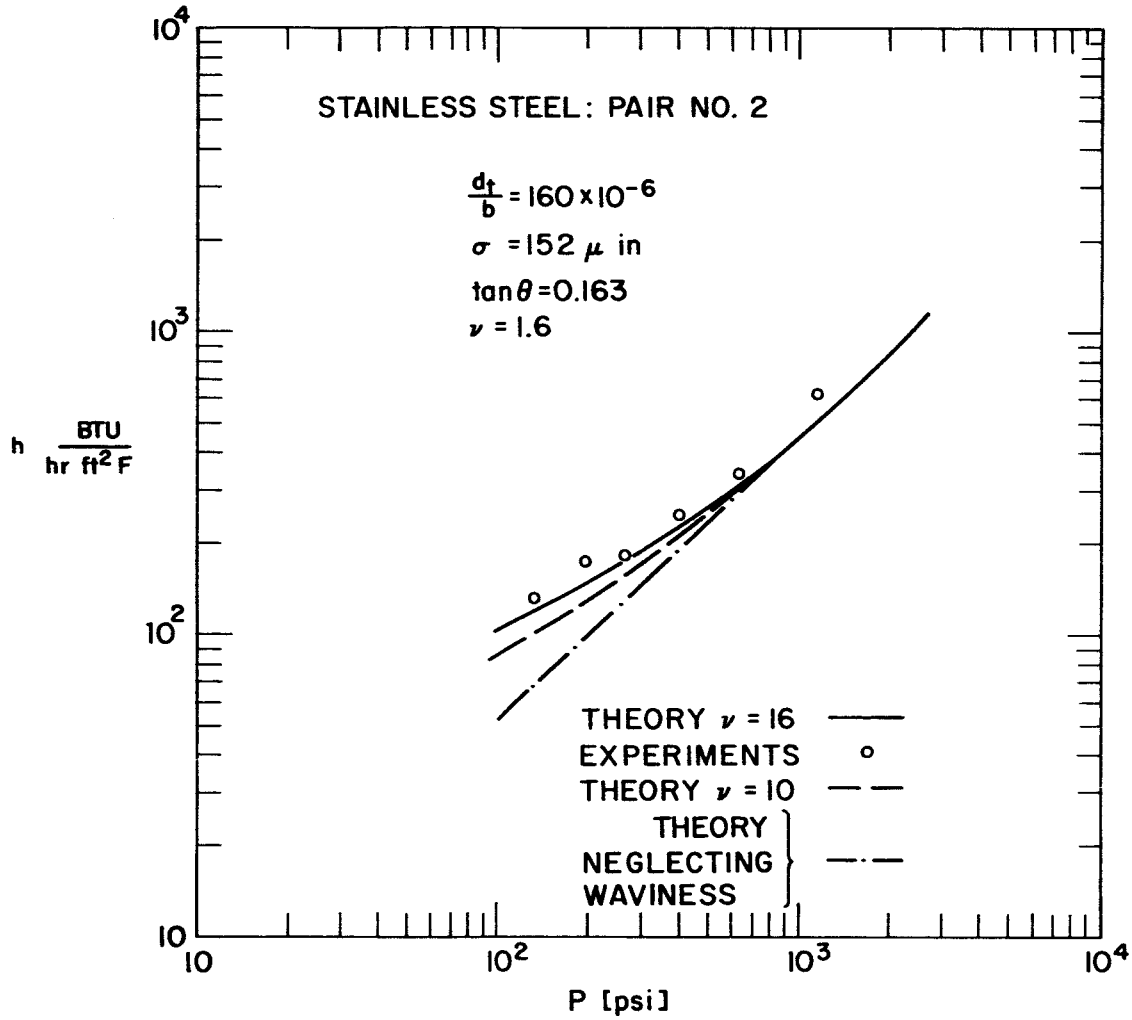


FIG. 27 CONTACT CONDUCTANCE VS. PRESSURE: STAINLESS STEEL PAIR NO. 2

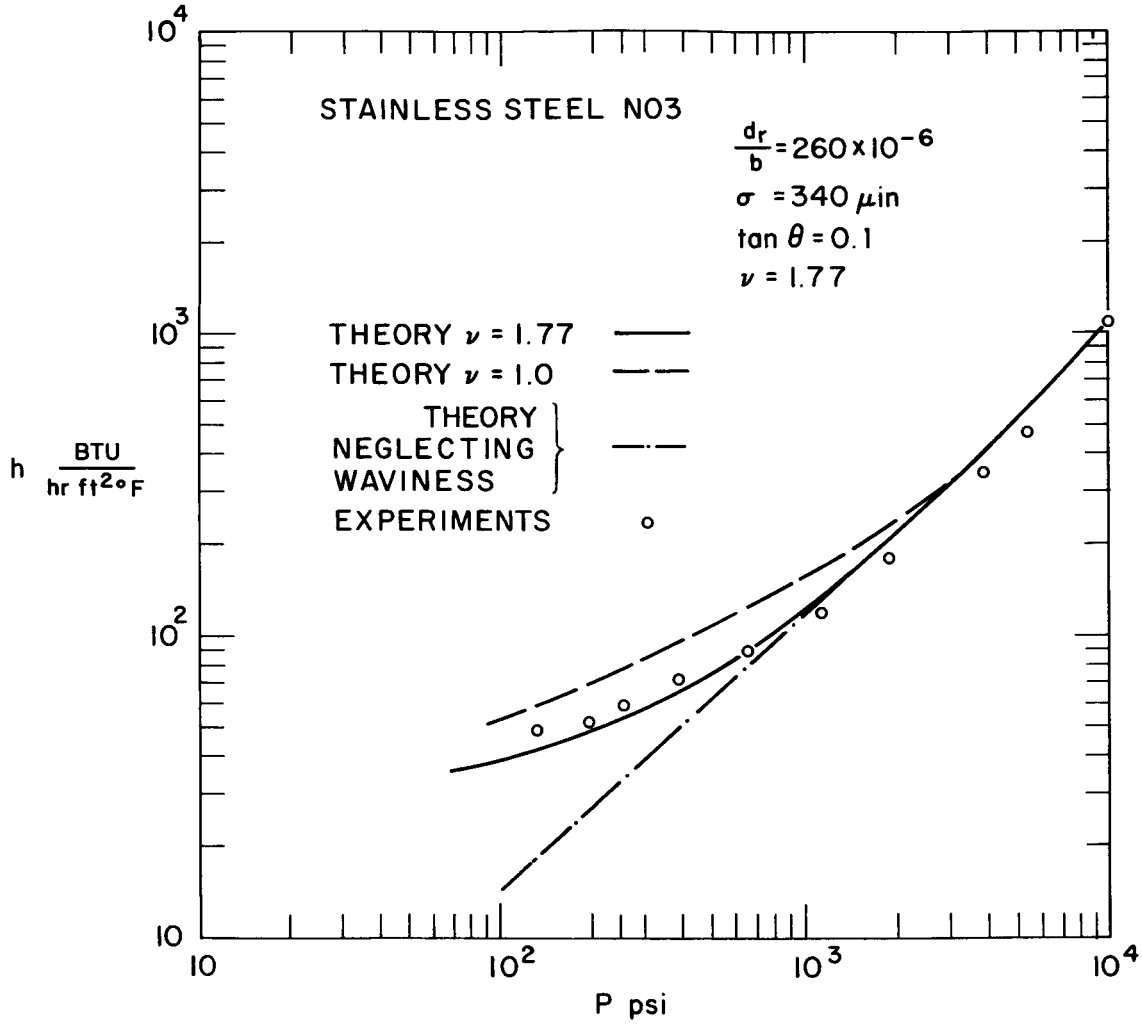


FIG. 28 CONTACT CONDUCTANCE VS. PRESSURE: STAINLESS STEEL PAIR NO. 3

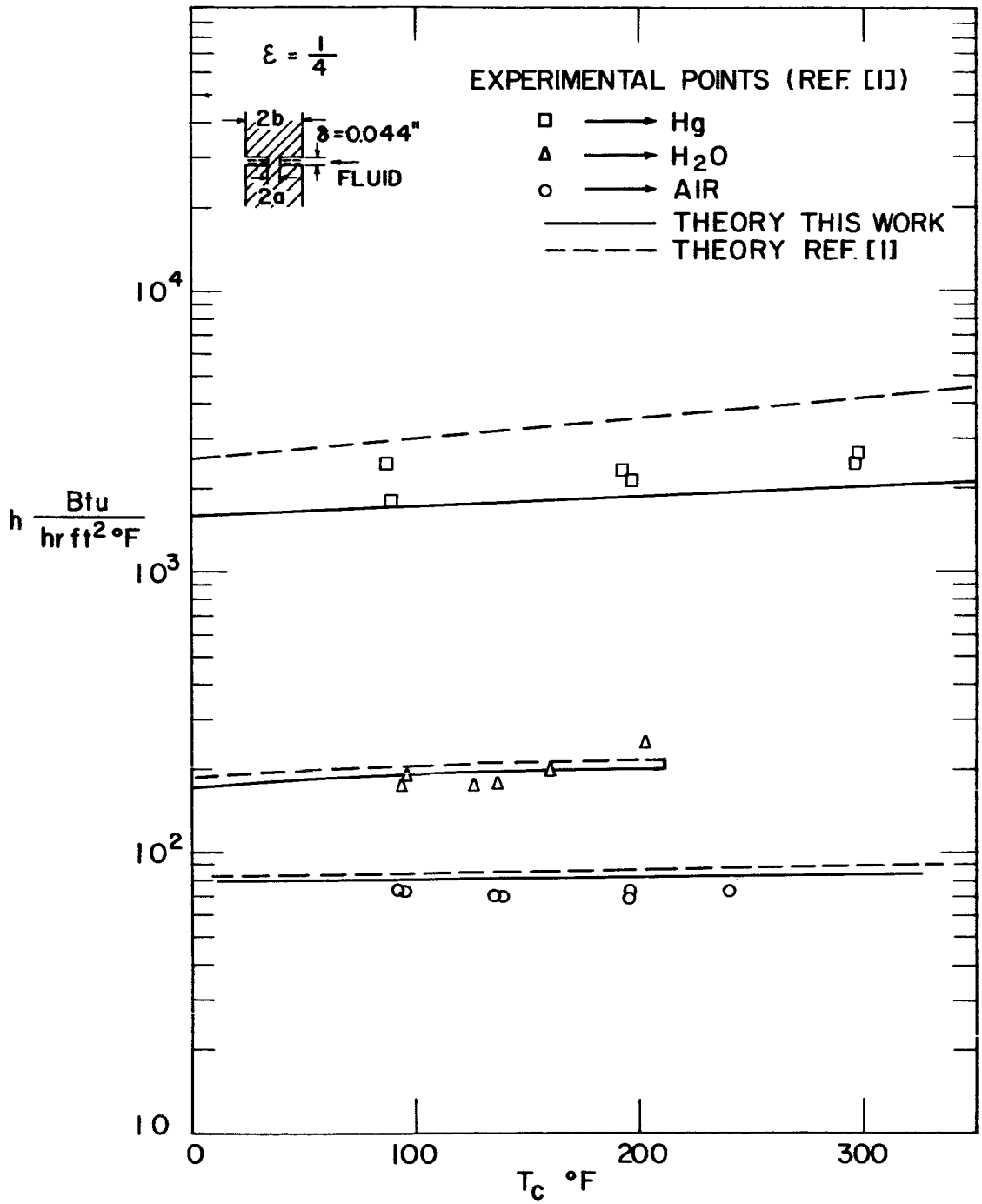


FIG. 29 IDEALIZED MODEL USED IN REF. [1] FOR A CONTACT SPOT IN A FLUID ENVIRONMENT : $\varepsilon = 1/4$

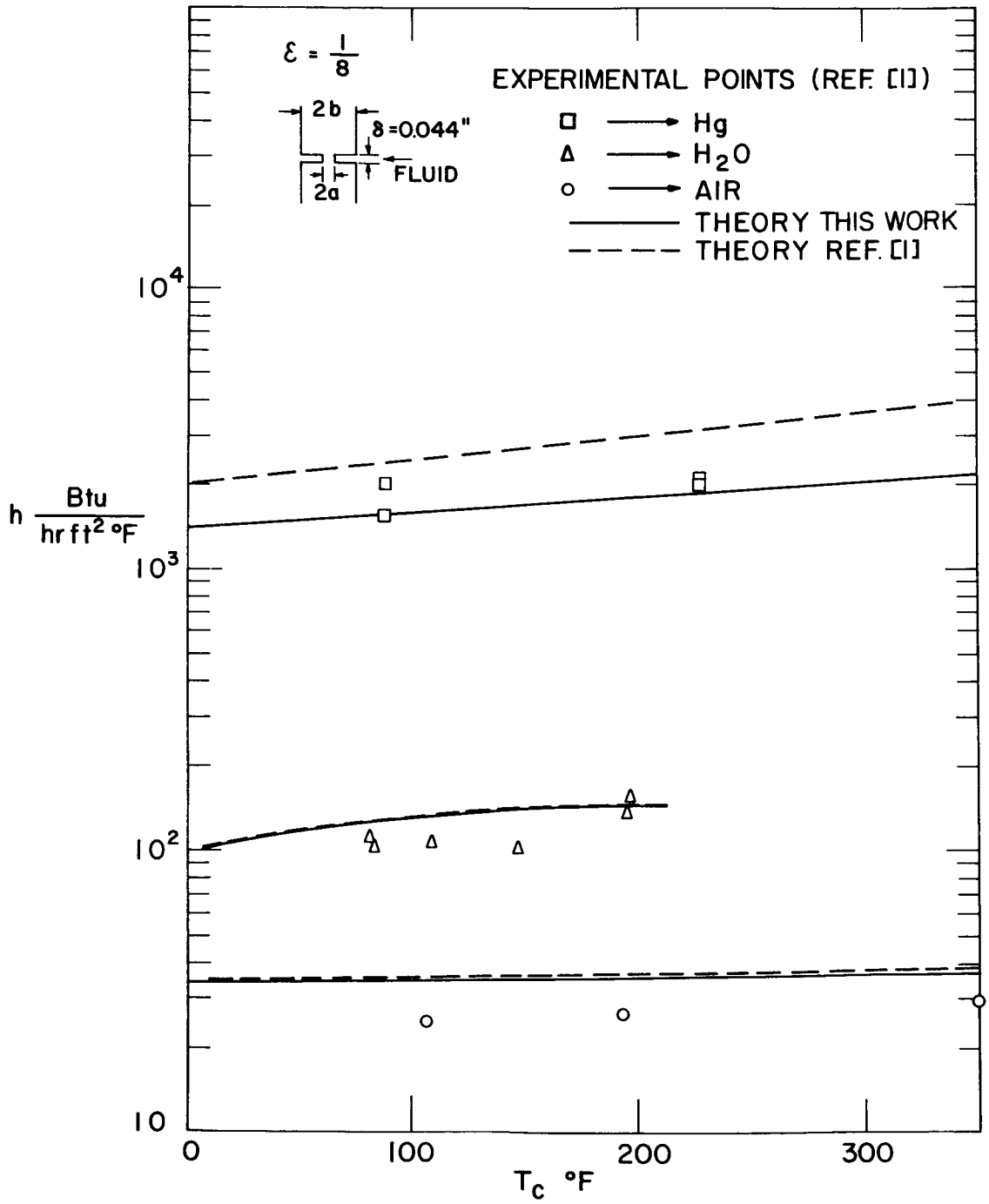


FIG. 30 IDEALIZED MODEL USED IN REF. [1] FOR A CONTACT SPOT IN A FLUID ENVIRONMENT: $\varepsilon = 1/8$

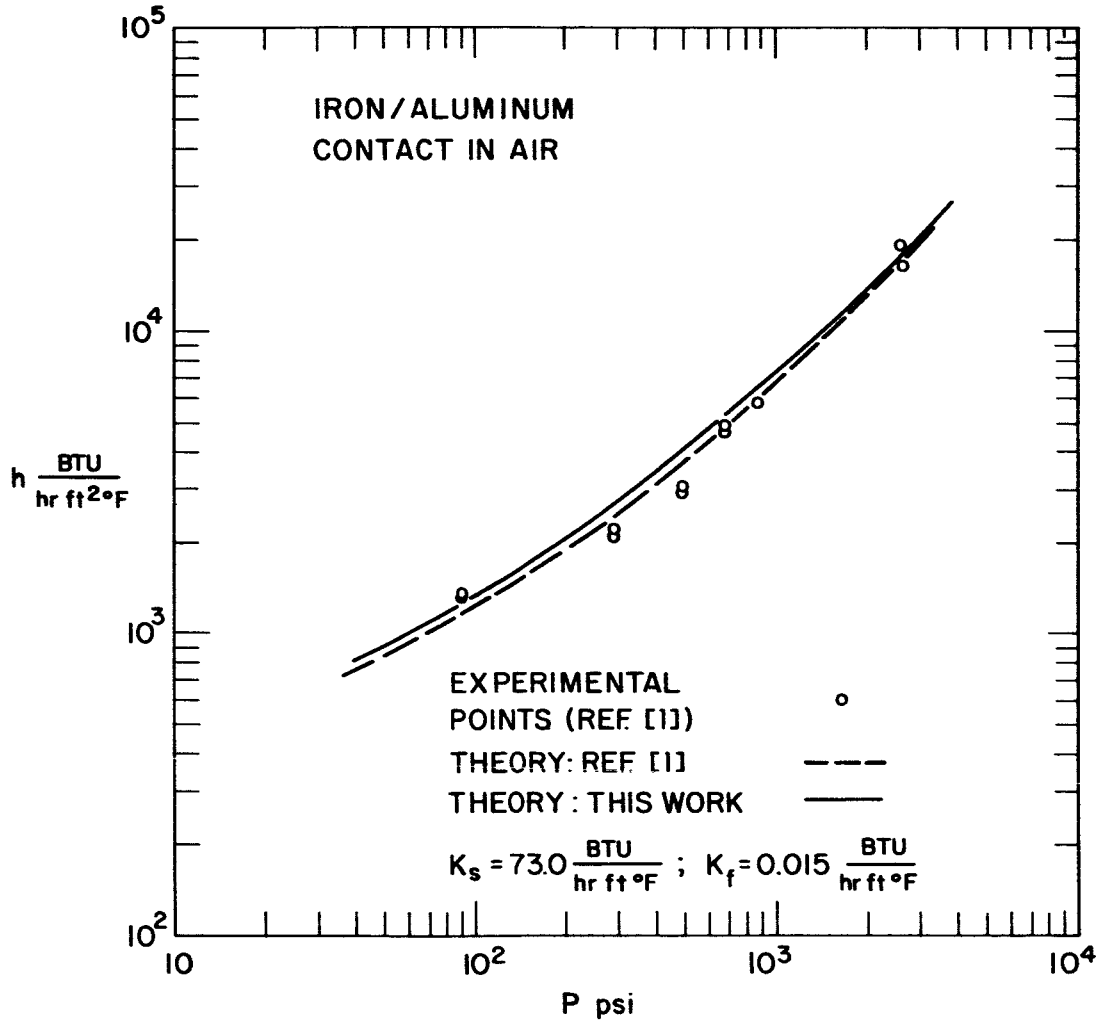


FIG. 31 CONTRACT CONDUCTANCE VS. PRESSURE FOR ROUGH NOMINALLY FLAT SURFACES IN AIR : IRON/ALUMINUM CONTACT

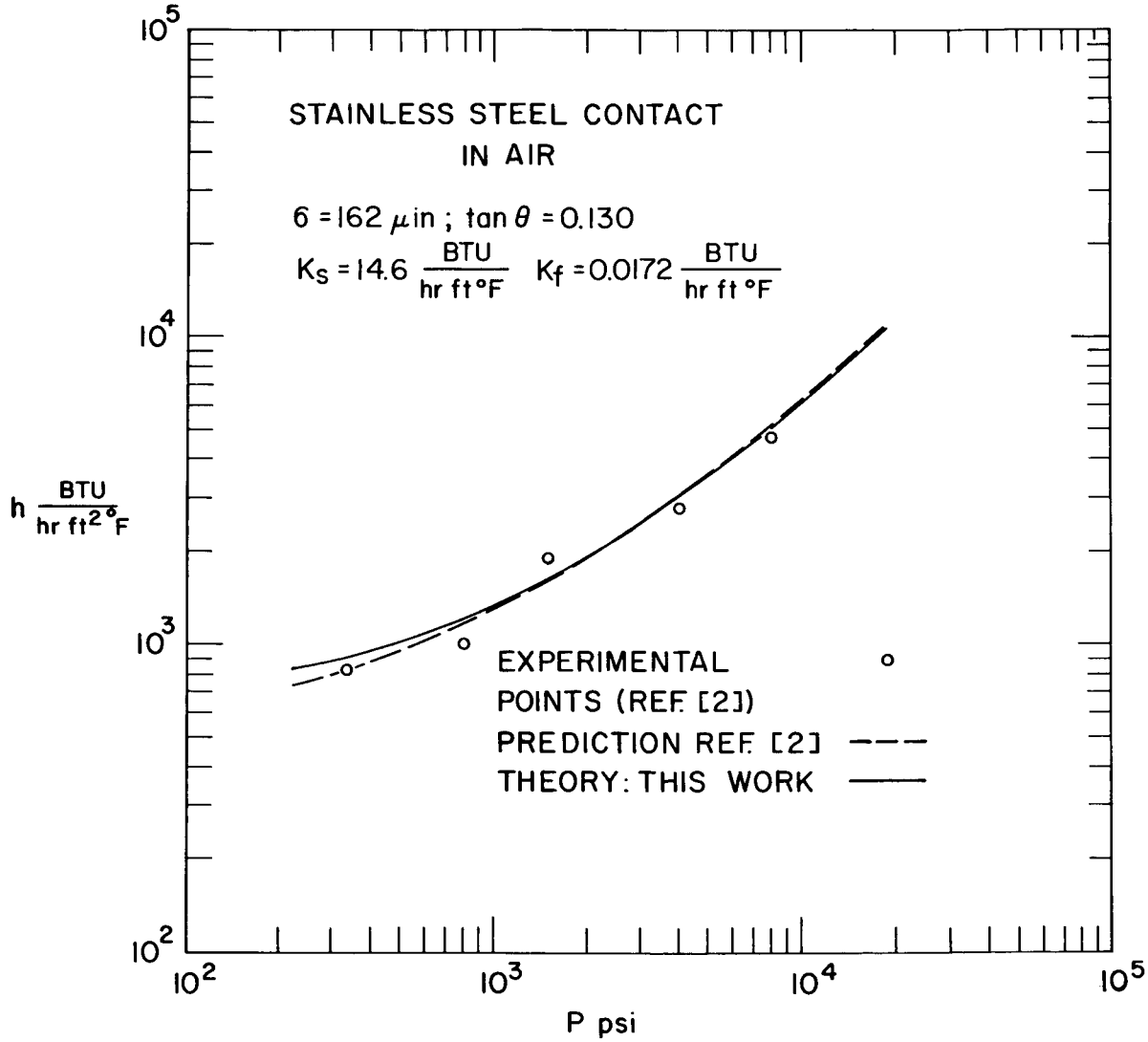


FIG. 32 CONTACT CONDUCTANCE VS. PRESSURE FOR ROUGH NOMINALLY FLAT SURFACES IN AIR: STAINLESS STEEL CONTACT

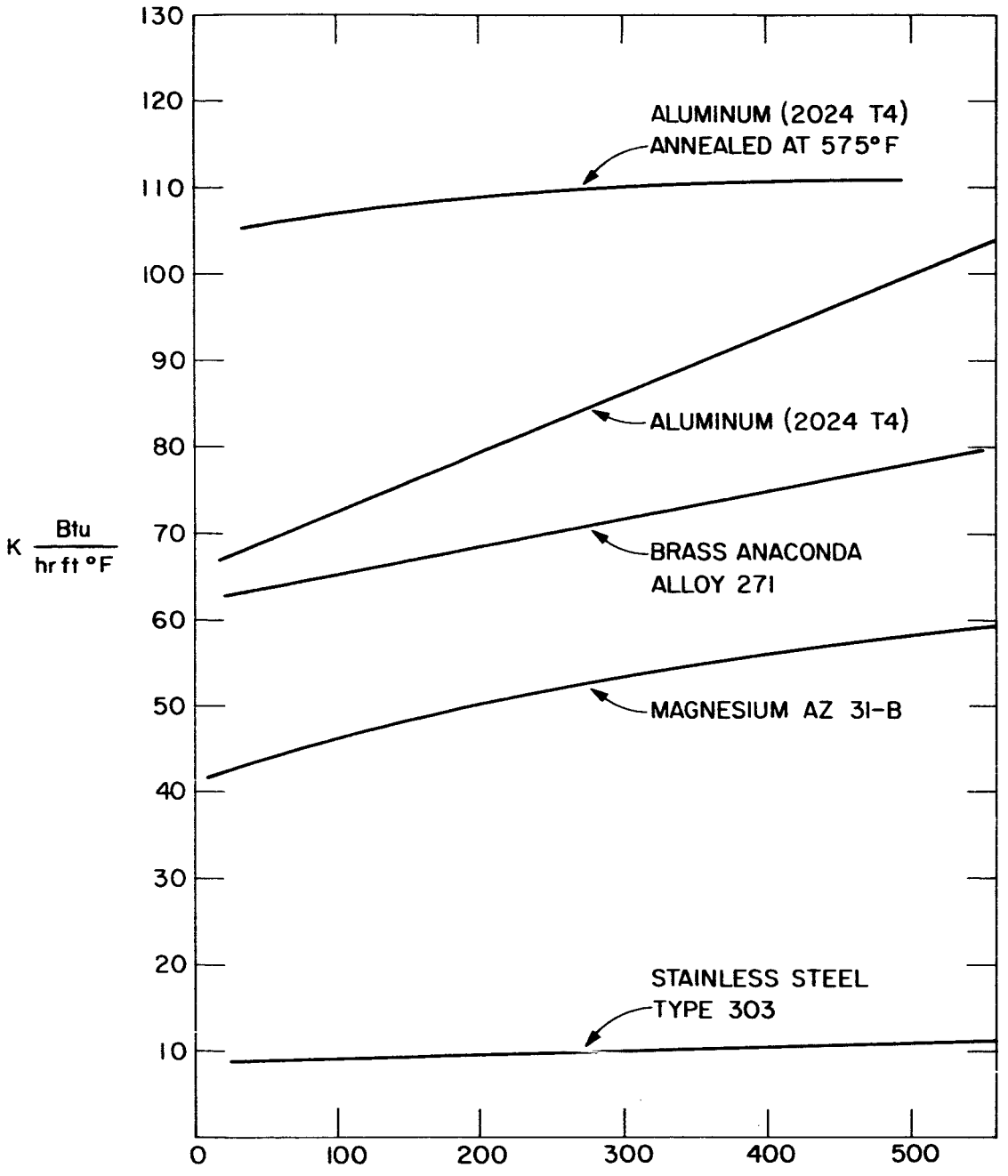


FIG. 33 THERMAL CONDUCTIVITY DATA (REF. [62])

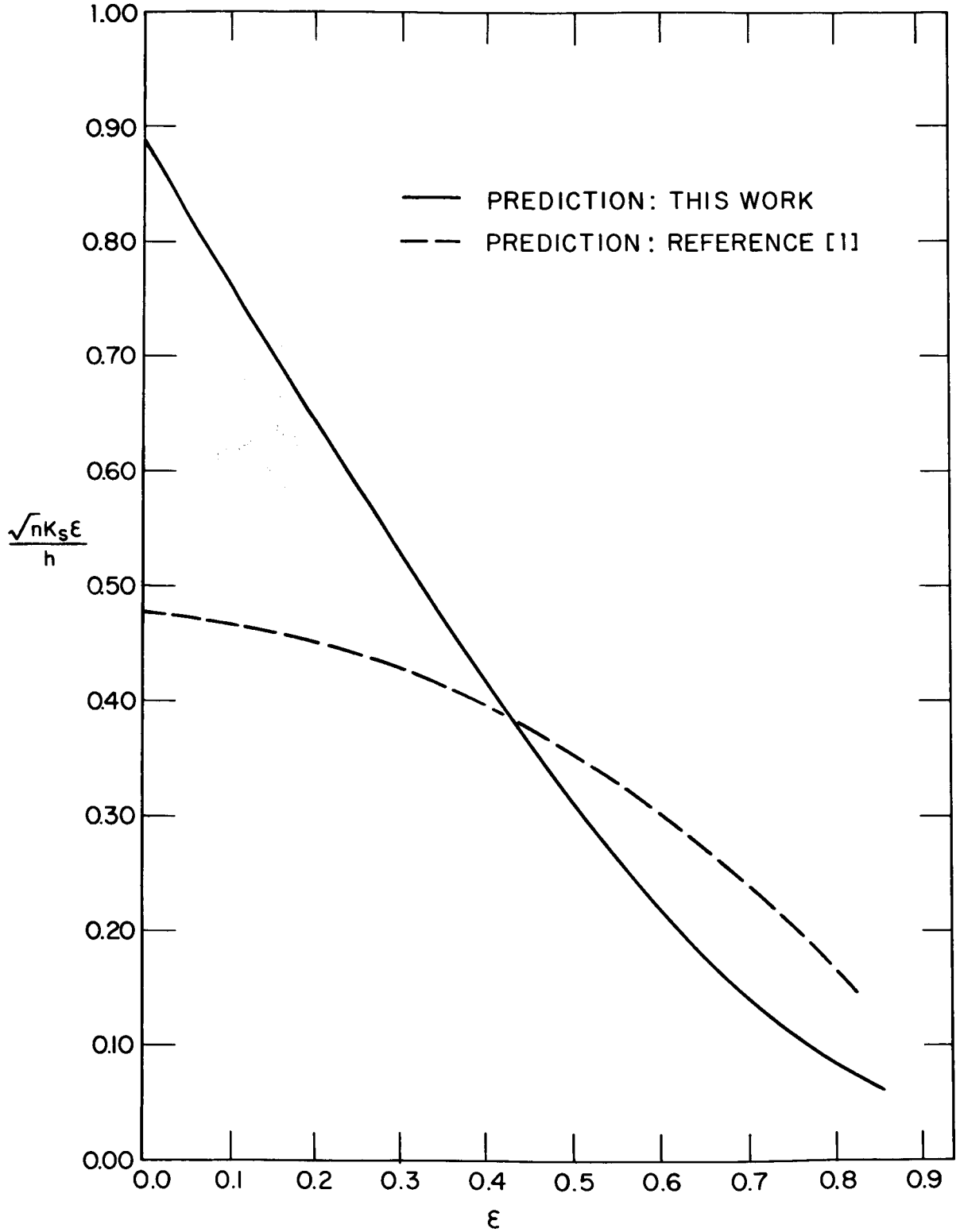


FIG. 34 COMPARISON BETWEEN THEORY OF REF. [1] AND THIS WORK